Visual Guidance of Target-Oriented Flight Behaviours in Birds

James Anthony Walker

Merton College

University of Oxford

Thesis submitted for the degree of Doctor of Philosophy

Trinity Term 2018

Visual Guidance of Target-Oriented Flight Behaviours in Birds
James Anthony Walker
Merton College, Oxford
DPhil. Thesis, Submitted Trinity Term, 2018

Abstract

Birds are highly dependent on vision to guide their flight during goal-directed tasks. They shift their visual attention primarily through head reorientation, with limited eye movement; however, measuring head orientation in free-flying birds is a significant technical challenge. While the gaze strategies of some birds have been studied in considerable detail in laboratory environments, studies of visual guidance in natural environments have largely been limited to inferences based on GPS-derived flight trajectories. This thesis aims to advance our understanding of how birds use their visual system to guide target-directed flight, using novel instrumentation to measure the gaze strategy of homing pigeons (*Columba livia*) and peregrine falcons (*Falco peregrinus*) flying in their natural environments.

We use GPS-derived flight tracks to explore the visual mechanisms available to pigeons to compensate for wind drift, finding that they partially compensate for lateral displacement caused by the wind performing better than a naive strategy requiring no knowledge of the wind. We then describe the development of a custom-built sensor, incorporating a GPS receiver and head-mounted inertial measurement unit (IMU), which measures bird position and head orientation. Using this instrumentation, we find that pigeons coordinate angular head saccades with their wingbeats. Our results also reveal that vertical head stabilisation is enhanced when flying with flock companions, largely via increased wingbeat frequency. The focus of pigeons' visual attention during homing flight is measured with the sensor, allowing specific points of interest to be identified in the landscape that do not lie on the bird's track. Finally, we find that in the closing phases of predatory pursuit, peregrine falcons continuously track their target position using either their frontally or laterally facing fovea. Refined iterations of the exploratory technique developed here have the potential to revolutionise our understanding of large-scale spatial cognition and short-range guidance in birds and may, in turn, lead to applications in the design of visually-guided unmanned aerial systems.

Acknowledgements

I undoubtedly owe my initial interest in birds to mornings spent in the woods with my Grandfather, whose life passion was recording bird song. I am very grateful to Charlie Ellington, who many years later agreed for me to undertake a couple of weeks of work experience in his lab at Cambridge building micro-aerial vehicles. I had no idea at the time that he was one of the founding fathers of the study of animal flight.

I met Graham Taylor for the first time at an Oxford open day where he was demonstrating some onboard video footage from the back of a steppe eagle. Fascinated by this, I applied to Oxford and was randomly pooled to be interviewed by Graham at Jesus College. Despite marking my first undergraduate essay as 'Fine', Graham later tried to convince me to do a PhD by introducing me to one of his students, Fergus McCorkell, who assured me that it would be light work. I thank Graham for his supervision, not just during the PhD but over the past 7 years, and for many engaging conversations that have led to the formation of this thesis. However, above all, I thank him for teaching me that pigeons and peregrines have different shaped beaks. I have been incredibly lucky to have Dora Biro and Tim Guilford as co-supervisors who have provided many valuable suggestions at various stages of this PhD.

The fieldwork undertaken for this thesis would not have been possible without the help of many people. In particular, I would like to thank Lucy Larkman and Takao Sasaki for help with the pigeons, Martin Cray for his expert handling of the peregrines, Malcom Beard for his expert handling of the drone, and Caroline Brighton for introducing me to the peregrine fieldwork. My two main fieldwork seasons were made considerably more enjoyable with the assistance of Eve Richardson and Victor Ajuwon who both made many valuable contributions from study design through to comments on chapter drafts. However, despite my best efforts, I didn't manage to dissuade either of them from applying for DPhils at Oxford. My collaboration with Fumihiro Kano has

been instrumental in refining the onboard sensor developed in this thesis, generating ideas for analysing the data in Chapters 4 and 5 and improving early chapter drafts.

I'd like to thank everyone from the flight group who provided an enjoyable place to work, even after moving offices seven times. In particular, I'd like to thank Sofia Minano Gonzalez, James Kempton and Robin Mills for useful comments on chapter drafts. Many friends in Oxford and London have contributed in their own way, but none more than the Smiths — Chris and James — who have both read the majority of this thesis and have hopefully learnt something about birds in the process.

Thanks also to John Krebs who encouraged me to apply for an internship at the Parliamentary Office of Science and Technology half way through the PhD, allowing me to appreciate science from a very difference perspective. I am grateful to the BBSRC for providing additional funding to support this internship on top of the studentship that has supported this PhD. I have also been very fortunate to receive generous research and travel grants from Merton College.

Finally, I'd like to thank my family who have all read parts of this thesis, but more importantly have been there to support me throughout and remind me that there is more to life than birds.

L’Oiseau c’est une aile guidée par un oeil,
ce qui exige la précision et la vitesse des fonctions rétiniennes

Rochon-Duvigneaud (1943)

Contents

Statement of Authorship

This thesis is structured as a series of papers, each with a self-contained introduction and discussion. Data from Chapter 4 (Figure 4.7) is published in PLOS biology (Taylor et al., 2019) and I have contributed to an additional publication (Kano et al., 2018) which is not included in this thesis but is built upon in Chapters 4 and 5. I developed the instrumentation used within this thesis in collaboration with Fumihiro Kano (Kyoto University) and performed all of the field tests for data used in this thesis. I designed the studies and conducted data analysis with help from my supervisors Graham Taylor, Dora Biro and Tim Guilford but the text of this thesis is entirely my own.

Chapter 1. General introduction

Birds display a number of target-oriented aerial capabilities that outperform most human-engineered autonomous flying vehicles, and do so in a way that is more robust to environmental disturbances and turbulence. Some examples of these sophisticated aerial capabilities include navigating to a fixed goal from unfamiliar or familiar locations (Wallraff 2005; Guilford & Biro 2014), flocking (Pettit et al., 2015; Usherwood et al., 2011; Nagy et al., 2010), avoiding collisions with obstacles (Lin et al., 2014; Bhagavatula et al., 2011), intercepting aerial prey targets (Brighton et al. 2017; Kane & Zamani 2014; Kane et al. 2015; Tucker et al. 2000), tight turning manoeuvres (Ros & Biewener 2017; Kress et al. 2015), and landing on perches (Lee et al., 1993; Davies and Green, 1990). These complex flight behaviours are largely guided by vision. As a result, birds are the most visually-dependent class of vertebrates with highly developed visual systems and larger eyes relative to their body size than any other animal (Jones et al., 2007). While it is evident that birds use visual information to command flight behaviours, the mechanisms by which this visual information is acquired and fed into guidance commands remains largely unknown.

Recent advances in high-speed video and miniaturised onboard sensors have allowed an insight into the precise trajectories, as well as the visual sampling strategies, used by birds during flight. This thesis aims to advance our understanding of the mechanisms underlying the visual guidance of target-directed flight in birds, and the way in which birds stabilise and direct their visual system to extract the information required to implement these mechanisms. This is achieved using novel onboard instrumentation to study homing navigation in pigeons (*Columba livia*) and predatory pursuit in peregrine falcons (*Falco*

peregrinus). The nature of this thesis is highly interdisciplinary, drawing on visual ecology, control engineering and biomechanics. However, the core contribution of this work examines the boundary between three related, but distinct, areas of avian research: visual ecology, visually-mediated guidance and visually-mediated navigation. The distinction between these areas of research, their modes of analysis and ultimate aims are detailed below.

1.1 Avian vision

Birds rely more heavily on vision that any other terrestrial vertebrate (Jones et al., 2007). This is demonstrated by their large eyes relative to the size of their heads occupying 50% of cranial volume compared with 5% in humans (Land, 1999). They also enjoy a world rich in colour often with four or five spectral classes of cones, compared to three in humans, with the additional colour sensitivity in the ultraviolet range (Jones et al., 2007). Like many sensory systems, visual systems tend to reflect the environment in which they operate and therefore there is much variation in sensory system within the avian class according to their ecology (Martin, 2009). One such variation is the regions of specialisation within the retina of with high photoreceptor cell densities, fovea. Although many animal species lack true fovea (primates are the only foveate mammals) (Fite and Rosenfield-Wessels, 1975), fovea are typically found in species for which acute vision is a distinct necessity for survival. The two species that form the focus of this thesis, homing pigeons and peregrine falcons, are both bifoveate with a fovea in the temporal region of their visual field in addition to the central fovea allowing them to fixate distant objects. This allows them to see clearly along more than one visual axis (Benson et al., 2017). Although no detailed measurements of peregrine falcon's visual fields exist, Figure 1.1 shows an orthographic projection of the

boundaries of the retinal fields in the American Kestral (*Falco sparverius*). This visual field configuration with a large region of binocular overlap and large blind area is common in diurnal raptors that rely on vision for aerial predation (O'Rourke et al., 2010). However, prey species such as the pigeon have much smaller regions of binocular overlap and smaller blind areas to maximise their perceptual range in help detect approaching predators.

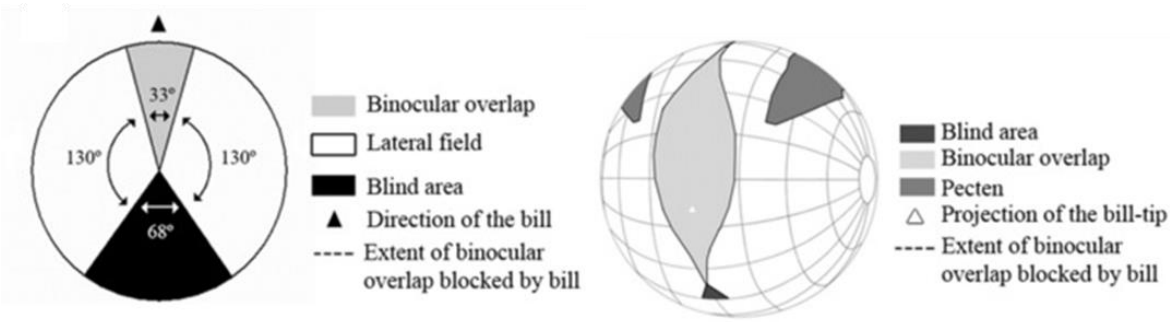

Figure 1.1 – Orthographic projection of the boundaries of the retinal fields of an American Kestral, reproduced from (O'Rourke et al., 2010).

1.2 Avian navigation

The study of avian navigation has a long history dating back over 100 years (Wallraff, 2005). Early experiments displaced wild birds to demonstrate their impressive ability to home from unfamiliar locations (reviewed in: Wiltschko and Wiltschko, 2003). This research is typically undertaken with the ultimate aim of better understanding animal spatial cognition (Guilford and de Perera, 2017). Despite the inherent difficulties in understanding the perceptual abilities of different species and how this relates to their spatial representation of the world, it has been possible, through experimentation, to understand the different mechanisms and cues involved in spatial reasoning and their relative importance. Amongst others, these cues include magnetic fields, polarised light, gravitation fields, visual landmarks, olfactory cues and path integration based on

proprioception. Homing pigeons have become the central model for the study of avian navigation, with research aiming to understand the hierarchy of cues used by birds to navigate at different spatial scales (Wiltschko and Wiltschko, 2003). In the past 20 years, the field has been transformed by the development of miniature GPS loggers that can be used to precisely track the trajectories taken by navigating birds (Meade, 2005; Biro et al., 2002; von Hünerbein et al., 2001).

Kramer's (1957) map and compass model represents the enduring paradigm for long-distance avian navigation from unfamiliar locations. Under this model, the navigational process consists of two separate steps: the map step where birds determine their own position in space and calculate the correct bearing to home, then the compass step where they use some compass mechanism to fly in the calculated direction. The specific sensory modalities that form the basis of each mechanism have been the focus of much debate since the model was proposed (Wallraff, 2005). For the map step, Papi (1971) and Wallraff (1970) have argued for the importance of atmospheric factors such as odour cues. They observed better homing performance from birds kept in lofts open to the atmosphere compared to those kept in protected lofts. In addition, Baldaccini et al., (1975) showed that deflecting the direction of the wind at the home loft leads to a predictable effect on birds' subsequent homeward orientation. A 90 degree deflection in air passing through the loft (so northerly winds appear to come from the east) led to an approximate 90 rotation of the vanishing bearings of the bird when released from a novel location. Although the exact nature of these atmospheric cues is unknown, Wallraff and Andreae (2000) showed evidence of a number of potential airborne hydrocarbons that vary across orthogonal gradients allowing positional information to be estimated. One of the most commonly cited alternatives to the olfactory map hypothesis is one based on geomagnetic fields (Walcott

1978). While the use of magnetic information as a navigational cue is seen in a variety of species (Walker et al., 2002), the evidence for a magnetic map in pigeons is tenuous (Wallraff 1983).

The sun and magnetic compasses are favoured in the literature as directional cues for pigeons navigating from unfamiliar locations. Kramer (1953) first suggested the role of solar cues in providing directional information. The use of the sun compass has been robustly demonstrated using clock shift experiments (Schmidt-Koenig 1958) which artificially manipulate birds' light/dark cycle leading to predictable deflections in homeward orientation: each hour that the birds are shifted away from their natural cycle leads to a 15 degree deviation in homeward trajectory from that shown by controls. However, in some cases, pigeons have been shown to navigate just as successfully in overcast skies (Wiltschko 1987) suggesting that the birds are not fully reliant on their solar compass. Keeton (1972) demonstrated instead that birds with magnets attached to their beaks homed worse than controls on overcast days indicating a role for a magnetic compass, however, these results have not been replicated. Wallraff (2005) suggests that the inconsistency of results from magnet experiments may be explained by the difficulty in humans detecting whether or not solar information is available and the relative importance of the sun compass under different experimental protocols.

Although the mechanisms described above are clearly also available to pigeons navigating within their familiar area, the extent to which different cues are used is unclear (Guilford and Biro, 2014). Early experiments which fitted pigeons with frosted lenses that impaired their vision did not find any negative effect on homing ability within 2 km of their home loft (Schmidt-Koenig & Schlichte 1972). However, recent experiments have shown that

the visual preview of a familiar site before release increases homing performance of pigeons compared with controls but has no effect at unfamiliar sites (Braithwaite & Guilford 1991). Further evidence for the use of visual features in familiar area navigation is provided by the observation that individuals will recapitulate previous routes when released multiple times from the same location (Meade et al., 2005). However, using only the birds' GPS tracks, it is difficult to infer the information content of the underlying landscape and as a result the precise nature of these visual cues remains elusive (Guilford & Biro 2014).

1.3 Short-range guidance

In contrast to navigation, the study of short-range visual guidance in birds has a more recent history, borrowing modes of analysis from the extensive insect literature on the topic (reviewed in: Altshuler and Srinivasan, 2018). In this context, guidance is defined as the process by which visual information is collected and applied to command flight manoeuvres. This research is typically undertaken by mechanical engineers who aim to understand the mechanisms underpinning avian flight in the context of human engineered systems, and ultimately to gain inspiration from birds to improve the design of unmanned aerial vehicles (UAVs). The majority of this work has been undertaken in a laboratory setting involving precise, high-frequency measurements of flight kinematics and aerodynamics, often using high-speed video footage. Such experiments have allowed researchers to begin to identify the underlying controller used by birds to steer flight (Lin et al., 2014) and the role of rapid head movements in turning (Kress et al. 2015; Ros & Biewener 2017), but do not necessarily represent natural flight behaviours. A few notable

exceptions have studied predatory pursuit in raptors using GPS loggers (Brighton et al., 2017) and onboard cameras (Kane et al., 2015; Kane and Zamani, 2014).

This thesis bridges the boundary between the fields of visual guidance and navigation by: (i) taking a guidance approach to studying short-range navigation and, (ii) measuring many of the quantities of interest in laboratory-based experiments, such as wingbeat characteristics and head movements, but for freely flying birds in their natural environment.

1.4 Thesis structure

This thesis is structured into a series of papers, each with a self-contained introduction and discussion. However, the experimental methodology and instrumentation detailed in Chapter 3 is not repeated across subsequent chapters to avoid repetition. Here, I provide a brief summary of the motivation and aims driving the work in each chapter.

In Chapter 2, I take a guidance approach to study the challenge faced by birds flying towards a target through a moving air mass: wind drift. Wind drift compensation has been studied extensively for migrating birds (Liechti, 2006; Green and Alerstam, 2002; Hedenstrom and Alerstam, 1995) and short-term gust responses have been studied in a laboratory (Quinn et al., 2017). However, the compensation for lateral drift is relatively poorly understood for birds flying over intermediate timescales in their natural environments. I borrow terminology from the missile guidance literature to frame this problem in the same context as pursuit, where the target is moving. This chapter uses GPS-tracked homing pigeons and guidance-based simulations to help understand the underlying visual mechanism used for drift compensation. However, it also highlights the complex nature of flight in natural environments and the limitations of simplifying models in

attempting to understand the nature of visual cues based only on GPS-derived flight trajectories.

In subsequent chapters, I explore the role of vision in guiding flight more explicitly by developing instrumentation to measure how birds direct and stabilise their gaze throughout flight. Like most animals with advanced visual systems, birds have specialised regions of their visual field (foveae) that they shift to interrogate their visual environment. However, unlike many other animals, gaze shifts in birds are predominantly determined by head movements as opposed to eye movements (Land 2014). This enables head movements to act as a good proxy for gaze shifts, and head orientation to act as a reliable indicator of gaze direction (Eckmeier et al., 2008).

In Chapter 3, I describe the development and validation of novel instrumentation that is used to simultaneously record the flight trajectories and head orientation of birds flying in their natural environments. The instrumentation consists of a dorsally-mounted GPS logger and a head-mounted inertial measurement unit (IMU) containing a three-axis gyroscope, accelerometer and magnetometer. The use of onboard GPS units to track bird flight paths has become common (Brighton et al., 2017; Wilmers et al., 2015; Freckleton and Iossa, 2010; Meade, 2005; Biro et al., 2002; von Hünerbein et al., 2001), and the use of accelerometers is becoming increasingly widespread (Taylor et al., 2017; Williams et al., 2015; Portugal et al., 2014). However, few studies have used integrated IMUs combining gyroscope and accelerometer readings to measure flight dynamics (Kano et al., 2018; Reynolds et al., 2014; Usherwood et al., 2011; Gillies et al., 2008). The instrumentation described here builds on previous technological developments to enable us to directly measure how birds interrogate their visual environment. Chapter 3 reviews the design of

this equipment and some of the limitations that should be carefully considered when analysing the output.

To effectively extract visual information from their environment, birds require a stabilised visual system. Image stabilisation simplifies the visual processing required by reducing motion blur and is achieved by combining visual, vestibular and cervical reflexes (Gioanni and Vidal, 2012; Wallman and Letelier, 1993). While extensive laboratory-based studies exist of gaze stabilisation in birds (Gioanni 1988a; Gioanni 1988b; Ros & Biewener 2017; Kress et al. 2015; Haque 2004), I am only aware of one study that explores gaze stabilisation for birds flying in their natural environment (Pete et al., 2015). Chapter 4 uses the head-mounted sensor described above to investigate the coordination between wingbeats and angular head saccades in pigeons during homing flights. By releasing birds with and without conspecifics, I was also able to compare the modulation of translational head stabilisation in response to close visual stimuli (their flock companions).

Understanding the function of shifts in gaze in birds, as well as the resulting focus of visual attention, has begun to attract growing scientific interest. However, experiments to date have been primarily laboratory-based (Kress and Lentink, 2015; Eckmeier et al., 2008), and gaze shifts have been under studied for birds flying in their natural environments where they have important adaptive significance for navigation and vigilance. In Chapter 5, I use the head-mounted sensor to examine the periods of fixation between gaze shifts in freely homing pigeons. I attempt to identify the factors underlying shifts in gaze, and points in the landscape that align with lines projected from the birds' foveae during each fixation period. This novel and exploratory approach to studying visual attention could identify the

salient cues of bird navigation in natural environments with important implications for spatial cognition.

In Chapter 6, I build on previous work that used GPS data to determine the guidance law implemented by peregrines during pursuit (Brighton et al., 2017) by incorporating information on head movements using the head-mounted sensor. This allowed me to differentiate between possible gaze strategies adopted during pursuit in relation to the visual environment and to the target. This was achieved by taking the reverse approach to that described in Chapter 5; instead of determining the focus of visual attention using head orientation by assuming a set of fovea angles, I assume that the peregrine is focussed on the target and determine where on their visual field the target is fixated. This also allowed me to explicitly test existing hypotheses relating to the region of the visual field used to fixate the target at different distances from the pursuer (Tucker et al. 2000).

1.5 Overarching themes

The primary aim of this thesis is to advance our understanding of the ways in which birds deploy their visual system to guide target-directed flight. However, a number of additional topics are tackled across multiple chapters. Firstly, although wind is most explicitly dealt with in Chapter 2, I treat wind as an important factor to consider when interpreting ground tracks to infer navigation and guidance mechanisms. This is true in Chapters 5 and 6 for the interpretation of body orientation from GPS data in a moving air mass where I incorporate wind estimates into the analyses. Secondly, the use of the same instrumentation to study two species of bird with very distinct behavioural repertoires enables a direct comparison of their gaze strategy. This allows an analysis of the different visual requirements of an aerial predator and its prey and also demonstrates that the technique

developed here is applicable to the study of a broad range of species. Finally, in each chapter, I describe how further developments from the findings of this thesis could be used to aid the design of human-engineered systems. Visual sensors are emerging as an important source of input for autonomously controlled UAVs because they are lightweight and can capture large amounts of spatial data. However, engineers are confronted by many of the same challenges faced by birds such as image stabilisation, target tracking, visual processing and drift detection. As such, the development and implementation of robust vision-based guidance algorithms for autonomous flight in turbulent, unpredictable, GPS-denied environments, inspired by avian visual systems, is an important goal with significant commercial interest. I carefully consider the potential of avian research in achieving this goal but highlight the need to appreciate the evolutionary constraints under which avian visual systems have evolved.

Chapter 2. Homing pigeons partially compensate for wind drift when released within sight of their goal

2.1 Abstract

When left uncorrected for, wind causes birds to drift away from their desired path. To reach their destination, birds must compensate for wind drift by adjusting their heading and speed. The compensation for wind drift has been widely studied in migrating birds but has received relatively little attention for birds guiding their trajectory over shorter distances. Recent technological advances have allowed detailed flight trajectories to be examined in relation to the wind field using onboard tracking devices. Here, we analysed GPS tracks from 44 homing pigeons (*Columba livia*), released within sight of their destination, along with time-averaged local wind data to differentiate between the possible visual mechanisms used by the birds to compensate for the effect of wind. We found that pigeons are capable of compensating for wind, but they do so imperfectly, resulting in curved trajectories which are displaced laterally in the direction of the crosswind. Track simulations revealed that in high crosswinds, pigeons perform better than a naive drift compensation strategy ('pure pursuit') which requires no knowledge of the wind field. The analyses presented here suggest instead that the birds are able to directly or indirectly detect the wind field and partially compensate for drift using a range of mechanisms that include guidance and the use of landscape features.

2.2 Introduction

The task faced by a bird flying through the air to a desired goal requires an impressive display of guidance relying on a variety of cues (Chapman et al., 2008). This task is made substantially more complex when the air mass is moving at speeds of the same order of magnitude as the bird's airspeed (Emily L.C. Shepard et al., 2016). Without adjustment, a flying bird will experience wind drift when the wind direction is not parallel with the bird's intended heading, leading to lateral displacement from the desired path. The resulting ground track vector ($\vec{V}$) is the vectorial sum of the wind vector ($\vec{W}$) and the bird's air velocity vector ($\vec{U}$) (Figure 2.1). In order to remain on its intended track while experiencing a crosswind, a bird must therefore make compensatory adjustments to its air velocity vector (i.e. airspeed and heading). In a constant wind field with perfect knowledge of the wind vector, a bird can achieve perfect drift compensation by adjusting its heading by a deviation angle (δ). Given the large energetic cost associated with flight (Pennycuick, 1978), it is reasonable to assume that birds have evolved wind drift compensation mechanisms that allow them to minimise their cost of transport (Liechti et al., 1994). Indeed, empirical evidence for compensatory adjustments to heading or airspeed has been found in the analysis of soaring in steppe eagles (*Aquila nipalensis*) (Taylor et al. 2016), in migrating birds (Hedenström et al. 2002, Hedenström & Åkesson 2016) as well as in insects (Reynolds et al., 2010; Chapman et al., 2008).

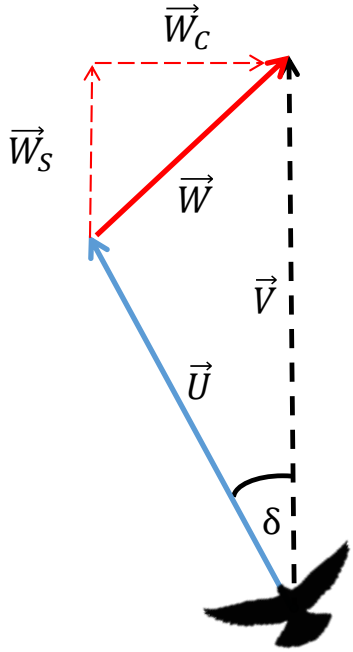

Figure 2.1 — Triangle of velocities representing the flight of a pigeon. The pigeon is flying with a certain air velocity vector ($\vec{U}$: airspeed and bird heading) while being drifted by the wind vector ($\vec{W}$: wind speed and direction). The bird's resulting movement across the ground ($\vec{V}$: groundspeed and track angle) is the vectorial sum of the air and wind vectors ($\vec{V} = \vec{U} + \vec{W}$). If $\vec{V}$ is the desired track and the wind field is constant, the pigeon can, in principle, add a deviation angle (δ) to its heading to fully compensate for the effect of wind. Wind support ($\vec{W}_s$) and crosswind ($\vec{W}_c$) are the two horizontal components of the wind vector resolved with respect to the mean ground vector.

A large body of work has used optical techniques and radar tracking to study bird migration paths in response to wind conditions (Hedenström et al. 2002, Green et al. 2004, Alerstam 1979). Recent technological advances have allowed detailed flight trajectories to be examined in relation to the wind field using onboard tracking devices (Taylor et al. 2016, Tarroux et al. 2016, Mandel et al. 2008, Bohrer et al. 2012). The orientational abilities of homing pigeons have attracted considerable research attention in recent decades (Biro et al., 2003; Burt et al., 1997; Wallraff, 1994)with investigators attempting to identify the mechanisms and cues that pigeons adopt when orienting within both unfamiliar (Wallraff,

2005) and familiar (Guilford & Biro 2014) areas. Free-flying homing pigeons also offer a convenient study system for investigating guidance and control over shorter timescales by precision tracking their homing trajectories in relation to the wind field. Here, homing pigeons (*Columba livia*) were fitted with GPS loggers and released within sight of their target, the home loft, to explore the underlying mechanisms available to the bird to compensate for wind drift where the goal is visible.

Given that wind drift can have a large impact on the energy and time required for efficient orientation (Liechti et al. 1994), leading to large errors if uncorrected, it is reasonable to assume that pigeons have evolved mechanisms that allow them to compensate for the effect of the wind on their flight path. When the bird's target is in sight, there are a number of possible visual mechanisms that could be used to compensate for drift. Here, we consider them from a guidance perspective, borrowing terminology from the missile guidance literature typically used to describe pursuit. Although pursuit strategies are typically used to describe guidance with respect to a moving target, this is equivalent to the pursuit of a stationary target in a moving air mass. The mechanisms that we consider are: (i) pure pursuit - requiring no knowledge of the wind field, (ii) deviated pursuit – where the wind is sensed and drift is corrected for before it has happened, and (iii) the use of landscape features directly below. These mechanisms are discussed further below.

(i) If the goal is in sight, the simplest mechanism available to a bird to compensate for wind drift is to adjust its airspeed vector so it always points at the target. This guidance strategy is referred to as 'pure pursuit' in the missile guidance literature (Shneydor 1998). It requires no knowledge of the wind vector and corrects for the effects of wind drift after they have happened. This geometric rule has been shown to match pursuit trajectories in flies (Land,

1993), goshawks (Kane et al., 2015) and fish (Lanchester and Mark, 1975). This strategy will be used here as a null model against which to test short range navigation in pigeons where the target, the home loft, is stationary. If this simple strategy is adopted, and a bird flies directly towards a single landmark directly ahead when there is a non-zero crosswind, the bird will be subject to wind drift. This will result in a curvilinear track, displaced in the direction of the crosswind (Guilford and Taylor, 2014).

(ii) With some knowledge of the wind vector, a bird can perform better than pure pursuit by adding a deviation angle to its heading, orienting itself into the wind. This guidance strategy is referred to here as 'deviated pursuit'. It corrects for the effects of wind drift (whether wholly or partially) before they have happened but requires some explicit or implicit knowledge of the crosswind to compute the deviation angle (δ — Figure 2.1). If a perfect deviation angle is selected by the bird, and is constantly adjusted for the changing wind field, this would enable the bird to take the direct line between its current position and the target.

The deviation angle can be estimated by the bird in a number of ways. Prior to take-off, the bird may use mechanoreceptors near its feather follicles that are sensitive to the magnitude of flow to estimate wind direction (Brown and Fedde, 1993). However, in steady conditions, it is not possible to mechanically detect the wind speed of a mass of air in which you are drifting (Chapman et al., 2011). In contrast, there are a number of possible visual mechanisms that allow drift to be sensed when airborne. For example, using the relative parallax between landmarks in front of and behind the target, or using a fixed azimuthal reference such as the sun or a magnetic compass, against which to compare the azimuth of your goal (Srygley and Oliveira, 2001). If the azimuth of the goal relative to the reference

changes while the bird is flying towards it, this indicates that wind drift has occurred that can be compensated for by adjusting the deviation angle until the azimuth of the loft remains unchanging. Alternatively, translational optic flow, the pattern of apparent motion of the visual scene across an animal's retina, can theoretically be used estimate lateral drift in low-altitude flight (Taylor et al. 2016; Guilford & Taylor 2014). Lateral translational optic flow, perpendicular to the animal's air vector, can be used to sense crosswind speed and direction and has been observed in bumblebees to help reduce lateral drift due to wind (Riley et al., 1999). Although the use of optic flow has been demonstrated for gap negotiation in budgerigars (*Melopsittacus undulatus*) (Bhagavatula et al., 2011), it is unclear whether birds are able to use optic flow cues during variable altitude flight.

(iii) Homing pigeons often incorporate linear landscape features such as roads, hedge lines, field boundaries and rivers into their habitual routes (Meade et al. 2005; Mann et al. 2011; Guilford et al. 2004; Lau et al. 2006). In addition to providing a navigational aid, linear features could provide an obvious mechanism to detect and compensate for drift (Bruderer, 1978) that is distinct from the guidance mechanisms discussed above. Some observational evidence for the use of linear features for drift compensation exists for migratory birds that were found to preferentially align their flight path with the Hudson river during high crosswinds (Bingman et al., 1982). Additionally, Richardson (2000) observed that higher concentrations of migrants were found over linear features in high crosswinds during the day than for similar wind conditions at night. This was taken as further evidence that linear features were being used, when available, for drift compensation. If pigeons are making use of linear features to compensate for wind, the extent of linear feature following should vary with wind characteristics.

The mechanisms described above make some specific predictions regarding the flight trajectories that pigeons are expected to take in relation to the wind field. We attempt to differentiate between some of these mechanisms using simulations to compare the tracks expected under these mechanisms against GPS-derived flight data. However, given the complex nature of navigation, the detailed structure of homing trajectories will also reflect a combination of mechanistic and functional factors such as the navigational mechanism used, homing experience, predator avoidance and homing motivation. Releasing the birds within sight of their target from familiar release sites goes some way to reducing their reliance on navigational mechanisms, allowing the impact of wind on flight structures to be more clearly assessed and giving a greater degree of certainty relating to their preferred track.

2.3 Methods

2.3.1 Subjects

Forty-four homing pigeons (*Columba livia*), aged between 2 and 8 years and reared at the University of Oxford Field Station at Wytham (51.782872 N, -1.317358 W), were used as subjects. Experiments took place over 3 years from 2015 to 2017 from April to August each year. All subjects were familiar with the area surrounding the loft and had been recently released from each release site prior to experimentation. The feather condition and flight behaviour of birds were monitored throughout the study and water and food was provided *ad libitum*.

2.3.2 Release sites and testing

Two release sites were selected within direct sight of the white buildings surrounding the pigeons' home loft in opposite directions from the loft (Table 2.1). GPS logging devices (Qstarz BT-Q1300ST, approx. 15 g) were attached dorsally using custom made elasticated harnesses around the subject's body which were worn throughout the study duration. For every flight, the GPS devices logged geographical longitude and latitude at 5 Hz. Between testing, when the birds were in their home loft, the elastic harnesses were fitted with Plasticine dummy weights equivalent in size to the GPS loggers. The GPS units typically provide an absolute horizontal positioning accuracy of ≤7.8 m (95% of data falls within this range of the actual position) although dynamic tests with these devices have found that the relative positioning accuracy is substantially better than this over short flights (Brighton et al., 2017). GPS devices were turned on and attached to the bird at least 5 min before each release in an attempt to minimise initial positioning errors. Each bird was allowed 15 seconds to survey the landscape after fitting the GPS prior to release and each release was separated by a two min period after the previous subject had been released in order to eliminate group homing behaviour. Testing was only conducted on clear days when the sun's disc was visible in the sky with the exception of one release in July 2017 that was carried out in misty conditions from Wytham Hill where the visibility was ~30 m. The five flights conducted on this day were not included in the main analysis but were used as a comparison for when the loft was not visible from the release site.

Site	Latitude	Longitude	Bearing to loft (deg)	B*eeline* Distance to loft (m)	Number of flights
(1) Wytham Hill	51.774825 N	-1.321878 W	19.4	950	115
(2) Kings Mill Lock	51.789200 N	-1.307700 W	221.3	950	32

Table 2.1 - Release sites selected equidistant from the home loft in opposite directions. Latitude and longitude given in decimal degrees.

Wind data were recorded using a WS2083 Professional Wireless Weather Station (Aercus Instruments, UK) installed at the loft, 5 m above ground level which logged average wind direction and wind speed every minute. Wind data were processed using Cumulus Weather Station Software (Sandaysoft, v1.9.4).

2.3.3 Track and wind analysis

Data processing and analysis was conducted using MATLAB (MathWorks, vR2017a). Time-stamped positional fixes were downloaded after recovery of the GPS trackers using dedicated software (Qsports v3.7, Qstarz). In the case of logger failure, the track was eliminated from subsequent analysis (n = 11). GPS data were screened for accuracy and precision using methods described by Brighton et al. (2017) by analysing the discrepancy between differenced groundspeed estimates and the Doppler velocity from the GPS device. This resulted in the elimination of 1 track leaving 147 flight tracks for subsequent analysis. Latitude and longitude were converted to meters using a Universal Transverse Mercator projection and cropped to between 50 m and 800 m from the home loft. At the start of the track, this excluded take off and the first few seconds of the flight and the initial climbing phase. By this point, the bird will have had the opportunity to assess the wind vector based on the drift experienced. At the end of the track, the crop excluded circling from subsequent analyses. Each track was then translated so that the start position was aligned exactly to the

position of the release site in order to minimise the error arising from GPS inaccuracy. This meant that track positioning error is therefore zero at the start of the flight, but expected to drift through time and hence expected to be largest at the end of the flight. See Chapter 6 for an assessment of the importance of this correction. Altitude data from the GPS devices were found to be insufficiently accurate to explore whether the birds maintained the constant flight altitude required for drift corrections using lateral optic flow and were not analysed further.

The lateral displacement was calculated throughout each flight — the distance between the bird's current position and the beeline, measured perpendicular to the beeline – and then averaged across the flight. This gave a measure of the extent and direction of lateral displacement of each flight relative to the beeline between the release site and the loft. If pigeons were minimising the cost of transport, and were capable of perfect drift compensation, they would fly the beeline distance to the loft and have a mean lateral displacement of zero which is equivalent to a route efficiency of 1 (Meade et al. 2005) .

Mean airspeed (U) was estimated using the ground velocity vector ($\overrightarrow{V}$) and wind vector ($\overrightarrow{W}$) and used to parameterise the pursuit model describe below. The effect of wind support on the bird's choice of airspeed was then analysed using a regression analysis, as has been done for other species (Hedenström & Åkesson 2016; Taylor et al. 2016). For each track, wind support ($\overrightarrow{W}_s$: the length of the wind vector parallel to the direct line between the release site and loft) and the crosswind ($\overrightarrow{W}_C$: the length of the wind vector perpendicular to the direct line between the release site and loft) were calculated using wind data collected at the loft and averaged over the flight time. These quantities have been defined in relation to the bird's intended ground vector similar to Liechti et al. (1994) rather than in relation

to the bird's air velocity vector as in (Safi et al. 2013; Taylor et al. 2016) and averaged over the entire flight rather than calculated instantaneously. Positive wind support values represent a tailwind and negative values represent a headwind while positive crosswind values represent wind moving from right across the bird's track and negative values represent the reverse. For each flight, the predicted deviation angle (δ — Figure 2.1) was calculated using the equation: $\delta = \sin^{-1}(\frac{W_C}{U})$. The crosswind vector was multiplied by the duration of the flight in seconds to give the required 'crosswind effect', the distance that the birds would have drifted laterally if no attempt to compensate for wind drift had been made.

2.3.4 Track simulations

Trajectories were simulated for each flight using the naive 'pure pursuit' model described above, parameterised by the mean wind vector (wind direction and speed) and the bird's mean airspeed (estimated by subtracting the bird's ground vector from the wind vector). Starting at the first track point, the simulated bird always keeps its heading aligned with the target, moving at a constant airspeed until it reaches the loft. The mean lateral displacement was then calculated using the method described above for each of the simulated tracks and compared in a linear regression model against observed data. Figure 2.2 shows an example of two GPS-derived tracks (orange) along with simulated tracks under pure pursuit (blue) for the given wind field (red arrow) where the bird is displaced less (Figure 2.2A) or more (Figure 2.2B) than predicted using this model. Due to the uncertainty in the model input parameters, pure pursuit trajectories were also simulated for the whole range of airspeeds (10.3 – 23.5 m/s), wind speeds (0 — 11.4 m/s) and wind directions (0 – 360 deg) which were recorded. This allowed us to graphically compare the

range of crosswind correction and mean lateral displacement predicted from simulations against the observed data.

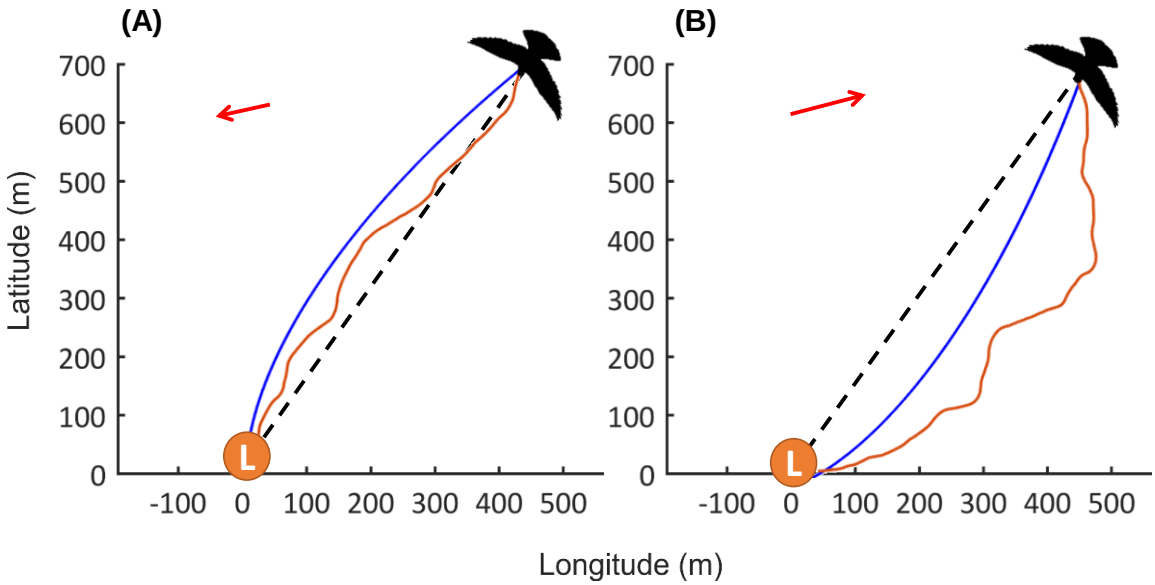

Figure 2.2 — Examples of pure pursuit simulated track (blue) and GPS derived track (orange) for 2 flights with different wind conditions (red arrow) flying towards the home loft (L). The dotted black line is the direct line between the flight start and loft used to calculate the mean lateral displacement (MLD). (A) Bird experiences less lateral displacement (MLD: -28.9 m) than track simulated using pure pursuit (MLD: -58.1 m) with the following parameters: wind speed = 3.7 m/s, wind direction = 70 deg, mean airspeed = 18.9 m/s. (B) Bird experiences more lateral displacement (MLD: 122.0 m) than track simulated using pure pursuit (MLD: 52.0 m) with the following parameters: wind speed = 4.8 m/s, wind direction = 271 deg, mean airspeed = 15.6 m/s. In both cases, the bird is laterally displaced in the direction of the crosswind experienced.

Deviated pursuit trajectories were simulated for each flight by adding a constant deviation angle (δ) to the pure pursuit model across the flight. For each flight, the deviation angle was optimised to fit the GPS data by minimising the sum of distances between each GPS derived point and the simulated bird trajectory for that same point in time. Figure 2.3 shows an example of a GPS derived track (orange) along with a track simulated using pure pursuit (blue, δ = 0 deg) and a track simulated using deviated pursuit with an optimised deviation

angle (green, $\hat{\delta} = 17.6$ deg). Additional trajectories are simulated for a range of deviation angles around the optimum.

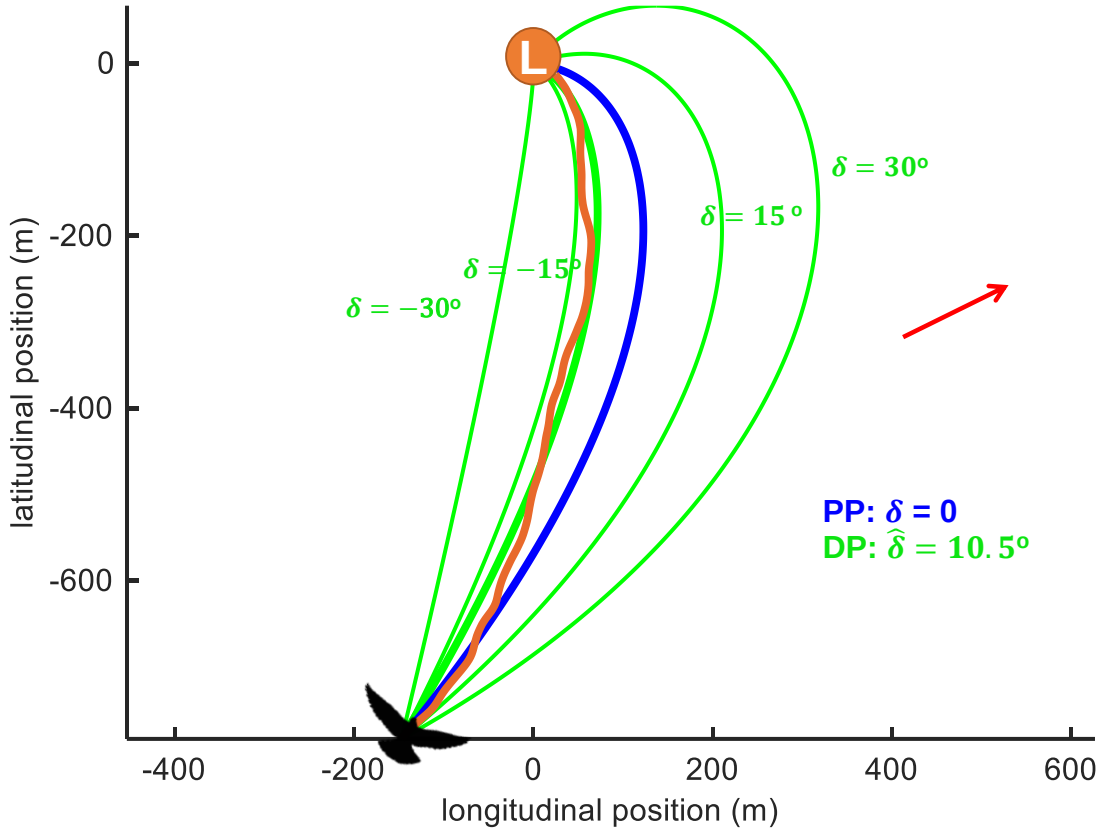

Figure 2.3 – Example GPS track (orange) plotted with simulated tracks using pure pursuit (blue) and deviated pursuit (thick green) for a deviation angle that is optimised to the track ($\widehat{\delta}$ = 10.6 °) along with 4 additional trajectories for a range of deviation angles (thin green). Pure pursuit is a special case of deviated pursuit where δ = 0. The 'predicted deviation angle', the angle that would lead to a direct track between release site and loft given a constant wind field for this flight is -31.8 deg. The red arrow indicates the wind vector used to parameterise these simulations (wind speed = 10.4 m/s, wind direction = 252 deg), along with mean airspeed = 18.4 m/s.

2.3.5 Linear feature detection

To evaluate the use of linear features as an aid for wind drift compensation, we took three steps. Firstly, we developed a method to objectively determine whether or not the tracks from each site have a greater tendency than expected by chance to fall over linear features,

described below. Secondly, where there was evidence for linear feature following at a site, we determined whether the extent of linear feature following varied with the crosswind experienced. Finally, we attempted to determine whether any relationship between crosswind and linear feature following was simply a result of a greater tendency to be blown over linear features in a crosswind as opposed to the birds selecting to align their track with linear features. This was achieved by repeating the second analysis but instead comparing the linear feature following from simulated null trajectories against the crosswind.

In order to objectively identify linear features in the area of interest, an edge image was produced (Figure 2.4B) by running a Canny edge detection on an aerial image (Figure 2.4A) covering the region of interest using similar methods to Lau et al. (2006). The resulting binary image was scaled so that each pixel represented 1 m^2 with a value of 1 over edges or 0 between edges. The tracks were then overlaid on top of the binary image (Figure 2.5) and each GPS point was categorised as either over an edge (if an edge occurred within the 5 m^2 area around the point, to account for GPS error), or as not over an edge. This allowed the proportion of the track following linear features to be estimated. This method has distinct advantages over previous efforts to quantify the degree of linear feature following (Lipp et al., 2004) as it does not require linear features of interest to be subjectively identified.

To objectively identify whether the trajectory taken by the bird overlies edge features of the landscape to a greater degree than expected by chance, we compared the proportion of the trajectory that fell over edges against a null distribution. This distribution was generated for each flight using 1,000 simulated deviated pursuit trajectories (parameterised by the

wind vector, start position and air speed). We used evenly spaced deviation angles between the predicted deviation angle (leading to a direct track between release site and loft) and a deviation angle of zero ($\delta = 0$, pure pursuit) (Figure 2.3). For each simulated trajectory, the proportion of points over edges was calculated using the binary edge image and added to the distribution against which to compare the value from the GPS-track. The range of deviated pursuit trajectories generated for each flight represents a plausible set of tracks — 80% of null distributions cover the range of the GPS-derived track against which it is compared. However, the interpretation of edge alignment values against these null distributions should be treated with caution as they clearly do not represent all possible paths that the bird could take to the loft. Nevertheless, this allowed us to characterise each flight using an edge alignment percentile relative to the null distribution.

2.3.6 Statistical analysis

Statistical analyses were conducted in R (v3.5.1; R Core Team 2008). To test for the effects of learning across multiple flights, we applied a linear mixed model (LMM) using the R package 'lme4' (Bates et al., 2014). We tested for the effect of release number (the number of releases from each site) on route efficiency, including bird ID as a random factor. We tested the significance using a likelihood-ratio test comparing the full model with a model without the effect in question. The assumptions were verified using visual inspection of plotted residuals. The regression analyses, used to compare guidance model simulations against GPS-track data, treat each flight as independent and do not control for bird ID in order to simplify the interpretation of the slope coefficients.

Figure 2.4 — Linear Feature detection method. Canny edge detection of an aerial image (A) to produce a binary image (B) of the flight area. Release sites 1 (Wytham Hill) and 2 (Kings Mill Lock) are labelled along with the home loft 'L'.

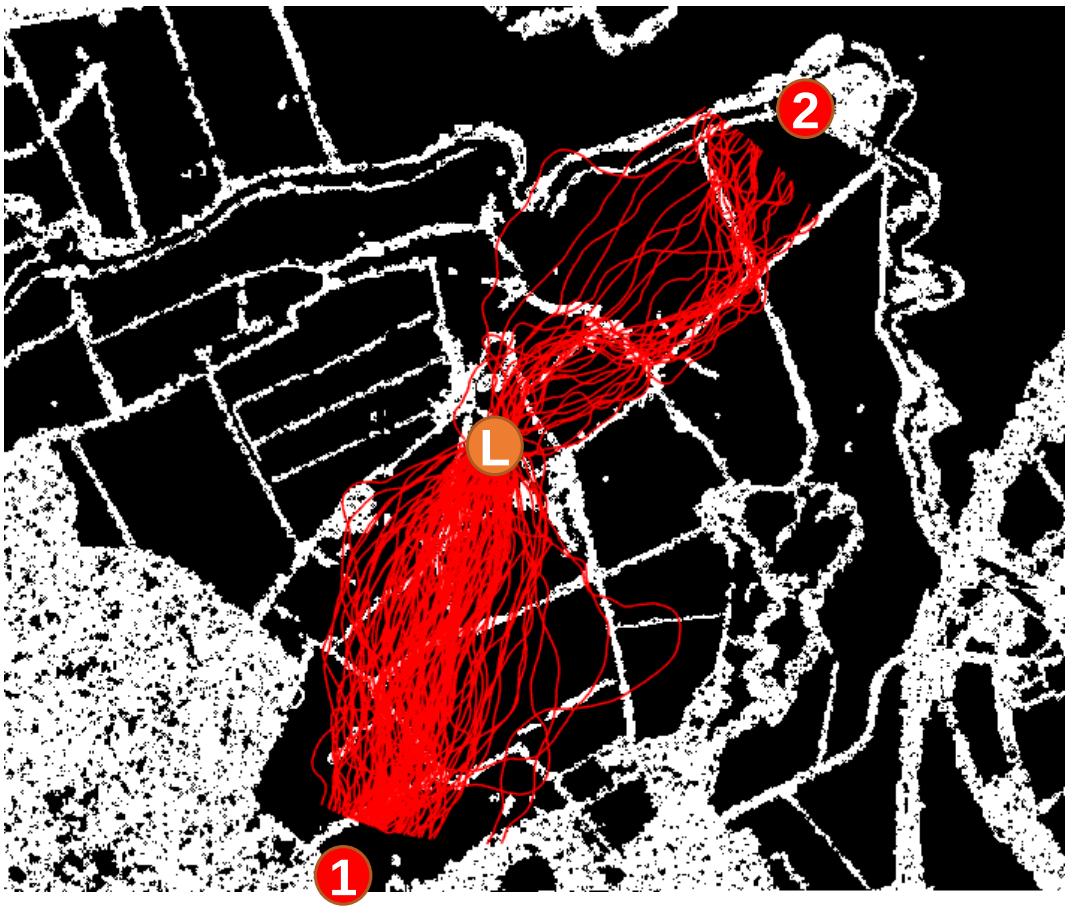

Figure 2.5 – Binary edge image with all cropped GPS-derived tracks overlaid in red. 147 trajectories are plotted from 44 birds.

2.4 Results

All birds arrived home in non-zero wind conditions and therefore must have adopted some mechanism that allowed them to compensate for wind drift, either before or after the drift had the opportunity to take effect. The birds all homed immediately after release without stopping en route, suggesting that they were highly motivated to home and that their patterns of movement were dominated by navigational decisions to this end. Unsurprisingly, given the proximity of the release sites to the loft, and the familiarity of all birds with the surrounding area, route efficiency (the beeline distance between the release site and the loft divided by the length of the path flown) was not found to increase significantly with release number from the same site (LMM, $\chi^2 = 0.063$, df = 1, p = 0.80). Visual inspection of flights for each individual indicated little route stereotypy for any individual.

A linear regression model was used to examine the relationship between mean groundspeed (V) and mean wind support (W_s) for each flight; data were bootstrapped to control for the effect of unbalanced sampling of individuals. Parameter estimates are the means of 1,000 regressions, each generated from a sample including one randomly selected flight per bird (n = 44). Note that mean wind support is the component of the wind vector parallel to mean ground vector (Figure 2.1) and therefore in the absence of a change in airspeed in response to wind, we would expect these two variables to be linearly related with a slope of one. Indeed, we found mean groundspeed to increase with wind support (F (1, 144), $R^2 = 0.57$, $p < 0.001$), according to the following equation $V = 20.7 + 1.16\ W_s$ with a slope that did not differ significantly from one (95% CI: 0.93 — 1.41). Therefore, we found no evidence

for airspeed adjustments but the strength of this relationship gives some confidence in the wind data collected.

2.4.1 Crosswind explains some variation in lateral drift

When all tracks are plotted and coloured by the crosswind effect (Figure 2.6), it becomes obvious that much of the track variation is accounted for by crosswind (the component of the wind vector perpendicular to the beeline track) where the direction of lateral displacement is typically in the same direction as the crosswind experienced. This indicates that the mechanism adopted by the pigeons to compensate for wind is not perfect and the bird uses a poor estimate of the wind field, either detected visually once airborne or mechanically before take-off, to adjust its heading. Figure 2.7 demonstrates this relationship for all flights where the mean lateral displacement (the average distance between each point and the most direct track) is plotted against the crosswind correction (the lateral distance that the bird would have been drifted over the duration of the flight if no corrections had been made). A chi-square test of independence confirmed the relationship between the sign of the crosswind effect and the sign of mean lateral displacement (χ^2 (1) = 43.5, p <0.001). To test whether the extent of lateral drift increases with larger wind speeds we used Spearman's rank correlation coefficient to test whether absolute mean lateral displacement increases monotonically with absolute crosswind speed. We found this to be statistically insignificant (r_s (147) = 0.137, p = 0.0782), although only marginally so.

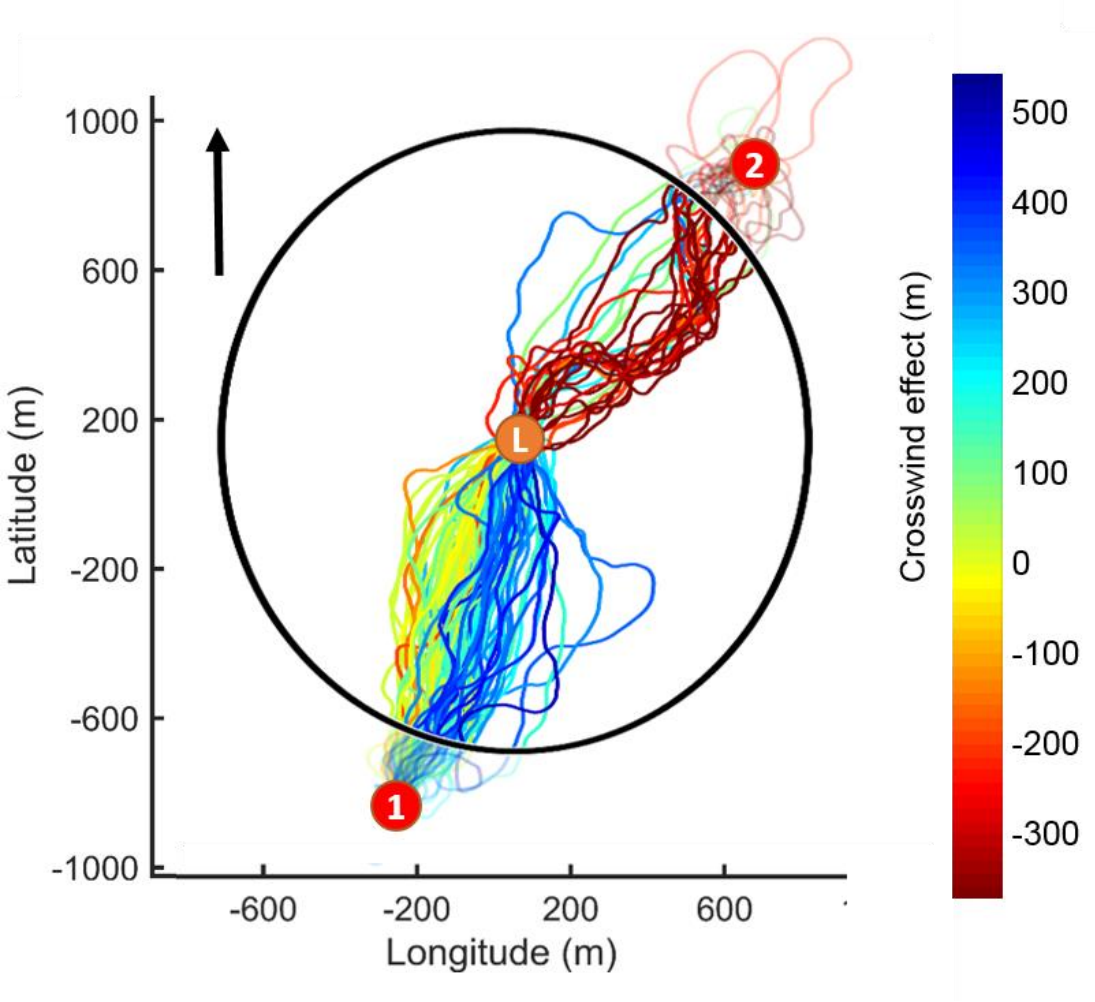

Figure 2.6 – 147 GPS-derived trajectories from 44 pigeons released from sites 1 or 2 and coloured by crosswind effect (the product of crosswind and flight duration), cropped to between 800 m and 50 m of the home loft (L). The circle indicates the 800 m cropping radius with the start of tracks plotted at 50% opacity. Crosswind effect is positively signed when blowing across the track from the right (clockwise deflection from direct line between release site and loft) and negatively signed when blowing across the track from the left. Figure scaled to meters with the loft at the origin. The black arrow indicates north.

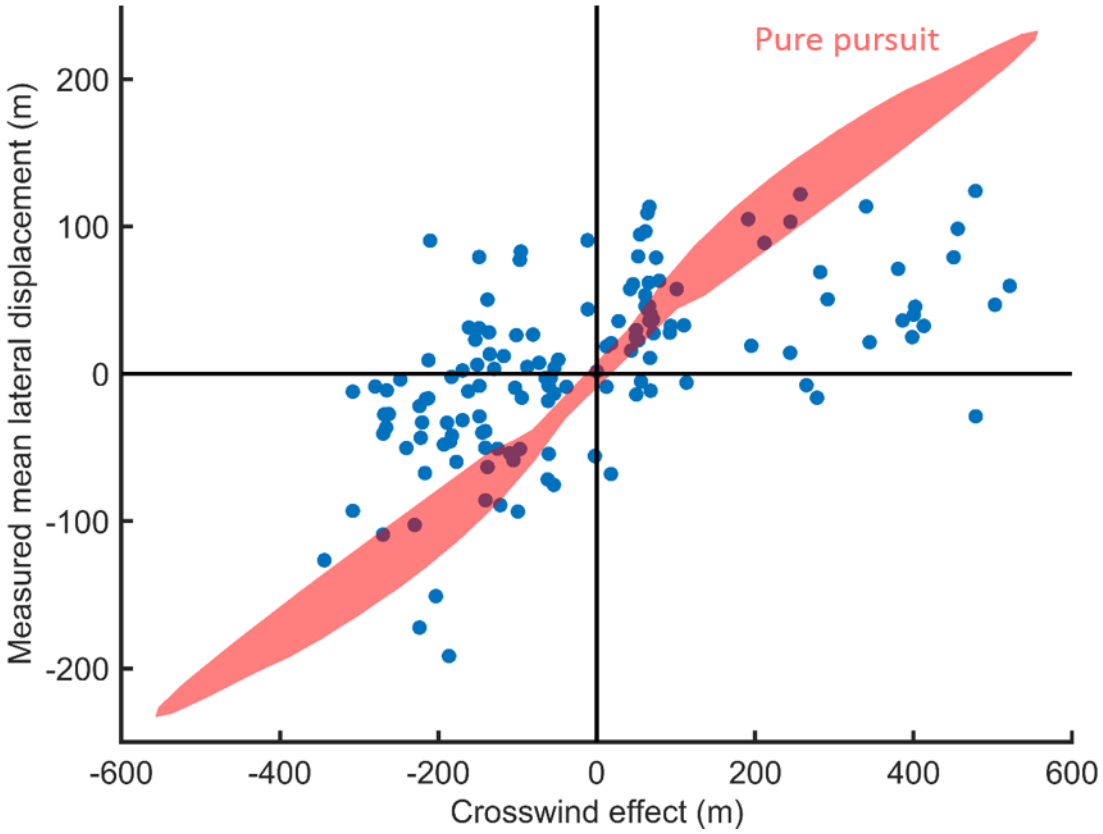

Figure 2.7 — Crosswind effect (crosswind speed multiplied by flight duration) against the mean lateral displacement, both in meters, for all flights (n = 147). The red shaded area represents pure pursuit simulated data for each combination of the whole range of airspeeds (10.3 – 23.5 m/s), wind speeds (0 — 11.4 m/s) and wind directions (0 – 360 deg) recorded across all flights. For positive crosswind effects, when the blue dots fall below the red shaded area the bird has experienced less drift than predicted by pure pursuit and vice versa for negative crosswind effects.

2.4.2 Guidance model simulations

GPS-track data were compared against data simulated using the naive pure pursuit model for the given airspeed, wind speed and wind direction and used to predict the mean lateral displacement from the beeline. There was a positive correlation between observed mean lateral displacement and data simulated under the pure pursuit model ($R^2 = 0.35$, n =147), with a slope of observed versus predicted of 0.59 (t = 8.11, $p < 0.001$, n =147). However, the 95% confidence interval (0.45, 0.74) does not include 1 suggesting that the birds are

compensating by more than expected under this strategy, which indicates that the birds are behaving as if they have some knowledge of the wind. Pure pursuit model output for the whole range of wind and airspeeds recorded within and across all flights is shown as the red shaded area in Figure 2.7. This shows that at low crosswind speeds (and hence lower crosswind effect), the strategy used by birds sometimes leads them to be displaced more than predicted by pure pursuit. However, at higher crosswind speeds, the birds are able to compensate for crosswinds better than predicted by pure pursuit. The simulations also revealed that birds took 27.6% $\pm$ 11.2 (mean $\pm$ sd) less time to reach the loft than predicted under pure pursuit. Note, however, the model does not account for variation in airspeed through the flight, because it uses the mean airspeed for each flight simulation. The simulations demonstrated that it is always possible to reach the loft using pure pursuit either when wind support is positive, or when the wind support is zero (pure cross wind or no wind) but the bird's airspeed is greater than the wind speed. However, the analysis presented in Figure 2.7 suggests that the birds are using a different strategy.

Deviated pursuit should theoretically allow the bird to compensate better for crosswinds if an appropriate deviation angle is selected. To assess whether the birds were using deviated pursuit, we analysed the relationship between predicted deviation angle (which would lead to a direct track between release site and loft, given the wind conditions) and the optimised deviation angle (the deviation angle that was found to best fit the observed GPS-track). The strength of these correlations gives an indication of how complete the drift correction is. At the Wytham hill release site we found a weak positive relationship between predicted and optimised deviation angles ($R^2 = 0.33$, $p < 0.001$, $n = 115$) with a slope that differs significantly from 1 (95% CI: 0.95, 0.53). The relationship is less clear for Kings Mill Lock release site ($R^2 = 0.19$, $p = 0.084$, $n = 32$) but again the slope is significantly lower than 1

(95% CI: 0.92, 0.17). The slope of less than 1 for both release sites indicates that if the birds are using deviated pursuit, they tend to select deviation angles that are smaller than required for perfect drift compensation.

2.4.3 Linear features analysis

Our results suggest that linear features may aid drift compensation when there is a positive crosswind (across the track from the right) at Kings Mill Lock. To demonstrate this, we first conducted a sign test on the edge alignment percentile, an indicator of linear feature following (see 2.3.5), for each site to test the hypothesis that the median edge alignment percentile was 50. We found no evidence for linear feature following at Wytham Hill (median edge alignment percentile = 54.5, sign = 59, n = 115, p = 0.67), but we did find evidence for linear feature following at Kings Mill Lock (median edge alignment percentile = 81.4, sign = 27, n = 32, $p < 0.01$). We subsequently set out to test whether this linear feature following was associated with the crosswind experienced by running a regression model on the proportion of the track that aligned with linear features against the mean crosswind for each flight (Figure 2.8A). Regression lines were fitted separately for both positive and negative crosswinds, as this relationship will depend on the availability of linear features in either direction from the track. We found that positive crosswinds (from the right) are strongly associated with the proportion of the track that aligns with linear features ($R^2 = 0.54$, $F(1,25) = 27.2$, $p < 0.001$) while negative crosswinds (from the left) do not show a significant relationship with linear feature alignment ($R^2 = 0.18$, $F(1,5) = 0.98$, $p = 0.39$). We cannot conclude much for negative crosswinds given the small sample size (n = 6). However, for positive crosswinds, the birds' tracks are more likely to align with crosswinds when the crosswind is stronger. This could be because the birds are using

the linear features to compensate for drift in high crosswinds, or it could simply result from landscape bias meaning they are more likely to be drifted over linear features with a strong wind from the right.

We found that the median proportion of linear feature alignment from simulated trajectories was not associated with positive ($R^2 = 0.01$, $F(1,25) = 0.2$, $p = 0.65$) or negative ($R^2 = 0.04$, $F(1,5) = 0.158$, $p = 0.71$) crosswinds (Figure 2.8B). This suggests that the result described above (Figure 2.8B) is not simply explained by the birds being more likely to drift over linear features in strong winds. The median proportion of linear feature following was determined from the 1,000 simulated deviated pursuit trajectories and is considered the null expectation for each flight. The simulations used evenly spaced deviation angles between the predicted deviation angle and a deviation angle of zero, described in 2.3.5.

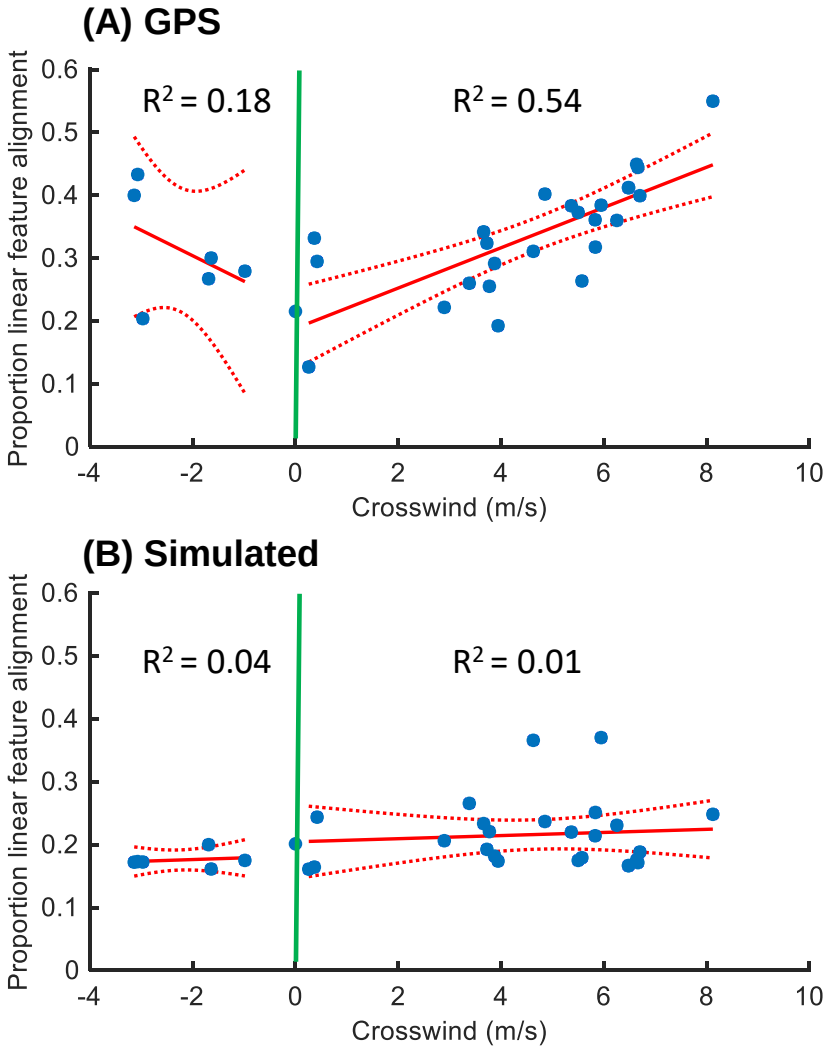

Figure 2.8 – Proportion of tracks aligning with linear features against crosswind experienced for 32 flights from Kings Mill Lock. Regression lines fitted with R^2 values shown separately for crosswinds coming from the right (right side of green line) and from the left. 95% confidence bounds are shown as red dashed lines. (A) Proportion aligning with linear features from GPS-derived tracks. (B) Median proportion aligning with linear features from simulated null trajectories using deviated pursuit (see 2.3.5).

2.5 Discussion

We investigated the visual mechanisms adopted by homing pigeons to correct for the effect of wind. The results indicate that pigeons are able to compensate for the effects of wind,

however, they do so imperfectly as their tracks are displaced in the direction of the crosswind experienced. While our simulations show that it is possible for birds to use a naive pure pursuit strategy to compensate for drift with no knowledge of the wind field, the birds tend to experience less lateral displacement than expected from this strategy. Our results also suggest that the birds may be using deviated pursuit but with too small a deviation angle that leads to only partial compensation. However, the weak fit of the predicted deviation angles to measured deviation angles may suggest that the birds are using a different mechanism. There is some evidence that linear features could help to augment drift compensation, at least for the Kings Mill Lock release site. Overall, our results highlight the complex nature of homing navigation and drift compensation, even when the target is in sight, and suggest that pigeons may flexibly use a range of visual cues depending on the wind field and the variety of cues available.

2.5.1 Pigeons are drifted less than expected by pure pursuit

Pure pursuit is the naive model for understanding how compensation for wind drift might be achieved. It requires continuous correction using information on the orientation of a single discrete target throughout the flight with no knowledge of the wind field or an external reference system, such as the sun compass. The pure pursuit model simulations above explain some variation in mean lateral displacement. However, at low crosswind speeds, birds tend to be displaced to a greater extent than predicted by the pure pursuit model, while at higher crosswind speeds, they experience less lateral displacement than predicted. At low crosswind speeds over the short distances flown here, the costs associated with incorrect drift correction are low and track variation is more likely to reflect other factors such as the navigational mechanism used, individual idiosyncrasies or predator

avoidance. The fact that the pigeons' tracks tend to be displaced less than pure pursuit at high crosswinds implies some knowledge of the wind. This could simply be learning from the drift experienced at the start of the flight to deviate the pursuit in the right direction, albeit not to the extent required to correct wind drift perfectly. The pure pursuit model presented here relies on the simplifying assumptions that the wind field remains constant throughout each flight and airspeed is not adjusted in response to wind. While we did not find any evidence for airspeed adjustments, adjustments over this scale may not be detectable using the course wind measurements used in this study.

2.5.2 Deviated pursuit

At higher crosswind speeds (>5 m/s), Figure 2.7 suggests that the birds are using a more effective mechanism to compensate for drift than pure pursuit. This could, in principle, be achieved by adding a deviation angle to their heading based on an estimate of the crosswind speed. However, we find only a weak correlation between predicted deviation angle (the angle which would lead to a direct track between release site and loft, given the wind conditions) and optimised deviation angle (the angle that was found to best fit the observed GPS-track) with a slope of less than one. This suggests that if the birds are using deviated pursuit, they are underestimating the deviation angle required to compensate fully for the wind, but the extent of under-compensation is not consistent between flights. Alternatively, the birds may not be using deviated pursuit in the simple form in which it has been modelled here and instead using a more sophisticated method of drift compensation. Our findings could also reflect the limitations of our model in capturing a flight using wind data averaged across the flight.

Our results do not allow us to differentiate between possible mechanisms for detecting lateral drift which could be used to estimate the best deviation angle to use. However, assuming that the birds in this study were motivated to take the most direct route back to the loft, our finding that trajectories are displaced in the direction of the wind suggests that information used to sense drift is imperfect. Given the reliance of pigeons on solar and magnetic cues for navigation (Wallraff, 2005), it is plausible that these play a role. If the pigeons in this study used only lateral optic flow to detect and compensate for wind drift, and did so near perfectly — as is observed in bumble-bees (*Bombus terrestris*) (Riley et al., 1999), this would have resulted in geographical tracks that were independent of wind direction. However, given that the crosswind analysis presented above shows that the birds in this study were laterally displaced by the wind, is it clear that this is not the case. The strength of optic flow cues will vary with altitude, and therefore the extent to which birds are able to use optic flow cues for drift compensation when flying at altitude is unclear and requires further investigation. Deviated pursuit is not the only mechanism that could be used to implement drift compensation using optic flow cues. For example, the birds could simply attempt to eliminate the component of translational optic flow perpendicular to their heading (Bhagavatula et al., 2011). In this case, the absolute value of optic flow, which varies with altitude, may not be of importance.

2.5.3 Linear features may aid drift compensation at Kings Mill Lock

Our results provide preliminary evidence that linear features, such as hedgerows, are used by pigeons to compensate for wind drift compensation as well as acting as a navigational aid (Figure 2.8). We found that when the crosswind was positive (blowing across the track from the right), the birds spent more time over linear features in stronger winds. Our results

suggest that this is not simply because the structure of the landscape leads them to be drifted over more linear features when wind blows from that direction as we found that simulated deviated pursuit tracks did not align with linear features to a greater extent in stronger winds. However, this result must be treated with caution as it assumes that the simulated trajectories are a plausible set of trajectories for the given wind speed. Nevertheless, there is one hedgerow in particular at Kings Mill Lock that appears to act as a bound for trajectories that have been drifted south or east relative to the beeline track (Figure 2.5). This could, therefore, be acting as a convenient visual measure of drift for birds from this site where instead of seeking the linear feature as a means of drift correction, the birds may follow a simple rule that tells them not to cross a linear feature from the direction of the lateral drift relative to their intended track that is sensed by some other means. Although it is not possible to conclusively determine whether linear features are aiding drift compensation from Kings Mill Lock, our analysis shows that it is either something that should be controlled for in future studies of drift compensation, or should be explicitly tested. However, designing such an experiment is problematic as it is difficult to manipulate the landscape or select release sites that make it possible to differentiate the track structure arising from drift compensation mechanisms from navigational mechanisms.

We found no evidence for linear feature following at Wytham Hill. The difference between release sites may reflect the difference in alignment of linear features with the intended track direction (seen clearly in Figure 2.5). Given that the loft was clearly visible from both release sites, linear features are unlikely to offer much navigational assistance. However, the Wytham Hill release site is elevated by 40 m relative to the loft which may mean that the loft is a more obvious initial target for the birds upon release, when compared with

Kings Mill Lock, leading to less reliance on other navigational cues. The difference in use of linear features between release sites may explain the different findings from the deviation angle analysis at each site; birds released from Kings Mill Lock in high winds may not use deviated pursuit because they have access to a different mechanism.

2.5.4 Limitations

Due to the complexity of the underlying navigation mechanism, it is not possible to infer precisely the intended flight track or ultimate motives of the birds, even when in sight of the loft. However, it is assumed in the analysis above, that the costs in terms of energy and time are significant enough, even over short distances, for pigeons to attempt to minimise lateral drift and that these adjustments are apparent from their ground track. The validity of this assumption is hard to test, but the poor fit of the data to the guidance models demonstrates either that the birds are using a different strategy, or that it is not possible to determine the relationship based on GPS-derived tracks. Additionally, we assume that the most direct route to the loft is always the most efficient but this might not always be the case. Our results highlight the limitations in reducing complex flight behaviours to simple guidance models. A further limitation of the guidance models used in this Chapter is that they assume that the bird is focussing on their target, the loft, at all times. In Chapter 5 we show that this assumption is unlikely to be true which may further help to explain the poor fit of the data here to the guidance models.

The largest source of error in the analysis presented in this chapter arises from the fact that wind was measured at the loft rather than along the track and treated as constant throughout the flight. Despite the short flight durations (~ 60 s), in reality the wind is likely to have varied considerable in speed and direction throughout the flight and may be substantially

different at the loft compared with the flight altitude of the bird. Without better quality wind data, discussed below in future directions, it is hard to develop the analysis of visual mechanisms far beyond that described here.

2.5.5 Future directions

Future studies of wind drift compensation in short range flights in birds should make use of higher quality, high frequency wind data in order to build a more detailed picture of the effect of flow on flight trajectories. This should also account for the altitude at which birds fly as flow can be laminar at high altitudes but highly turbulent near the ground with strong gusts that have a large effect on flight (Emily L. C. Shepard et al., 2016). In a laboratory setting, wind tunnels provide a convenient way to challenge birds to fly in a known airflow (Quinn et al. 2017). For free-flying birds, however, collecting data on airflow is more challenging. Data from onboard airspeed sensors (pitot tubes) can be combined with track data to provide an accurate estimate of the wind vector. These sensors have been used effectively in steppe eagles (Reynolds 2016) and Andean Condors (Williams et al., 2015). However, both these species have a body mass >5 times that of the pigeons used in this study and the sensors are not yet sufficiently miniaturised to be deployed on smaller birds (but see Takahashi & Shimoyama (2018) for recent developments). As a minimum, we recommend that future studies use a portable anemometer to measure wind conditions at the release site for comparison with the data collected at the loft.

The analysis presented here has shown that wind plays an important role in shaping the structure of homing pigeon trajectories and is a crucial factor to consider when interpreting ground tracks to infer navigational mechanism. As an example, when analysing the deflection of pigeon tracks released from the same release site used in this study (release

site 1 — Wytham Hill), Armstrong et al., (2013) concluded from releases over 3 days that this site biases the orientation of the pigeons in a generally clockwise manner, possibly due to the topography. The crosswind analysis presented above shows that from 16 days of releases from this site, the direction of lateral displacement can be largely explained by wind direction and no apparent bias was found. Historical wind data from Upper Seeds Weather Station (ECN meteorology data accessed July 2015) revealed that on all three release days used by Armstrong et al., there was a moderate westerly wind which is sufficient to account for the apparent 'release site bias' that the authors reported. Therefore, we recommend that future studies include wind in their analysis whenever they are concerned with the structure of trajectories.

At present, the development of robust control algorithms for flight in turbulent, high flow environments remains a major challenge for drone autonomy in GPS denied environments and bio-inspired visual algorithms are likely to play an important role in future developments. The insights gained from the wind compensation mechanisms employed by birds could, therefore, have great potential for the implementation of robust vision-based guidance algorithms in autonomous unmanned aerial vehicles.

Chapter 3. Instrumentation and data analysis

3.1 Abstract

The use of onboard sensors has become widespread in the study of bird flight to track the trajectory and dynamics of their flight. However, few researchers have attempted to use onboard devices to assess the sensory information available to birds. An understanding of the ways in which birds direct their visual system in order to extract visual information is an important prerequisite for an understanding of guidance and cognition. Therefore, the development of sensors capable of accurately recording gaze shifts during flight is an important goal with significant value. We developed a sensor combining a head mounted inertial measurement unit (IMU) and a back-mounted GPS receiver capable of recording bird head orientation and body position during flight in natural environments. This chapter describes the development of this sensor, the analysis of sensor data to draw biological insight, and validation experiments that aim to assess the performance of the sensor and the effect that it has on the behaviour of birds. While we find no detectable effect of a head-mounted sensor on flight performance, we highlight the need for further miniaturisation of future iterations of head-mounted devices.

3.2 Introduction

Most animals with advanced visual systems have one or more specialised regions of their retina with high visual acuity (foveae) that they shift to attend to visual targets using both head and eye movements (Land 2014). Visual attention can offer valuable insights into cognition and lead to a deeper understanding of complex behaviours in non-verbal subjects.

Eye-tracking has been used successfully as a technique to study visual attention in human and non-human primates for several decades (Kano and Call, 2014; Holmqvist et al., 2011). However, unlike primates, birds have limited eye mobility and therefore tend to use head movements to shift their gaze, aided by their light heads and highly flexible necks (Gioanni 1988). Laboratory studies have found that during walking and feeding, 80-90% of gaze shifts in pigeons are accounted for by head movements (Haque, 2004). A recent study tracking both head and eye movements in free-flying pigeons confirmed that eye movement is restricted to less than 5 deg during flight (Ivo Ros, pers. comm.). As a result, bird head orientation provides a good proxy for gaze direction and a number of laboratory-based studies have therefore measured only head orientation when studying the gaze strategy in birds (Friedman 1975; Erichsen et al. 1989; Stamp Dawkins 2002; Eckmeier et al. 2008; Fux & Eilam 2009; Kress et al. 2015; Ros & Biewener 2017). However, measuring head movements for freely flying birds in their natural environment is a significant technical challenge that has rarely been attempted (but see: Land 1999).

The miniaturisation of microelectronic sensors in recent decades has spurred new avenues of research, allowing animal-borne instrumentation to give fresh insights into their movement and behaviour. A rapidly growing body of research has adopted the use of these devices to study the dynamics of bird flight. The use of onboard GPS units to track bird flight paths has become common (Brighton et al., 2017; Wilmers et al., 2015; Freckleton and Iossa, 2010; von Hünerbein et al., 2001) and the use of accelerometers is becoming more widespread (Taylor et al., 2017; Williams et al., 2015; Portugal et al., 2014; Usherwood et al., 2011). However, the use of integrated inertial measurement units (IMUs) combining gyroscope and accelerometer sensors to study bird flight dynamics is still relatively uncommon (Kano et al., 2018; Reynolds et al., 2014; Gillies et al., 2008). A

significant proportion of the work undertaken in this thesis was contingent on the development of a head-mounted IMU designed to measure the head movement of pigeons (*Columba livia*) and peregrine falcons (*Falco peregrinus*) in free flight. This chapter will outline the rationale for using this equipment over other approaches, the technical details involved in the development of the sensor and an assessment of the device performance. We will also discuss the limitations and constraints surrounding the use of this instrumentation and quantify the effect that head-mounted sensors may have on flight performance in pigeons.

Past approaches adopted to study how birds direct and stabilise their gaze during flight have relied on ground video analyses of flight in natural environments (Land, 1999), head-mounted cameras (e.g. Kane & Zamani, 2014), or took place in closed flight arenas using high-speed cameras (Kress and Lentink, 2015; Eckmeier et al., 2008). While high-speed video footage in closed flight arenas allows the most precise measurement of head orientation during flight, this approach is limited to very short-range flight behaviours. The setup developed here allows gaze direction to be studied in free flight during guidance tasks outside the confines of a flight arena, allowing long-range flight behaviours to be studied. The sensor also has distinct advantages over head-mounted video data in that it does not require the analysis of unstabilised video footage. Unlike video data, where the field of view is limited to the lens being used, this sensor can capture information on the bird's entire visual field.

The instrumentation described in this Chapter was developed in collaboration with Fumihiro Kano of Kyoto University and was used to collect the data reported in Chapters

4 – 6 of this thesis. It was also used to collect additional pigeon data reported by Kano et al., (2018).

3.3 Instrumentation

The primary objective was to develop a sensor capable of simultaneously recording bird position and head movement during free flight. To accurately capture natural flight dynamics and behaviour, the sensors needed to have minimal effect on the subject to which it was attached. The main limitation in the design of animal-borne sensors is their weight and size. For flying animals, many studies apply the rule that the instrumentation must weigh less than 5% of the animal's body mass (Kenward, 2001). However, the evidence supporting the use of this arbitrary value is limited (Portugal & White 2018) and we made every effort to reduce sensor weight beyond this value. To capture the rapid head movements and detailed flight trajectories of the peregrines and pigeons in this study, we required the sampling frequency and logging capacity of the device to be sufficiently high which dictated the choice of sensor and microprocessor. While numerous commercially available devices containing a GPS and IMU exist, such as drone autopilot systems, the requirement here was to have a lightweight detachable sensor mounted on the bird's head with the logging unit mounted dorsally meaning that the device needed to be custom-built for this purpose.

3.3.1 Sensor hardware

We designed, built and programmed the head-mounted sensor and logging unit using commercially available electronics (Figure 3.1). The microcomputer (Adafruit M0 Feather, USA, New York), running an ARM Cortex M0 processor, was attached to a GPS receiver

(Adafruit MTK3339 GPS, -165 dBm sensitivity, 66 channels) along with a micro-SD card (32 GB; SanDisk, USA, California), and a LiPo battery (110 mAh, 3.7V). The 9-DOF inertial measurement unit (Adafruit BNO055 Absolute Orientation Sensor) contained a

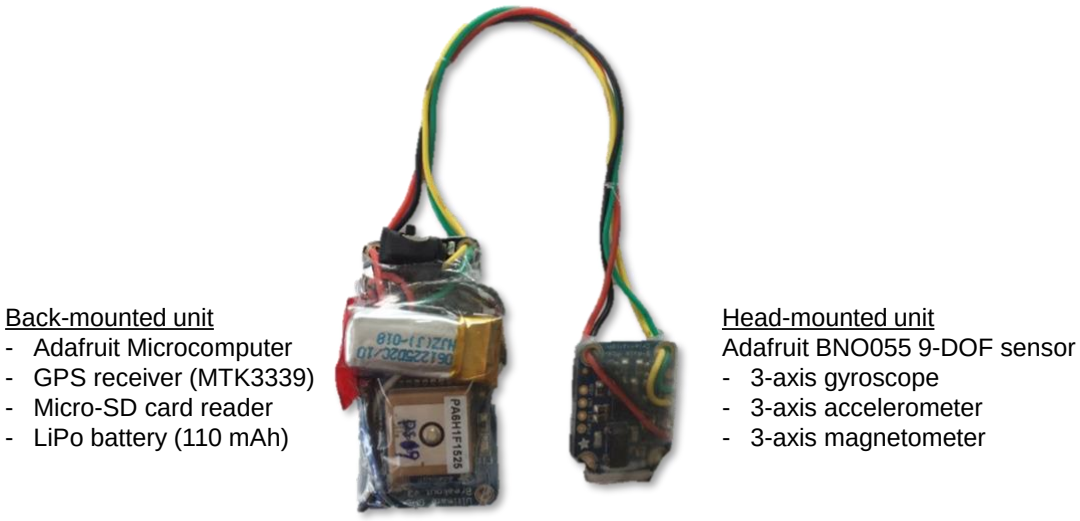

three-axis gyroscope, accelerometer, and magnetometer. The GPS receiver logged position data at 10Hz while the inertial measurement unit logged at 60 Hz. The sensor was connected to the microcontroller via four thin, flexible cables (28 AWG) with a length chosen to allow the sensor to be attached to the bird's head without restricting its movement (pigeons: 130 mm, peregrines: 180 mm). These cables were periodically replaced during experiments, or whenever sensor data became scrambled. The sensor cables were connected to the logging board via a plug which could be easily detached as a safety mechanism allowing the bird to detach the sensor if the wires were to get tangled.

Figure 3.1 – Complete onboard instrumentation unit with an inertial measurement unit (IMU) (right) attached via thin cables to the logging unit, GPS module and battery (left).

The device weighed 21.7 g, 1 g of which was the head-mounted unit, and had the physical dimensions: 120 × 21 × 8 mm. The head-mounted sensor was attached using 3M double

sided tape to a custom-built wire mask (3.6 g) for the pigeons (built by Fumihiro Kano) and a modified eye-less leather hood (4.9 g) for the peregrines (built by Martin Cray). The pigeon mask was constructed from thin wire covered in soft fabric, twisted to follow the outline of the bird's skull. The mask avoided contact with the bird's throat and instead was secured around the base of the beak meaning that it would not interfere with breathing. The GPS module and logging unit were carried in custom-built elasticated backpacks for pigeons, described in Chapters 2 and 4. For peregrines, the device was attached dorsally using Velcro to a 3D printed attachment (designed and built by Malcom Beard) to a removable harness with Teflon ribbon straps (Marshall Direct Ltd, Lancashire, UK), described in Chapter 6.

3.3.2 Data logging

The device was programmed using the open-source Arduino IDE (v1.8.5) to simultaneously log time-stamped IMU and GPS data to separate text files. The code was optimised to maximise the sampling rate of the board by logging only the minimum recommend GPS sentence output ($GPRMC). Altitude data were excluded as it was found from static tests to produce an unacceptably large error, as was found in previous tests of GPS performance (Reynolds 2016). The output from the log files is summarised in Table 3.1. The microprocessor board had two LEDS, one of which was programmed to flash at high frequency when the IMU data were logging successfully, and the other when the GPS had a satellite fix. Logged data were downloaded from the microSD card and imported into MATLAB (R2017b, Mathworks) for post-processing and analysis.

Sensor	Logged parameter	Unit	Sampling frequency
IMU	x,y,z acceleration	m/s^2	60 Hz
	x,y,z rate of angular rotation	deg/s	
	x,y,z magnetic field strength	µT	
GPS	Position	decimal degrees	10 Hz
	UTC time	hhmmss.ss	
	Satellite fix	binary	
	Doppler groundspeed	knots	
	Course	deg	

Table 3.1 — Summary of sensor measurements used in this study.

3.4 Data processing

3.4.1 GPS processing

As a first check for loss of satellite signal, GPS tracks were overlaid onto satellite images using Google Maps API (Bar-Yehuda, 2015) in MATLAB R2017b, Mathworks. No unexpected jumps in the position measurements were found in any of the tracks which would have resulted from the loss of satellite signals in any of the tracks. Latitude and longitude were then converted from decimal degrees to meters using a Universal Transverse Mercator projection for the given latitude. GPS data were then screened using an internal validation method for loss of precision by comparing the highly accurate Doppler shift groundspeed estimate against the noisier differenced groundspeed estimate, see methods described in Brighton et al. (2017).

3.4.2 IMU calibration and sensor fusion

While the microelectromechanical sensors used in the device detailed above offer a convenient means of state estimation for a range of applications, these sensors are only accurate if properly calibrated. Prior to each experiment, three calibration procedures

(outlined below) were performed allowing calibration data to be collected and used during post-processing. The gathering of calibration data for each sensor is described below.

For an ideal set of three orthogonal magnetometers with an equal gain and no magnetic field distortions, the length of the magnetic field vector should be constant in all directions. Therefore, the xyz components of the magnetic field vector will lie on a perfect sphere in the sensor board axes. However, both hard and soft iron distortions are caused by magnetic fields generated by ferromagnetic materials on or around the instrumentation unit leading the magnetic field vectors to form an ellipsoid. For the hard iron case, the magnetic fields generated are permanent leading to a sensor bias error. For the soft iron case, the materials generate a magnetic field that depends on its alignment with the Earth's magnetic field lines, and therefore causes a scale factor error (Renaudin et al., 2010). Distorted magnetic field vectors can therefore be transformed to lie on a sphere using a certain offset and scale factor (Caruso, 2000). Optimised offset and scale factors were calculated for each flight using methods and code adapted from Reynolds (2016). Prior to each flight, the sensor was rotated about all axes in an attempt to record the magnetic field vector in as many orientations as possible. This guaranteed that enough orientations were considered in the computation of the calibration offset and scale factors. For the pigeon experiments, which made use of a wire mask, this calibration was conducted with the mask attached to the sensor in order to account for ferromagnetic distortions arising from the mask. Calibrated magnetometer readings were subsequently used to estimate the board yaw direction. This first required corrections to be applied for the difference between true north and magnetic north (declination angle) and for the difference between the horizontal plane and the magnetic field vector (inclination angle) for the specific location.

Accelerometer readings are also affected by scale factor and offset errors. These can be accounted for using the same method described above for the magnetometer, but by assuming that an ideal set of orthogonal accelerometers will form a sphere of radius *g* (9.81 m/s^2) in the sensor axes. Unlike the magnetometer case above, the acquisition of accelerometer calibration data is done statically as the objective is to gather measurements of the gravity vector in all three accelerometer axes; movement of the sensor would record accelerations other than the gravity vector. A 3D printed cube was designed and built for this purpose (by Malcom Beard) with a slot for the sensor allowing it to be placed in each of the 6 orientations and held for 5 seconds. These static positions were automatically detected in MATLAB and transformed to a sphere centred at the origin with radius *g* using a scale factor and offset for each flight. These calibration variables were then used to transform the raw accelerometer data.

When integrated, angular rate data from gyroscope sensors can be used to estimate the state of the board if the initial attitude is known. However, gyroscopes suffer from random noise and systematic errors which can lead to large cumulative error and therefore are often fused with accelerometer data. To calibrate the gyroscopes, static tests were carried out for 1 minute prior to each flight to calculate the systematic error associated with each axis. This error was then subtracted from each flight. The offset was never more than ± 3.2 deg/s. Gyroscope readings are also known to drift over time due to temperature variations which was not accounted for here. However, the effect of this is unlikely to be significant over the range of temperatures (~10 deg – 20 deg) and logging durations (max 30 min) used in this study (Xia et al., 2009).

3.4.2.1 Sensor fusion

To determine the direction of the bird's gaze, the absolute orientation of the board (the board attitude) was estimated by fusing data from the inertial measurement sensors. This was done using a state-estimation algorithm based on an extended Kalman filter (EKF), designed for a drone autopilot and available open-source (Barton, 2012). The algorithm provides an estimate of the board attitude, expressed as Euler angles: roll, pitch and yaw. The version of the code used in this thesis was customised by Reynolds (2016) for a similar application. Some further modifications were implemented for the data analysed in this study to account for the magnetic inclination and different sampling rate. The extended Kalman filter iteratively predicts the Euler angles based on values from previous time steps which are updated with current observations from all three sensors. The performance of this algorithm is quantified below.

3.4.3 Sensor performance

The quantification of GPS error when studying bird flight dynamics has been reported on in great detail elsewhere (Brighton et al., 2017) and therefore here we only discuss a basic test to verify the reliability of this device under expected flight conditions. During testing, attempts were made to minimise GPS error by always allowing 5 min of sitting time for the device to acquire an accurate satellite fix before starting experiments. We also ensured that the patch antenna was not obscured and had a clear view of the sky by placing the antenna pointing away from the bird.

In order to benchmark the performance of both the GPS and IMU sensors, the device was mounted on a commercially available quadcopter (Phantom 4, DJI) to mimic some of the manoeuvres that the board was likely to experience when mounted on a bird during flight.

The device was attached using 3M tape to the top of the drone body (~8 cm above the drone's centre of mass). The drone was commanded to perform fast rotations (~200 deg/s, similar to bird head saccades) and sharp banks, which are known to negatively affect GPS accuracy (Reynolds 2016). The Phantom has a built-in GPS and IMU producing data which is fed into the drone's autopilot and used to control its attitude and position. While the exact nature of the algorithm used to filter and fuse GPS and IMU data for state estimation is proprietary, the estimated Euler angles and GPS position data are available to download from the drone after each flight (recorded at 10Hz). Given the impressive ability of this drone to hold its altitude and position, and to recover its attitude after sharp manoeuvres, it was assumed that these represent highly accurate estimates of the drone's state. A close correspondence between these values and those calculated independently using the device developed here using the extended Kalman filter would therefore give confidence in the methods used in this study. To minimise the effects of ferromagnetic distortions from the drone on our sensor, calibration data were collected using the methods described above after being mounted on the drone.

We found a close correspondence between the independent state estimates from the drone and our instrumentation giving confidence in the calibration procedure and sensor fusion methods detailed above. Figure 3.2 shows a 45 s sample of drone flight with time-matched yaw, roll and pitch data plotted for the Phantom drone (blue) and our instrumentation (orange). Data from our sensor was resampled at 10 Hz (down from 60 Hz) to correspond to the Phantom drone data and synchronised to the nearest 0.1 s by aligning accelerometer readings from the drone's initial take-off. In order to compare both signals, the correlation coefficient was calculated for all Euler angles over the section of flight shown in Figure 3.2 for corresponding points in time (yaw: $r = 0.998$, roll: $r = 0.947$, pitch: $r = 0.989$). The

yaw estimate from the IMU is particularly informative for determining head orientation in relation to visual features of interest.

The large discrepancy between estimates of roll between the IMU device and the Phantom could be due to the difference in placement of the in-built IMU of the Phantom (located near the drone's centre of mass) and the placement of the sensor mounted on top of the drone. Alternatively, this difference could have arisen if the Phantom sensor fusion algorithm is using a different Euler angle set (the axis rotation sequence used to fuse IMU data) to the ZYX (Yaw, Pitch, Roll) set used in the extended Kalman filter described above (Pio, 1966). Figure 3.3 shows a comparison of the GPS data for the same section of flight described above, again showing a high degree of correlation between data derived from the Phantom drone and that derived from our instrumentation (latitude: $r = 0.997$, longitude: $r = 0.997$). The documentation of both GPS devices states a 50% circular error probability of 3.0 m meaning that 50% of GPS readings fall within 3.0 m of the true position. Therefore, the <3 m discrepancy observed for all time points between the two GPS devices suggests that the GPS device on our instrumentation is performing well within the expected range of error. At 9.6 s, the Phantom and mounted sensor experience a large (~50 deg) change in roll (see second panel of Figure 3.2). However, this doesn't appear to have a noticeable effect on the discrepancy between position estimates of the Phantom and IMU device (see 'x' in Figure 3.3).

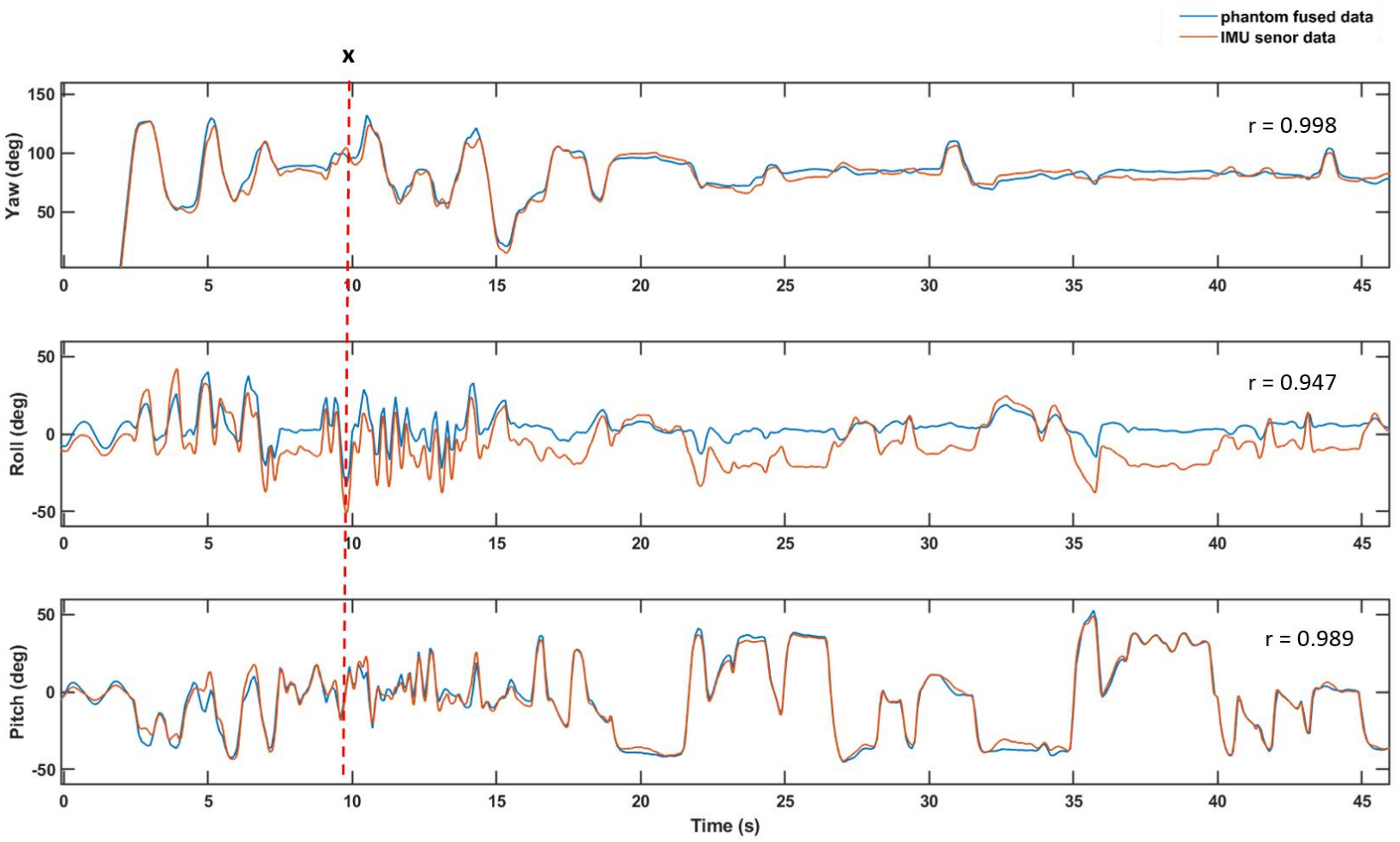

Figure 3.2 – Time-matched Euler angles from the Phantom drone plotted with the Euler angles derived from the IMU mounted on the Phantom for a 45 s sample of flight. The dashed red line corresponds to the time point 'x' in the Figure 3.3. Correlation coefficients (r) between the Phantom and device are shown for Euler angle.

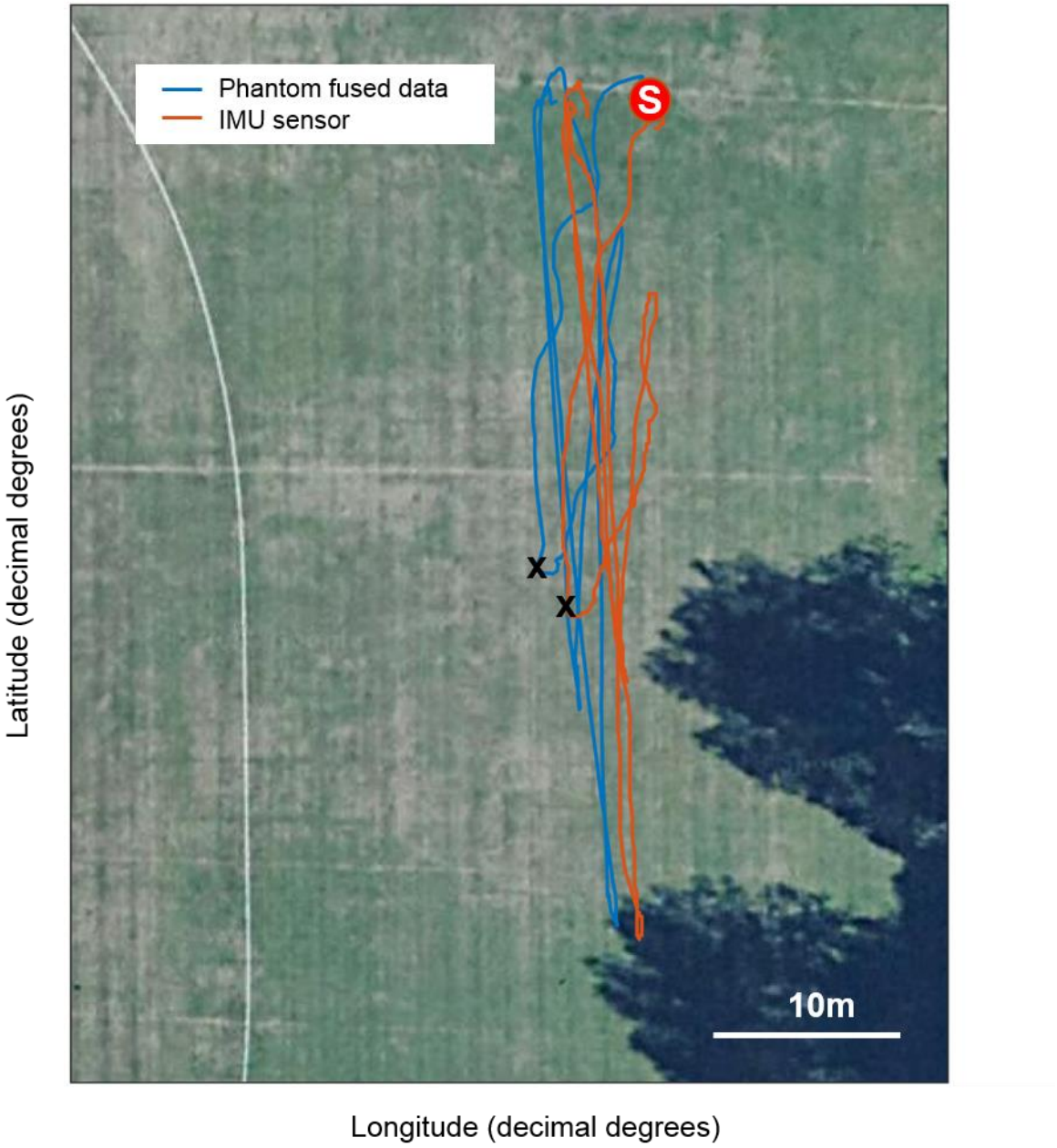

Figure 3.3 – GPS data from Phantom drone and IMU device mounted on the Phantom for a 45 s sample of flight. Flights are plotted in decimal degrees starting at the position marked 'S' onto satellite imagery (Google Maps, 2017). The point 'x' corresponds to the rapid change in roll from Figure 3.2 which results in no detectable change in the correspondence between GPS devices on the Phantom and our instrumentation.

3.5 Technique validation

3.5.1 Adverse effects of head-mounted instrumentation

A number of challenges exist when implementing onboard instrumentation to quantify animal behavioural dynamics. These challenges are particularly pertinent when the species in question place an evolutionary premium on being lightweight; birds have lightweight pneumatised skeletons and balance their energy intake with their body mass in order to maintain an optimum flying mass. The peregrines used in this study weighed between 750 – 952 g while the pigeons were 548 – 632 g. The total load of sensor, mask/hood, logging unit and backpack was therefore 4.4% of body mass for the smallest peregrine at its lowest flying mass and 5.1% of the body mass of the smallest pigeon. Given that this sensor is head-mounted, it is also important to consider the mass of the head-mounted unit relative to the bird's head mass. A study in herons found that head mass is 8-13% of body mass (Katzir et al., 2001) which, if true for peregrines and pigeons, would equate to approximately 7.5 g and 5.5 g respectively for the smallest birds. The sensor and mask/hood therefore add approximately 70% of mass to the bird's head that needs to be supported by its neck muscles. This is equivalent to an average man wearing a metal helmet weighing 3 kg and is therefore highly likely to have an effect on the bird's behaviour. This will result in changes in the centre of mass and centre of inertia of the bird's head and likely lead to differences in the rotational rate and amplitude of angular head saccades.

Aside from the effects of the instrumentation mass on the bird, the device is also likely to have further adverse aerodynamic and sensory effects on the bird. Aerodynamically, birds have specialised feather arrangements and the attachment of any instrumentation dorsally will disrupt air flow. This is particularly important for birds travelling at high speeds, such

as the peregrines used in this study. Head-mounting the sensor potentially leads to further aerodynamic challenges as it requires attachment via wires down the bird's neck. In addition, onboard instrumentation can also have an adverse effect on the bird's sensory perception when mounted on its head by impairing its vision, magnetoception, olfaction or auditory senses. All of these sensory modalities are thought to play some role in pigeon homing navigation (Wallraff, 2005) and therefore, if impacted by the sensor, could critically affect the bird's ability to orientate.

3.5.2 Quantifying the effect of a head-mounted sensor on flight performance

Despite the potential concerns detailed above, a number of relatively recent studies have used head-mounted devices on free-flying birds. These head-mounted devices include an eye tracker in pigeons (Ivo Ros pers. comm.), a video camera in falcons (Kane and Zamani, 2014) and an accelerometer in frigatebirds (Rattenborg et al., 2016). To assess the effect of head-mounted devices on flight performance, all of these studies relied largely on behavioural observations. However, Vyssotski et al. (2006), who attached a 7 g neurologging head unit to pigeons flying up to 22 km, described a more detailed assessment of the effect of the sensor. The authors reported no bird losses across their 26 subjects, and no abnormalities in either the structure of flight paths or in flight speeds. Vyssotski et al.'s experiment bears greatest resemblance to the experiments conducted in Chapters 4 and 5 and therefore offers some reassurance that head-mounted devices do not necessarily alter flight performance. However, we attempt a further validation experiment below.

We designed an experiment to test the effects on flight performance of mounting a sensor on a pigeon's head. Six birds were selected that had undergone the mask habituation protocol described above. All birds had experience flying in the local area and had been

released from the chosen release site (Wytham Hill: 51.774212 N, -1.322886 W) multiple times within previous days. Each bird was released twice from the release site on the same day. One release was conducted with the sensor mounted on the pigeon's head (H), using the custom fitted mask with the logging unit in an elasticated backpack, and the other with the sensor placed alongside the logging unit in the backpack on the body (B) with no mask attached to the head. The order of H and B treatments was randomised for each bird to reduce the effect of other factors that could vary systematically between releases such as wind conditions or presence of predators. Flight performance was quantified using three metrics: (i) route efficiency (using methods described in Chapter 2), (ii) GPS-derived groundspeed, and (iii) wingbeat frequency. Adverse effects on flight performance may manifest themselves in a reduction in groundspeed or route efficiency (Taylor et al., 2017): if the sensor has a negative effect on the bird's aerodynamics, we might expect a decrease in groundspeed, while a negative effect on sensory capabilities required for navigation may result in reduced track efficiency. The calculation of wingbeat frequency and its link to flight performance is discussed below.

Wingbeat frequency and amplitude are strongly related to the power required for flight (Pennycuick et al., 1996) and can be used as a proxy for energy expenditure (Usherwood et al., 2011). While it is not possible to compare wingbeat amplitude between H and B conditions, because the amplitude of head and body oscillations will vary due to sensor position, it is possible to compare the wingbeat frequency. Wingbeat frequency in pigeons is known to change in response to route familiarity (Taylor et al., 2017) and presence of conspecifics (Usherwood et al., 2011). Therefore, a significant change in wingbeat frequency may indicate an increased aerodynamic cost of transport. Accelerometer readings from the IMU allow wingbeat frequency to be calculated using established

methods (Taylor et al., 2017; Usherwood et al., 2011), see Chapter 4 for further details. Dorsal (Z-axis) accelerometer measurements were filtered and used to detect wingbeats from peak accelerations allowing wingbeat frequency (Hz) to be calculated for each wingbeat. Flight data were trimmed to include only the region between 800 m and 50 m of the loft, as in Chapter 2, to avoid abnormal wingbeats associated with take-off and landing.

3.5.3 No evidence for adverse effects on flight performance

We did not find evidence for a decrease in flight performance due to the head-mounted sensor using any of the metrics described above. Due to the low sample size (n = 6), the use of statistical tests was evaluated for this comparison of flight performance metrics using a power calculation for a paired sample t-test where $\alpha = 0.05$. For all flight metrics, the statistical power was too low to justify the use of statistics (wingbeat frequency: 0.101, velocity: 0.145, efficiency: 0.126) and instead the head and body conditions were compared graphically. Figure 3.4 shows that for the six birds tested at this release site, there was no obvious tendency for wingbeat frequency, velocity or route efficiency to increase or decrease when the sensor was mounted on the bird's head. These results suggest that the flight performance metrics may not be affected by the attachment of a sensor and mask to the bird's head. However, due to the small sample size these results must be treated with caution. While these results show that some flight performance metrics are not detectably altered by head sensor attachment, it is highly likely that other flight performance will be adversely affected in some way as discussed below.

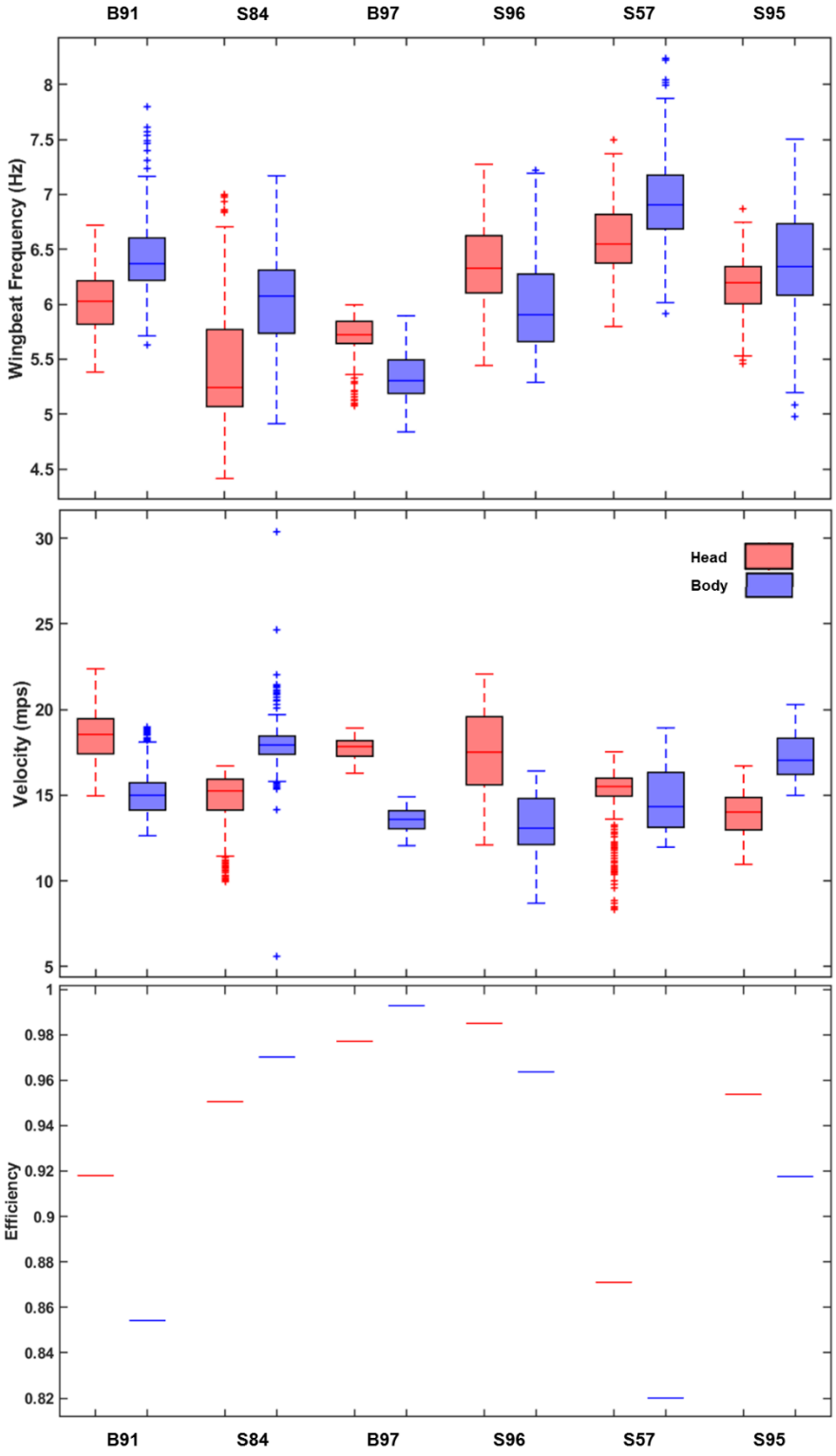

Figure 3.4 — Boxplots of wingbeat frequency, velocity and route efficiency for 6 birds each taking 2 flights from Wytham Hill, one with a sensor mounted on a mask on their head (red) and the other with the sensor attached to their body (blue).

3.6 Discussion

The device described in this chapter was used to record position and head orientation in over 200 flights of peregrine falcons and pigeons. The data extracted from the device is used in the following three chapters to characterise their gaze direction and visual stabilisation during target-directed tasks. Onboard sensors such as the technology described here have considerable potential in the study of bird flight dynamics. However, they present challenges in terms of the welfare and flight performance of the birds being tested.

While we found no significant difference in the flight performance metrics tested here, the attachment of any sensor will inevitably lead to changes in behaviour, many of which are hard to detect and quantify. The short flights used in the validation experiments described above (< 60 s), and throughout this thesis, may not be long enough to result in detectable differences in performance. We recommend that future experiments using head-mounted devices in birds should devise additional behavioural validation experiments that can better quantify the effect of the sensor on flight performance. As an example, the use of a motion capture system capable of tracking points at high frequency could be used to track points on the birds' heads with and without the head-mounted sensor. This would enable saccade characteristics to be compared between the conditions. However, motion capture technology is typically restricted to a laboratory context which limits the range of flight behaviours that can be tested.

The experiments conducted using the instrumentation described in this chapter were all approved by the Oxford University, Department of Zoology, Local Ethical Review Committee, and were considered not to pose any significant risk of causing pain, suffering, damage or lasting harm to the animals involved. Habituation protocols were devised for

the pigeons and peregrines used in this study (described in Chapters 4 and 6 respectively) allowing the behaviour of the birds to be closely monitored when initially wearing the head-mounted device. Once habituated, no significant differences in flight behaviour were observed for birds used in testing when fitted with the device and no new ethical issues were encountered.

3.6.1 Future directions

Future iterations of this technology should have animal welfare as their primary concern and aim to minimise the size and weight of any head-mounted units. Further miniaturisation of the electronics could be achieved by designing custom printed circuit boards to house the sensors and microprocessor. In addition, further improvements could be made to the head-mounting masks to make them more customised to each bird and to cause less sensory and aerodynamic disturbance during flight. The sensor sampling frequency could be increased by incorporating higher quality sensors and a microprocessor with more processing power. This would enable more precise measurements of wingbeat and head saccade characteristics. Given that GPS altitude was found to be unreliable, the device could be improved with the addition of a barometric altimeter. This would give a greater insight into vertical gaze location when combined with head pitch data from the IMU.

Gaze tracking has large potential in the study of a range of behaviours in birds besides flight control and visual guidance. As examples, previous studies have used visual attention to study sexual selection (Yorzinski et al., 2013), predator detection (Yorzinski and Platt, 2014) and foraging (Land 1999) . The head tracking technology developed in this chapter provides a relatively cheap and non-invasive method of obtaining data on visual attention for birds either in a laboratory setting or in their natural habitat. Refined iterations of this

technology could therefore lead to a deeper understanding of a range of visually guided behaviours in birds such as mating preferences, social cognition and the interrogation of new environments.

Chapter 4. Homing pigeons stabilise their gaze in relation to wingbeat timing and the presence of conspecifics

4.1 Abstract

Birds rely on stabilised visual cues to guide their flight, and therefore require the ability to eliminate the sensory clutter arising from flap-induced body oscillations. Unlike humans, birds have a limited range of eye movement and therefore visual stabilisation is facilitated by compensatory motion of the sophisticated avian head–neck system. While gaze stabilisation has been studied in laboratory settings in a range of bird species, little is known about how birds accomplish gaze stabilisation when flying in their natural environment. To address this, we fitted homing pigeons (*Columba livia*) with head-mounted inertial measurement units (IMU) and GPS loggers and released them from sites within their familiar area. This setup allowed us to characterise both angular and translational head movement during flight. By comparing the phase of rapid angular head movements (saccades) and wingbeats, we found that large saccades show a phase bias, i.e. they are initiated at a certain wingbeat phase. This is possibly to coordinate with wing occlusion of the visual field or to help guide flight manoeuvres. We found that vertical head stabilisation is enhanced when flying with conspecifics and that this is largely modulated by an increase in wingbeat frequency. This stabilisation may only be possible with the close visual stimuli provided by flock mates, but may also only be necessary when other conspecifics are near to avoid collisions and increase control. The avian head stabilisation mechanism described in this chapter could provide valuable inspiration for the design and tuning of image stabilisation systems in autonomous flapping drones.

4.2 Introduction

Flapping flight provides birds with an effective means of locomotion, but the rapidly alternating forces cause their bodies to experience extreme angular and translational displacement (Warrick, 2002). Birds primarily rely on visual information to guide their flight and therefore require their visual system to be stabilised relative to their surroundings. This stabilisation is required to simplify visual processing by minimising motion blur and separating the rotational from translational components of optic flow (Eckmeier et al., 2008). This is vital for a manoeuvring bird as translational optic flow produced by self-motion can be used to estimate important spatial parameters, while optic flow experienced during rotational self-motion cannot. Therefore, without image stabilisation mechanisms, birds would have difficulty differentiating the motion of a target or obstacle from head or body motion and would not be able to hold their gaze on close-range objects such as flock companions.

The gaze strategy of most birds is saccadic, with periods of fixation punctuated by rapid rotational shifts in head orientation (Land 2014). This strategy separates rotational from translational movement during locomotion which facilitates the extraction of spatial information from the visual input (Kress and Egelhaaf, 2014). Laboratory experiments on restrained pigeons have revealed that gaze stabilisation is achieved by combining cues from the visual system (via optic flow cues), vestibular system (via semi-circular canals) and proprioceptive system (via cervical mechanoreceptors; Gioanni 1988a; Gioanni 1988b) . A number of experiments have demonstrated that visual signals are by far the most important, generally overruling conflicting signals from other sources (Frost, 2009; Friedman, 1975). This visual information is used to control reflexes that lead to compensatory movements of

the eyes or head that limit retinal slip and therefore minimise visual blur (Gioanni and Vidal, 2012; Wallman and Letelier, 1993). While visual stabilisation can be accomplished through both head and eye movement, birds have limited eye mobility (Gioanni 1988a; Land 1999) and instead exhibit an impressive ability to stabilise their head with respect to the horizon using cervical reflexes. Optical nystagmus (involuntary eye movements) have been found to contribute very little to gaze stabilisation in body restrained pigeons (Gioanni 1988a) and show less that 5 degrees of eye movement during flight (Ivo Ros, pers. comm.). This finding has led researchers to focus on head movement when studying gaze stabilisation in birds and neglect eye movements for methodological convenience.

Laboratory-based experiments, using high-speed video to track head movements, have observed rotational head stabilisation in free-flying zebra finches (*Taeniopygia guttata*) (Eckmeier et al., 2008), lovebirds (*Agapornis roseicollis*) (Kress et al. 2015), and pigeons (Ros and Biewener, 2017; Warrick, 2002; Davis and Green, 1988; Bilo et al., 1985). This indicates the importance of rotational stabilisation for flight control. A recent study using head-mounted inertial measurement units (IMUs) to track pigeon head movements also found that pigeons stabilised their head with respect to the environment in all three axes of head rotation when flying in their natural environment (Kano et al., 2018). This chapter aims to extend the work by Kano et al. using the instrumentation described in Chapter 3 to investigate: (i) the coordination between pigeon wingbeat and angular head saccade timing, and (ii) the modulation of translational head stabilisation in response to close visual stimuli (i.e. their flock companions). Specifically:

(i) Given the disruptive motion caused by flapping, it is reasonable to expect birds to time periods of gaze fixation, when visual information is extracted, with periods of the wingbeat

phase associated with the least visual clutter. The timing of angular head saccades relative to wingbeat phase has previously been studied in a laboratory setting in pigeons (Ros and Biewener, 2017) and lovebirds (Kress et al. 2015) during rapid turning manoeuvres. Both studies identified wingbeat kinematics and head saccades by tracking points on the birds' heads and wing tips. They found that head saccades are consistently initiated at the end of the wingbeat downstroke, or at the downstroke-upstroke transition. This study aims to explore the phase relationship between wingbeats and head saccades, for the first time, in birds flying at high speed in their natural environment. We achieve this using a head-mounted accelerometer and gyroscope.

(ii) Vertical head stabilisation has been well studied in humans (Paddan and Griffin, 1988; Pozzo et al., 1990) and has received some research attention in stationary, walking and landing pigeons (Theunissen and Troje, 2017; Necker, 2007; Troje and Frost, 2000; Davies and Green, 1988), but has been under studied for birds during flight. However, one recent study (Pete et al., 2015) used high-speed videos of swans flying over a lake to track head and body displacement to find that a swan's neck passively attenuates flap-induced body oscillations. The authors concluded that birds tune the stiffness of their neck muscles to stabilise their head throughout flight. In another recent study (Taylor et al., in review), which found that pigeons increase their wingbeat frequency when flying in pairs, the authors suggested that increasing wingbeat frequency may be a mechanism to enhance visual stability. This is because increased wingbeat frequency leads to a reduced amplitude of translational body (and head) motion. Unlike rotational stabilisation, which is important when attending to objects at any distance, translational stabilisation becomes more important the closer the visual cues are to the bird. Therefore, when flying alongside conspecifics, translational stabilisation is essential to reduce motion blur and minimise

motion parallax. The stabilised visual information received on flock companions is then required for coordinating group dynamics and hierarchies. In this study, we used head-mounted accelerometers to explore the precise relationship between wingbeat frequency and vertical head displacement. This allowed us to directly test Taylor et al.'s hypothesis that flying in pairs requires increased head stabilisation by comparing head displacement when pigeons were flying solo or with flock mates. This method allowed us to explore translational head stabilisation when different levels of close-range visual information are available.

This chapter presents the findings from these two research goals and discusses the implications for both the mechanism and function of visual stabilisation in birds.

4.3 Methods

4.3.1 Subjects

We selected 20 homing pigeons, aged between three and ten years old, for experimentation from a flock of approximately 140 birds bred at the Oxford University Field Station, Wytham (51.782872 N, -1.317358 W). Birds were selected based on their weight, with the largest birds chosen in an attempt to minimise the effect of sensor load on their flight performance; the birds weighed 589 ± 32 g (mean ± sd). All birds had experience flying within 5 km of the home loft and took part in group training releases from the North, South, East, and West of the loft at the start of the season.

4.3.2 Instrumentation

We designed, programmed and built a device to simultaneously record pigeon position and head movement during flight (see Chapter 3 for a detailed description of the device). The

device recorded synchronised GPS data at 10 Hz and IMU data at 60 Hz. The IMU was mounted using double-sided 3M tape on a custom-made wire mask (built by Fumihiro Kano of Kyoto University) that had been designed to fit each bird's head (Figure 4.1) while the GPS logger, SD card, battery, and microcomputer were placed in an elasticated backpack. The instrumentation weighed 21.7 g, and therefore when added to the mask and backpack totalled 27.1 g, constituting 4.9 % of the smallest bird's body mass. We built six devices, allowing up to six birds to be used in each release.

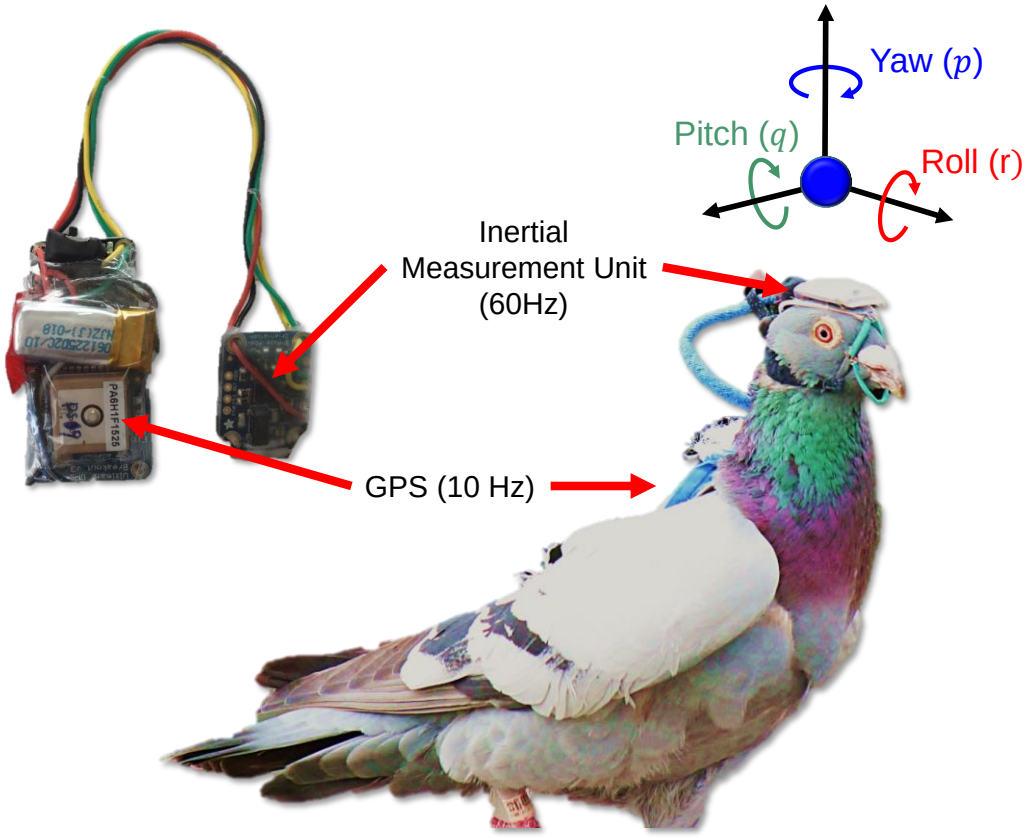

Figure 4.1 — Head-mounted Inertial Measurement Unit (IMU) glued to a custom-made wire mask connected via a blue cable to the back-mounted unit containing a GPS, battery and microprocessor. The three axes of rotation of the board (yaw, roll and pitch) are shown above the bird's head.

4.3.3 Habituation protocol

All 20 birds were fitted with an elasticated backpack for the GPS and logging unit that they wore for the season. Dummy loggers made from Plasticine were placed in the elasticated backpacks when the birds were not being used for experiments and masks were fitted at the start of each day of experimentation. The birds were habituated to wearing the custom-made mask for at least seven days prior to flight testing according to a protocol approved by the University of Oxford's Zoology Animal Welfare Ethical Review Board (No. APA/1/5/ZOO/NASPA/Biro/ PigeonsHeadmountedsensors). For each day of habituation, the bird was fitted with a mask matching its head size (small, medium or large) and carefully monitored for two hours within its home loft for signs of discomfort and abnormal patterns of locomotion. These signs included frequent head shaking, scratching the mask, removing the mask, abnormal flying, or abnormal walking. Two birds were dropped from the study because they still showed rapid head shaking with the mask on after two days of habituation. If, after seven days of habituation in the loft, the birds no longer attempted to remove the mask and did not show signs of vigorous head shaking, they were released outside the loft and allowed to fly freely under close observation. Four further birds were excluded from the study at this stage after showing abnormal flight with occasional head shaking or taking longer than thirty min to enter the loft after being released. The remaining 12 birds showed no signs of abnormal flight behaviour and were used for subsequent experiments. An analysis of the effect of the sensor on flight performance can be found in Chapter 3.

4.3.4 Release sites and testing

All flights in this study were conducted between June and September 2017 from three release sites within 3 km of the home loft (51.782872 N, -1.317358 W), see Table 4.1. The selected release sites were all familiar to the birds, in different directions from the loft, and surrounded by different landscape features in an attempt to remove any bias associated with a particular release site. Releases were only conducted during low wind (<5 m/s) and when the sun's disc was visible to minimise the chances of losses; no bird took more than an hour to return home to the loft across all releases in this study. Each day of testing, the participating birds were fitted with a mask and allowed to habituate to wearing it in the home loft before being transported by car to the release site. At the release site, the sensor was turned on at least 5 min prior to release to allow the GPS to acquire a satellite fix and to conduct the IMU calibration procedure described in Chapter 3. We released all six focal birds three times on the same day: once solo, once in a pair with a non-focal individual and once in a group of non-focal individuals. The order of release type (solo, pair, group) was randomised for each bird. Group releases were conducted with 8-11 other individuals.

Site	Latitude	Longitude	Bearing to loft	Distance to loft (m)	Number and type of flights
Wytham Hill	51.774825 N	-1.321878 W	19.4°	950	43 solo 6 pair 6 group
Swinford	51.771819 N	-1.353634 W	53.4°	2983	33 solo
Port Meadow	51.780972 N	-1.291521 W	273°	1785	12 solo

Table 4.1 — Release sites used in this study with a total of 100 flights of focal birds recorded across 12 birds.

4.3.5 Data processing and analysis

All raw IMU data were plotted in MATLAB (R2017b, Mathworks) for visual inspection each day after importing from the SD card. On three occasions, the IMU data were found to be scrambled and was discarded due to damaged cables connecting the logging unit to the board. Once these cables connecting the IMU to the logging unit had been replaced, the issue was instantly resolved. GPS data were overlaid onto satellite images using Google Maps API (Bar-Yehuda, 2015) in MATLAB for preliminary inspection. The data were then screened using an internal validation method for loss of precision by comparing the highly accurate Doppler shift groundspeed estimate against the noisier differenced groundspeed estimate using methods described in Brighton et al. (2017). This resulted in the exclusion of two flights from subsequent analyses where parts of the flight showed large discrepancies between Doppler and differenced groundspeeds. The GPS data were cropped to only include sections where the bird's Doppler groundspeed was greater than 5 m/s to exclude take-off and stationary flight, and sections where the bird was more than 50 m from the loft, to exclude circling flight at the loft.

4.3.5.1 Wingbeat timing analysis

Accelerometer data from the head-mounted IMU was used to calculate the wingbeat phase using established methods (Taylor et al., 2017; Portugal et al., 2014; Usherwood et al., 2011). Vertical (Z-axis) accelerometer measurements (Figure 4.2A) were smoothed by taking a running mean over five datapoints (0.083 s) and then filtered using a fourth order high-pass Butterworth filter with a cut-off frequency of 1 Hz (less than 25% of the wingbeat frequency) (Taylor et al., 2017). Head vertical velocity (Figure 4.2B) was calculated by integrating the vertical accelerometer measurements (Usherwood et al., 2011). Each

wingbeat was automatically detected using peaks in head vertical translational velocity with a minimum velocity of 0.3 m/s and a minimum distance of 0.08 s to the previous peak. Note that the peaks in translational velocity of the head (orange dots, Figure 4.2B) do not need to relate to any particular wingbeat kinematic to give information on wingbeat frequency and phasing (Portugal et al., 2014). However, we made use of findings from Ros & Biewener (2017) that pigeon translational head velocity had a consistent minimum occurring in the early downstroke, and a maximum occurring at the downstroke-upstroke transition, to estimate the wingbeat kinematics (timing of upstroke and downstroke) for our birds (see red shaded regions of Figure 4.2). This assumed relationship between wingbeat phase and head speed is in alignment with supplementary analysis from Taylor et al. (in review) that showed mathematically that the body's upwards acceleration peaks in the first half of the downstroke. It is also supported by Pete et al.'s (2015) finding in whooper swans (*Cygnus cygnus*) that the head lags the body phase by $\pi/2$ (see orange circles in Figure 4.2A). The wingbeat frequency (wingbeats per second; Hz) was calculated for every wingbeat using the wingbeat period identified as the time between vertical velocity peaks (mean wingbeat frequency = 6.5 Hz for the example flight section in Figure 4.2). Vertical head displacement (the oscillatory vertical translation of the head due to flapping) was calculated by integrating the vertical velocity described above to find the peak-to-peak vertical displacement of the head for each wingbeat (i.e. double the vertical head amplitude).

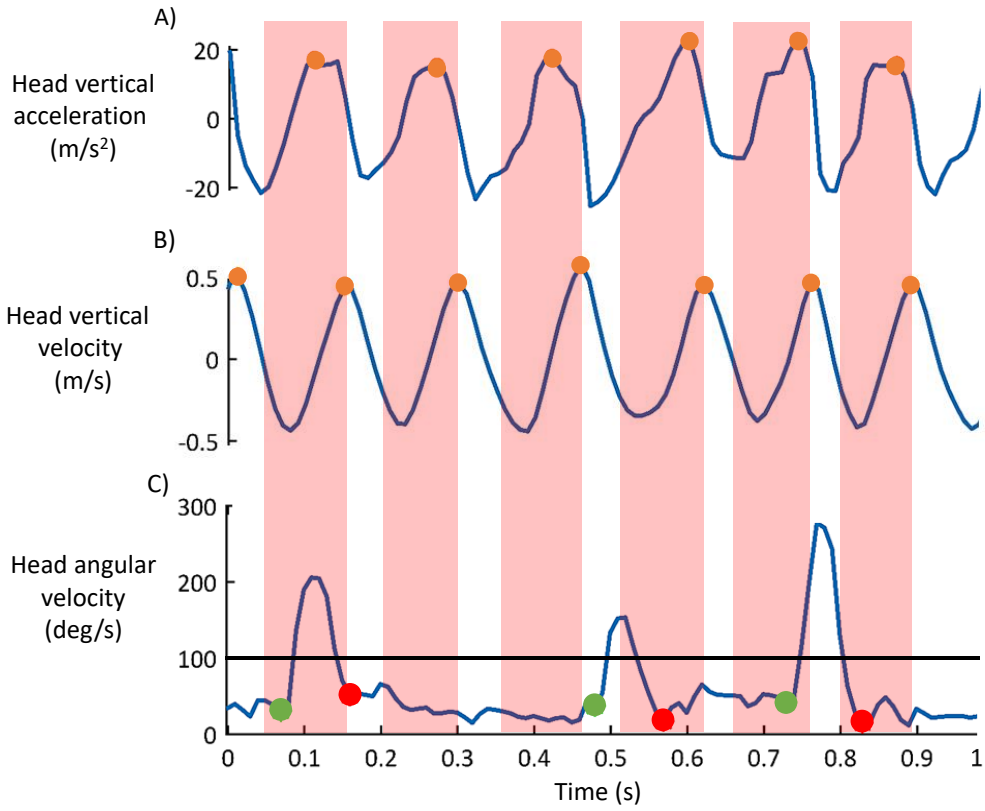

Figure 4.2 – Example of saccade and wingbeat analysis using gyroscope and accelerometer readings from the head-mounted IMU for 1 second of flight. (A) Vertical (Z-axis) head accelerometer data with peaks shown in orange. (B) Vertical translational velocity (integration of accelerometer data), again with peaks in orange used to identify wingbeats. (C) Combined (yaw, roll & pitch) head angular velocity from gyroscopes used to detect saccades (4.3.5.2). Start and end points of the saccades are labelled with green and red dots respectively. The 100 deg/s cut-off threshold is shown as a horizontal black line. (A-C) Estimated wingbeat downstroke timing (red shading) is displayed with reference to head vertical translational velocity based on observations from Ros & Biewener (2017). Upstrokes are unshaded.

4.3.5.2 Saccade identification

Gyroscope readings from the head-mounted IMU were used to detect head saccades. Saccades were defined as head rotations exceeding 100 deg/s for a duration of over 30 ms (Figure 4.2C). This definition is in line with previous studies addressing rotational head movements in free-flying birds (Kano et al., 2018; Kress and Egelhaaf, 2014; Eckmeier et al., 2008). Note that the head-mounted IMU recorded the pigeons' head movements with

respect to an inertial reference frame rather than the bird's body reference frame and therefore the gyroscope could also record body turns. However, given the threshold angular speed of 100 deg/s, a body turn would only be erroneously classified as a saccade if the pigeon (flying at 16 m/s – their average flight speed) had a turn radius of less than 8.5 m. While it is unlikely that many body turns would have a such a small turn radius, particularly for the direct homing flights recorded here, it remains a possibility that small bounding turns were detected as saccades. Saccades were first detected and analysed by considering each component of the angular velocity separately (yaw (p), pitch (q) and roll (r) rate — Figure 4.1), and then using the norm of the angular velocity: $\sqrt{\mathrm{p}^2 + \mathrm{q}^2 + \mathrm{r}^2}$. The start and end points of each saccade were defined as the first point before and after the saccade peak angular velocity where the derivative of the angular rate was zero (Figure 4.3C), i.e. where the angular acceleration changes direction. The amplitude of each saccade was estimated by integrating the angular rate between saccade start and end points.

4.3.5.3 Saccade timing analysis

We analysed the saccade and wingbeat phase by comparing the timing of identified peaks in vertical velocity data (from the accelerometer) with the saccade start and end points (from the gyroscope). For each saccade start and end point we calculated the wingbeat phase (φ) which varied between 0 and 2π rad, where $0/2\pi$ corresponds to a peak in vertical velocity (orange dots, Figure 4.2B). Each peak in vertical head velocity corresponds approximately to the wingbeat downstroke-upstroke transition (Ros and Biewener, 2017). Circular statistics were applied using MATLAB to analyse phase data using the CircStat toolbox (Berens et al., 2009). Finding no satisfactory and easily interpretable measure of effect size (the extent of departure from circular uniformity), we developed our own

measure *C*. This is calculated as the area of each histogram that lies outside a normalised uniform circular distribution (blue area, Figure 4.4) as a proportion of the area of the normalised uniform circular distribution (red area, Figure 4.4). If the distribution has a perfect circular uniform distribution, *C* will be 0. The greater the departure from circular uniformity, the larger the value of *C*.

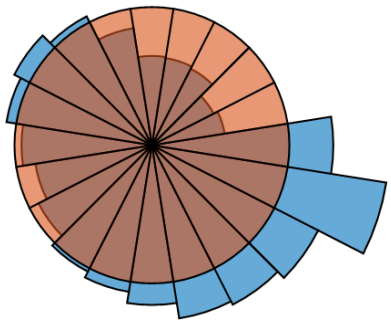

Figure 4.4 – Example of circular uniformity effect size calculation (*C*). The blue circular histogram is the distribution to be analysed and the red circular histogram is the normalised circular uniform distribution. This results in $C = 0.12$.

4.4 Results

4.4.1 Saccade-wingbeat timing

In accordance with previous findings (Kano et al., 2018; Ros and Biewener, 2017), pigeons were found to move their heads in a saccadic manner, with periods of fixation punctuated by rapid rotational movement. We pooled all saccades detected from 12 birds over 88 solo flights from three release sites to describe the timing of saccades and wingbeats. We found that pigeons initiate head saccades shortly before peaks (0 rad) and troughs (π rad) in head vertical velocity during wingbeats (probably coinciding with the downstroke-upstroke and upstroke-downstroke transitions respectively). However, larger saccades (> 20 deg) were

preferentially initiated only before peak head vertical velocity (the downstroke-upstroke transition). Figure 4.5A shows these data pooled for all saccades across all flights binned by saccade amplitude (θ). Four bin widths were arbitrarily chosen at 10 deg intervals; note the large difference in number of saccades within each bin. The Omnibus test (also known as the Hodges-Ajne test; Pycke 2010) was applied to test for circular uniformity rather than the Rayleigh test as it makes no assumptions about the underlying distribution; the Rayleigh test assumes that if there is a departure from the null hypothesis, that departure has a single peak. The Omnibus test found a significant departure from randomness in the saccade-start wingbeat phase ($m = 21353$, $p < 0.0001$) as well as for each of the four amplitude bins ($p < 0.0001$ for each group). The effect size (C), is shown for each circular histogram in Figure 4.5, where 0 is a circular uniform distribution and larger values represent a greater departure from circular uniformity. Figure 4.5 clearly shows that saccades of different sizes show different phase distributions with wingbeat timing; larger amplitude saccades show a stronger tendency to start and end at a particular wingbeat phase.

A parametric Watson-Williams multi-sample test for equal means (the circular analogue of a one-factor ANOVA) found that at least one amplitude bin group comes from a population with a different mean phase ($F(4,33262) = 208$, $\eta^2 = 0.011$, $p < 0.0001$). The eta squared (η^2) value of 0.011 shows that 1.1% of the total variance in phase is associated with bin grouping. This was true for pairwise comparisons of each adjacent amplitude grouping except $20 \text{ deg} < \theta \leq 30 \text{ deg}$ and $\theta > 30^{\circ}$ which were found to share a statistically indistinguishable mean phase ($F(2,1247) = 3.50$, $\eta^2 = 0.0015$, $p = 0.062$). This suggests that saccades with amplitudes over 20 deg do not differ significantly in their saccade-start wingbeat phase. Saccades were also categorised by the axis of head rotation (yaw, pitch or

roll – Figure 4.1) but were not found to differ significantly in the saccade-start wingbeat phase ($F(2,33262) = 1.31$, $\eta^2 = 1.2 \times 10^{-4}$, $p = 0.12$) or saccade-end wingbeat phase ($F(2,33262) = 2.13$, $\eta^2 = 2.9 \times 10^{-4}$, $p = 0.093$). Despite the low p values, given the large sample sizes, this test makes it clear that yaw, pitch and roll saccades do not vary significantly in their phase.

The mean saccade duration was 0.09 ± 0.019 s (mean ± sd) which was 68 ± 13 % of each wingbeat. Figure 4.5B reveals the pattern of saccade endpoints within the wingbeat which show similar departures from circular uniformity ($m = 16543$, $p < 0.0001$) but with larger spread and a shift in phase relative to the saccade start. For saccades over 20 deg, where the saccade start and end phases are unimodal, this results in a phase of the wingbeat with a lower probability of head saccades (i.e. a period of fixation). This is seen clearly in Figure 4.6 which displays the probability of a saccade occurring across 10 bins in the wingbeat phase for wingbeats which coincide with large (> 20 deg) saccades. This was derived from the number of saccades that occurred at each bin (fell between start and end points of a saccade) and the total number of saccades identified that occurred within wingbeats. The figure shows that pigeons are twice as likely to make large angular head movements at the start of the upstroke than they are at the mid-downstroke.

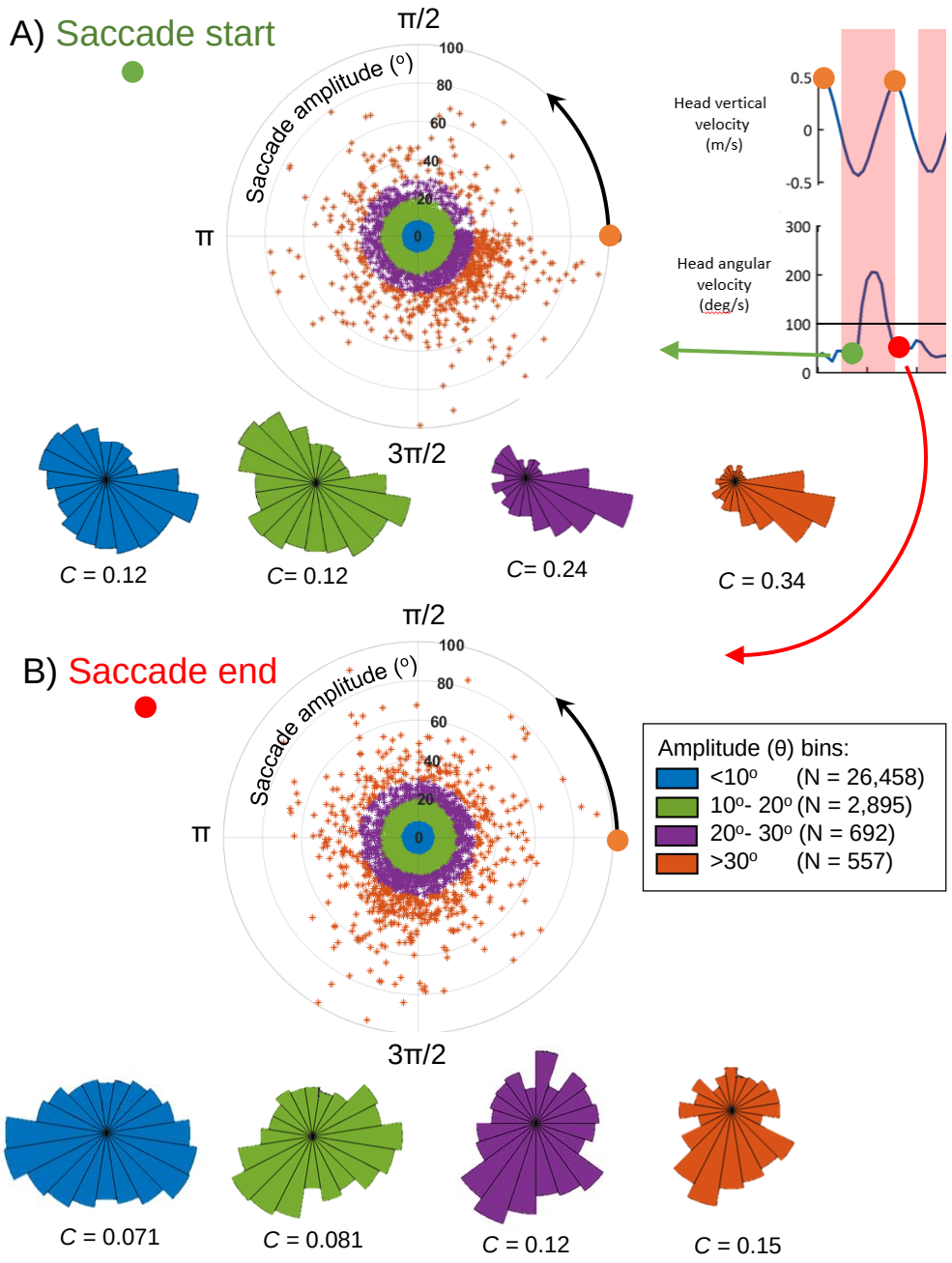

Figure 4.5 — Saccade start (A) and end (B) wingbeat phase binned by saccade amplitude for 30,602 saccades pooled across 100 flights by 12 birds. Section in top right taken from Figure 4.2 shows one saccade occurring in a wingbeat with saccade start (green), end (red) and peak vertical velocity from wingbeats (orange). Polar plots show the distribution of saccade phase within a wingbeat between 0 and 2π, where 0 is the vertical velocity peak per wingbeat (and assumed downstroke-upstroke transition Figure 4.2). Plot radius indicates the saccade amplitude and colours represent the four amplitude bins. The eight circular histograms represent saccade-wingbeat phase binned by saccade amplitude using the same colour scheme and the same axes as the polar plots from 0 to 2π. *C* values are given for each plot to show the extent of circular uniformity (Figure 4.4).

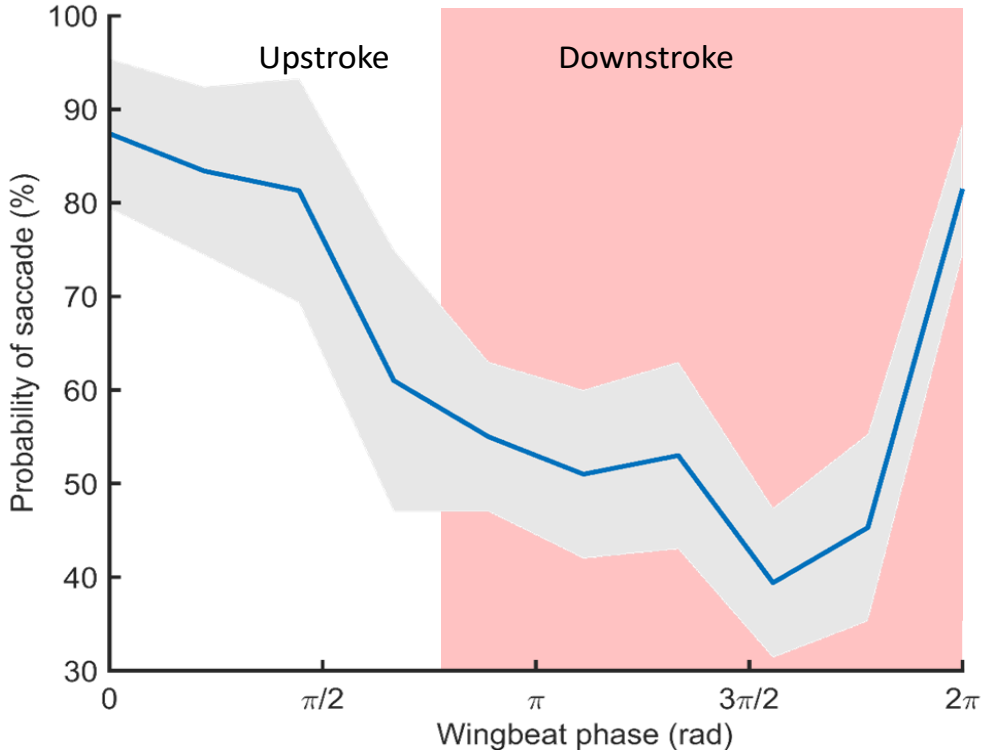

Figure 4.6 – The probability of a saccade occurring across a wingbeat phase for large saccades (over 20 deg), N = 3587 saccades. Solid blue line shows the average probability that a saccade is occurring in each of 10 wingbeat phase bins across the 12 birds, the grey shaded area is the standard deviation. Wingbeat phase measured relative to vertical velocity peaks. Estimated wingbeat downstroke (red shading) and upstroke timing is displayed with reference to head vertical translational velocity based on observations from Ros & Biewener (2017).

4.4.2 Head displacement analysis

We found that during flight, pigeon's heads experience flap-induced vertical oscillations with a peak-to-peak vertical displacement of 0.018 ± 0.005 m (mean ± sd). We found that this vertical head displacement is reduced when flying in pairs or groups. Figure 4.7 demonstrates the effect of release type (solo, pair and group) on vertical head displacement for six birds, each of which flew one flight solo, one with a pair and one in a group on the same day. This relationship was analysed using a linear mixed effects model testing the

effect of release type on median peak-to-peak vertical head displacement across six birds including bird ID as a random factor. We found that release type significantly predicts peak-to-peak head displacement ($\chi 2$ (1) = 45.24, $p < 0.0001$) with paired flight and group flight decreasing displacement by 5.3×10^{-3} m ± 6.6×10^{-4} and 7.7×10^{-3} m ± 6.6×10^{-4} respectively compared with solo flight. The p-value was obtained using a likelihood ratio test for a model with and without release type.

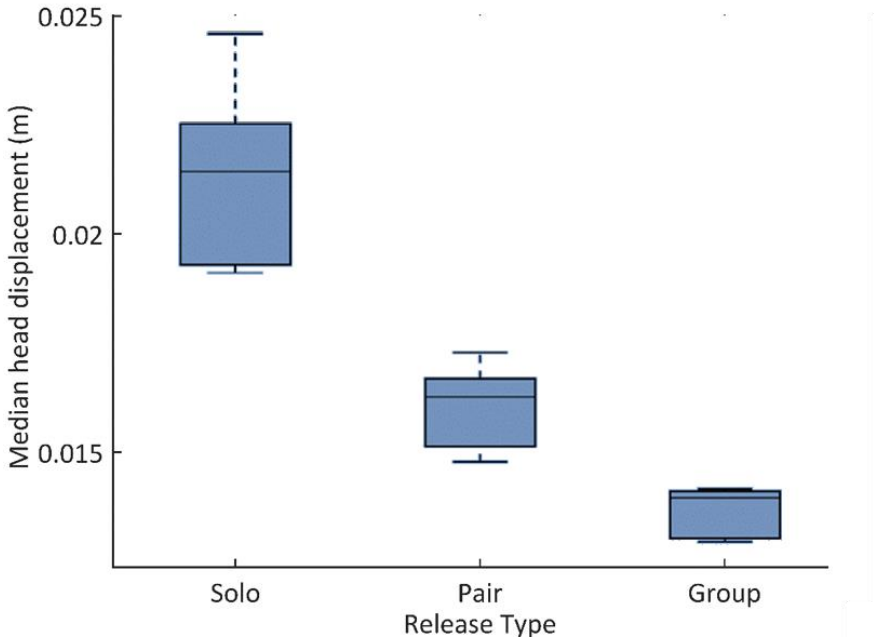

Figure 4.7 – Boxplot of median vertical peak-to-peak head displacement across 6 birds, each flying one flight solo, one in a pair, and one in a group. Bottom and top edges of the box indicate the 25th and 75th percentiles and the whiskers extend to the most extreme data points. Note that there is no overlap whatsoever between the median head displacements calculated for any of the three flight conditions.

The decrease in head displacement described above with more companions is accompanied by an increase in wingbeat frequency. Median wingbeat frequency was 5.5 ± 0.46 Hz (mean

± sd) for birds flying solo, 6.6 ± 0.42 Hz for pairs, and 6.7 ± 0.52 Hz for groups. Despite the low sample size and different sensor placement, this increase in wingbeat frequency across release type is a very similar result to those recorded from back-mounted accelerometers for pigeons flying in pairs (Taylor et al., in review) and groups (Usherwood et al., 2011). As a comparison, Taylor et al. found that when flying solo, birds had a wingbeat frequency of 5.48 Hz which increased to 6.48 Hz when flying as a pair. This result suggests that the change in wingbeat frequency between release type may be partially responsible for the change in vertical head displacement, as suggested by Taylor et al. This relationship is examined analytically in the equations below.

If the aim of a pigeon is to reduce vertical head displacement in order to minimise motion blur or parallax, this could be achieved by decreasing the peak-to-peak forces of the wingbeat or by increasing their wingbeat frequency, or a combination of both. This relationship can be shown analytically under the assumption that the forces produced due to the wingbeat (*F*) form a perfectly sinusoidal curve, where the bird is a rigid body with certain mass (*m*). The acceleration (*a*) experienced by the head, and measured by the accelerometers, will vary according to the following equation:

$$a(t) = \frac{F}{m} \sin(2\pi f t)$$

where *f* is the wingbeat frequency, *t* is time and $\frac{F}{m}$ is the amplitude of the acceleration. The oscillatory displacement (*s*) of the head can be found from the double integration of acceleration with respect to time yielding the following equation:

$$s(t) = -\frac{F\sin(2\pi f t)}{4\,\pi^2 f^2 m}$$

The peak-to-peak displacement measured at the head (referred to here as vertical head displacement) is double the displacement (s) amplitude. From the above equations, it becomes clear that displacement will scale with $1/f^2$. Figure 4.8 shows this relationship between vertical head displacement and wingbeat frequency within 3 flights of all 6 birds flying solo (red), in a pair (green) and in a group (blue). Each circle represents a single wingbeat within each flight. Theoretical lines, based on a rigid body assumption, are fitted to each flight using the mass (m) of each bird and finding a constant force (F) that minimises the root-mean-squared error (RMSE) to measured data. Force (F) values that minimise RMSE are shown in the figure for each flight. Each theoretical curve shows the expected relationship if wingbeat frequency was allowed to vary but the peak-to-peak force is kept constant throughout each flight. The figure shows that vertical head displacement decreases as wingbeat frequency increases both within flights and between flights when flying solo, with one additional partner or in a group. Within flights, some birds appear to fit the theoretical lines well but others do not (e.g. D12) suggesting that they may be adjusting something other than just wingbeat frequency. The fitted curves suggest that the birds may be adjusting the peak-to-peak wingbeat forces between release types with a lower force in groups relative to paired or solo flight.

Given that a pigeon is not a rigid body, some of the variation in displacement will also result from the placement of the sensor at an anatomically fixed point on the bird's body away from its centre of mass. This point will therefore vary periodically in displacement from the bird's centre of mass due to the wingbeat forcing leading to additional variation in acceleration. Given that the point of attachment is the bird's head, it is also expected that the neck will attenuate the oscillatory displacement of the body. This attenuation could be

tuned actively throughout the flight in response to wingbeat forces and the presence of other individuals, as discussed below.

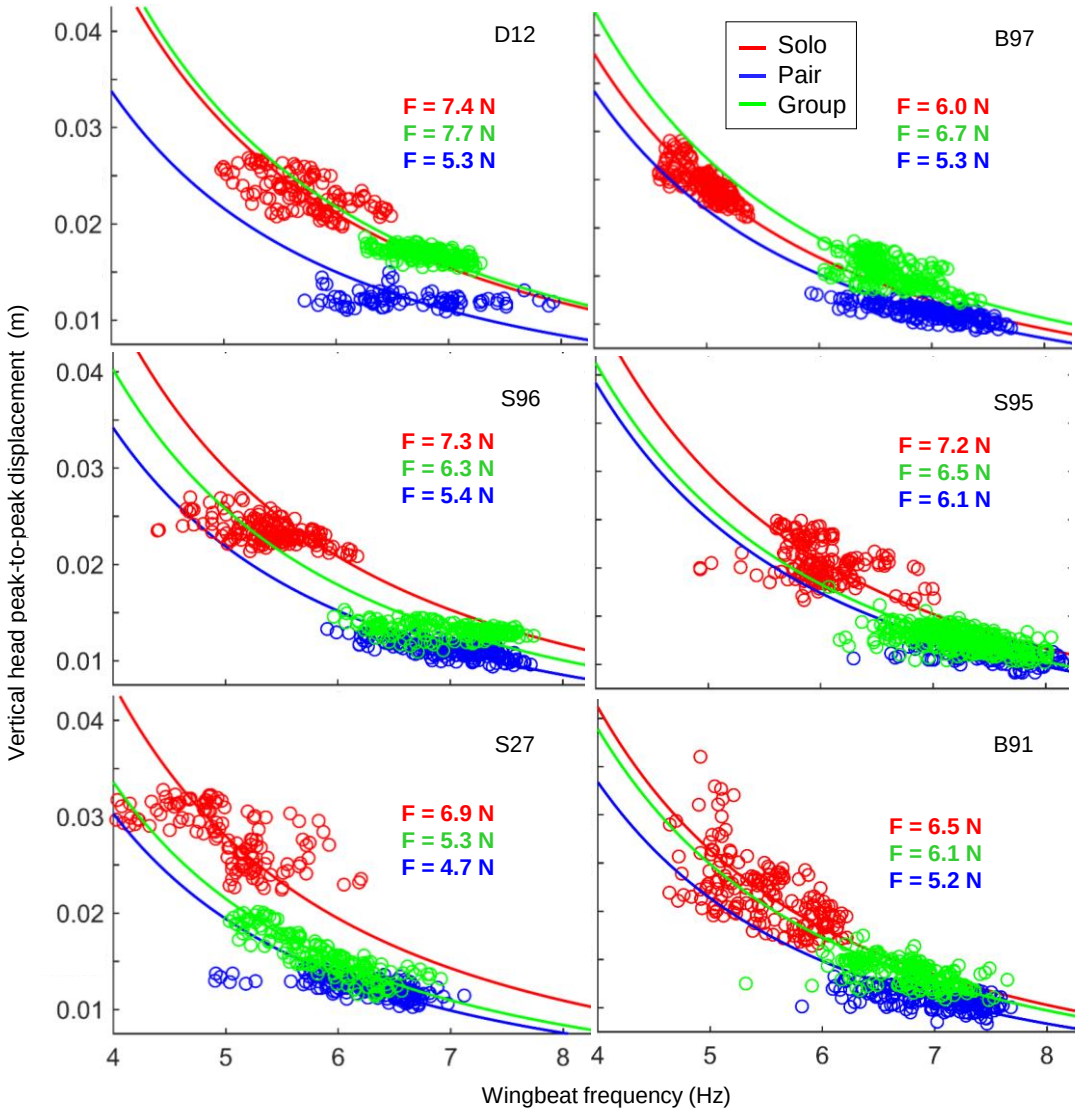

Figure 4.8 – Vertical peak-to-peak head displacement decreases with increased wingbeat frequency. Data shown within three flights (each circle is a wingbeat) by 6 birds (bird ID shown in top right of each panel) - one solo (red), one pair (green) and one group (blue). Theoretical curves according to the equations above are drawn for each flight, fitted using the bird's mass and assuming a constant force amplitude (F) throughout the flight (shown in each panel).

While inertial data were only collected in this study from the bird's head, it is possible to compare the head measurements made here against data from other studies. The comparison of median peak-to-peak head displacement data with median dorsal body peak-to-peak displacement data from two studies using back-mounted accelerometers (Taylor et al., in review; Usherwood et al. 2011) shows that pigeon necks attenuate vertical displacement by a factor of around half for paired and group flight (Table 4.2). The neck attenuation factor (head displacement/body displacement) for solo flights is marginally larger suggesting that the neck is dampening body oscillations to a larger degree in paired and group flights when proximate visual information is available. As an additional comparison, whooper swans flying solo were found to have a neck attenuation factor of 0.23 (Pete et al., 2015) demonstrating a greater degree of vertical head stabilisation, possibly afforded by their long relative neck length. These comparisons are made across different studies with different methodologies and must be treated with some caution.

Release Type	Body vertical displacement (mm)	Head vertical displacement (mm)	Neck attenuation factor
Solo	41.41	23.8	0.57
Paired	32.11	16.0	0.50
Group	27.32	13.6	0.50

Table 4.2 – Comparison of measured solo, paired, and group peak-to-peak vertical displacement for body and from literature (1: Taylor et al., in review; 2: Usherwood et al. 2011) against head displacement measured in this study. Neck attenuation factor is head displacement/body displacement and gives a measure of the fraction of the body displacement that is transferred to the head.

4.5 Discussion

In this chapter, we have demonstrated the effective use of a head-mounted IMU to reliably record the head movements of pigeons in order to demonstrate translational and rotational stabilisation during free flight.

4.5.1 Pigeons coordinate saccades with their wingbeats

We found that pigeons coordinate their angular head saccades with wingbeat phase, and that this coordination depends on the saccade amplitude (Figure 4.5). Smaller saccades, with an amplitude less than 20 deg, were found to show less of a phase bias than larger saccades but were still more likely to be initiated preceding peaks and troughs in vertical head velocity. This weak preference could be explained by birds attempting to coordinate periods of angular head movement, required to change gaze, with translational head speed, in order to minimise motion blur (Frost, 2009; Necker, 2007). It is likely that, similarly to humans (Krekelberg, 2010), birds suppress the intake of visual information during saccades (saccadic suppression) in order to simplify visual processing.

Larger saccades, with an amplitude over 20 deg, were initiated preferentially preceding peaks in vertical head speed. Although it is not possible to precisely relate accelerometer measurements to any specific wingbeat kinematic (Portugal et al., 2014), the observation that pigeon translational head velocity had a consistent maximum occurring at the downstroke-upstroke transition (Ros and Biewener, 2017) allowed us to infer that large saccades were initiated at the end of the downstroke. This leads to a period of relatively little head movement earlier in the downstroke (Figure 4.6), a period of fixation. This result is similar to findings from laboratory studies in pigeons (Ros and Biewener, 2017) and

lovebirds (Kress et al. 2015) which both found a tendency for birds to initiate saccades at the end of the downstroke or early upstroke. However, both studies found this tendency to be more rigid than the phase bias found in this study, likely because the data here captures a broader range of flight conditions. We discuss the possible reasons for the observed phase bias below.

Kress et al. (2015) suggest that the coordination between wingbeats and saccades in lovebirds maximises visual perception by overlaying two behaviours that impair vision — lovebird's wings occlude lateral vision at the end of the downstroke. We inspected high-speed video footage of pigeons flying in a laboratory (Ros & Biewener 2017 — Supplementary video 1) which showed that during slow flight, pigeons have a period where their wings occlude lateral vision at the start of the upstroke (φ: 0 - $\pi/2$). Therefore, it makes sense for pigeons to time the period of relative fixation (shown in Figure 4.6) to avoid this period of visual obstruction. However, it is not clear whether this is true for high-speed flight experienced by the pigeons in this study and further validation is required.

Ros & Biewener (2017) provide an alternative explanation showing that head saccades precede body turns and that cues inferred from head saccades (e.g. magnitude of neck bending relative to the body) correlate with subsequent changes in body position. If saccades are a prerequisite for all changes in body orientation, coordinating saccades with wing movements that actuate body movement would allow for increased control and collision avoidance. This effect is demonstrated by Kano et al. (2018) and is further corroborated in Chapter 5 using GPS devices to show that head movements precede large turns in trajectory for free-flying pigeons. However, head saccades may also be a prerequisite for all smaller bounding turns in fast flight that are undetectable using GPS

(on the scale of ~3 m, the GPS 50% circular positioning accuracy). As discussed in the methods, these sharp body turns may have been misidentified as saccades due to the high angular rate. However, this is unlikely given that saccade duration was normally distributed with a mean of 0.09 s, far shorter than expected from a body turn.

In order to differentiate between these alternative hypotheses, and conclusively determine the relationship between wingbeat phase and head mounted accelerometer readings, the use of high-speed video footage synchronised with the IMU would be necessary. Whatever the explanation for the observed coordination of angular saccades with respect to the wingbeat cycle, this result suggests that gaze changes are likely coupled to the central pattern generator network that drives the flapping wings (Grillner, 2006).

4.5.2 Flying with conspecifics enhances vertical head stabilisation

The results from the head displacement analysis show that pigeons can reduce flap-induced vertical head displacement by adjusting their wingbeat frequency (Figure 4.8), and possibly by adjusting their wingbeat forces and tuning their neck dampening system (Table 4.2). The reduced head displacement (and reduced variation in head displacement) seen for birds flying alongside other individuals may be partially explained by the observed increase in wingbeat frequency as suggested by Taylor et al. (in review). However, as these authors note, it is unclear whether the birds are increasing their wingbeat frequency (which comes at an energetic cost) in order to reduce head displacement and enhance visual stability (Pete et al. 2015; Land 1999) , or for other reasons such as a greater degree of control. If this is indeed a mechanism to enhance visual stability, this would likely be modulated by both visual and vestibular reflexes (Gioanni and Vidal, 2012; Wallman and Letelier, 1993).

Our finding that stabilisation is enhanced when flying with conspecifics is most likely made possible for two complementary reasons: firstly, the birds are required to keep their heads translationally stabilised when flying near conspecifics in order to avoid collisions and coordinate flocking behaviour, and secondly, it may only be possible for the birds to stabilise their heads translationally when close visual stimuli is provided by their conspecifics. Therefore, it is both only necessary, and only becomes possible, for birds to translationally stabilise their heads when flying alongside other birds. The latter implies a central role for vision in translational stabilisation. Although the relative importance of visual and vestibular cues used for stabilisation is well understood for grounded pigeons (Theunissen and Troje, 2017), it is poorly understood during flight. Therefore, future experiments using free-flying birds should attempt to isolate visual and vestibular cues more conclusively by manipulating visual stimuli. While this has been attempted in a laboratory setting (Bhagavatula et al., 2011), it is harder to manipulate the visual environment on a large scale to investigate the navigation studied here.

Our results also show that there is systematic variation in head displacement between release type (solo, pair, group) that is not fully explained by the theoretical model which only allowed wingbeat frequency to vary across the flight (Figure 4.8). This suggests that the birds may be reducing the amplitude of wingbeat forcing (Figure 4.8) or changing the extent to which their necks attenuate oscillations (Table 4.2) experienced by the body. It is unlikely that the birds will have the luxury of decreasing peak-to-peak forces because a certain minimum force is required to provide thrust to overcome drag and the lift to overcome their body mass. The analysis in Figure 4.6 assumes that these peak-to-peak forces stay constant throughout each flight. However, the aerodynamic power requirement of a flapping wing scales positively with the wingbeat frequency (Floryan et al., 2018) and

therefore the peak-to-peak wingbeat forces will also be a function of wingbeat frequency. This likely explains why, for each flight in Figure 4.8, we see that the empirical data is above the theoretical line at high frequencies but below the line at lower frequencies, i.e. the slope of the data is always flatter than predicted. Qualitatively, this is what we would expect as an increased wingbeat frequency requires more power input, and therefore higher forces, and results in an increased displacement. The neck attenuation comparison across release type shows a marginal increase in the extent of neck attenuation between solo flights and flights with conspecifics (neck attenuation factor 0.5 for solo compared with 0.57 for pairs and group). However, the neck attenuation result should be treated with caution as it compares data across different studies using different methods. For future work, the development of a device simultaneously measuring synchronised accelerations on the bird's head and body would allow for a better comparison of head and body displacements.

Image stabilisation is an essential task for a range of human engineered applications, particularly aerial robotics where vision often underlies autonomous control in GPS-denied environments. Multirotor drones often have gimbal-stabilised cameras which use visual and inertial information to provide rotational stabilisation in much the same way as a bird's head. Bird-inspired flapping drones also face the additional challenge of translational stabilisation. The avian neck-head system described in this chapter could, therefore, provide valuable inspiration for the design and tuning of a mechanism capable of attenuating flap-induced oscillations (Pete et al., 2015).

Chapter 5. Objectively identifying targets of visual fixation during navigation by free-flying homing pigeons

5.1 Abstract

Homing pigeons (*Columba livia*) rely heavily on visual information for both large-scale navigation and short-term flight control. They have a wide panoramic visual field extending over 340 deg but, like mammals, have foveae which they use to direct their visual attention to salient cues. Understanding the function of shifts in gaze, as well as the resulting focus of visual attention, is attracting growing scientific interest. However, experiments to date have been primarily laboratory-based, and gaze shifts have been under studied for birds flying in their natural environments where they have important adaptive significance for navigation and vigilance. Evidence from GPS-derived trajectories has shown that homing pigeons use visual landmarks when navigating in their familiar area, but the exact nature of these cues remains elusive. To investigate gaze strategy during free flight, pigeons were fitted with a head-mounted inertial measurement unit (IMU) and a GPS logger prior to release from sites within their familiar area. We were thus able to characterise the birds' pattern of saccadic head movement and gaze direction in relation to their track over the ground during flight and when grounded at the home loft. We found that shifts in gaze are largely governed by turning rate, with an increased saccade likelihood when turning steeply. We also observed a decreased saccade likelihood when birds are on the ground as opposed to flying. In addition, an analysis of gaze direction throughout each flight enabled us to identify points in the landscape that aligned with lines projected from the fovea during each fixation period. We found that such "points of interest" often aligned

with edge features of the landscape. Improved iterations of this novel and exploratory approach to studying visual attention could help identify the salient cues of bird navigation in natural environments and have important implications for spatial cognition.

5.2 Introduction

Shifts in visual attention can offer valuable insights into spatial cognition in animals that rely on visual guidance for orientation. Birds are heavily dependent on vision to guide their flight and are therefore equipped with highly specialised visual systems (Jones et al., 2007). Like most animals whose behaviour is guided by vision, birds shift their gaze in an alternating pattern of stable gaze fixations and fast saccades between fixations. However, unlike many animals, including mammals, birds predominantly change their gaze using head movements rather than eye movements (Land 2014; Gioanni 1988a; Maurice 2006). This has been confirmed by eye tracking experiments in body-restrained (Sridharan et al., 2014; Schwarz et al., 2013) and flying (Ivo Ros pers. comm.) birds which found that eye movement was confined within a five degree diameter area in the head reference frame. As a result, past studies of visual attention in birds have relied on the measurement of head orientation as a proxy for gaze direction. The majority of these studies have been in a laboratory setting (Stamp Dawkins 2002; Eckmeier et al. 2008; Warrick 2002; Ros & Biewener 2017; Kress et al. 2015; Green et al. 1994; Erichsen et al. 1989) meaning that remarkably little is known about how birds direct visual attention when flying in their natural environment.

Visual attention has been extensively studied in human and non-human primates through eye tracking technology (Kano and Call, 2017; Holmqvist et al., 2011). However, determining the focus of visual attention using gaze direction in birds is more problematic

than for mammals as many birds possess two acute regions of their visual field — one facing laterally (the central fovea) and one facing frontally (the temporal fovea). Behavioural and anatomical evidence from pigeons has suggested that bifoveate birds preferentially use the central fovea, which has a higher photoreceptor density, to view distant objects, and the temporal fovea, which is dedicated primarily to binocular vision, to view stationary or slow-moving objects at close range (Frost, 2009; Stamp Dawkins, 2002; Erichsen et al., 1989). The location of foveae on the visual field depends largely on the visual ecology of the bird: predatory species generally have a smaller visual field with forward facing eyes, while prey species tend to have flattened, more laterally positioned eyes (Martin, 2007, 2014). The few studies examining bird visual attention in natural environments (Kane et al., 2015; Kane and Zamani, 2014; Loretto et al., 2010) have relied on onboard video cameras to monitor prey pursuit in raptors and assume that the prey item is the focus of visual attention (but see Chapter 6 for a different approach to studying visually-guided pursuit).

5.2.1 Visual navigation in the homing pigeon

Owing to their impressive ability to navigate from unfamiliar locations, homing pigeons (*Columba livia*) have been used as the principal model to study avian navigation over the past century. Researchers have attempted to uncover the hierarchy of cues and mechanisms used by pigeons over various spatial scales and under different environmental conditions (Wallraff, 2005). Experiments in recent decades using GPS trackers have revealed the fundamental role of visual landmarks for pigeons homing within their familiar area (Guilford & Biro 2014). When pigeons are released from the same location multiple times, their trajectories often converge on high-fidelity “pinch points” that overlie distinctive

landscape features (Freeman et al., 2011) and often align with linear features such as roads or railways (Meade et al. 2005; Biro et al. 2004; Lau et al. 2006). Attempts to objectively identify the most informative regions of flight paths, using a Gaussian process model, found that salient visual features occur preferentially at the boundaries of forests and villages (Mann et al. 2011) . All these inferences have been drawn from GPS data and are therefore limited to conclusions relating to landmarks directly on the birds' flight path. Some additional experimental evidence from vanishing bearings suggests that pigeons are attracted to distant major landmarks such as power stations (Biro, 2002) or wind turbines (Mora et al., 2012). However, given the inherent difficulty in experimentally manipulating the landscape, the precise nature of the features used by pigeons for navigation remains relatively obscure.

Inferring visual attention during navigation in visually complex natural environments is a significant technical challenge. However, a recent study adopting a novel head-mounted inertial measurement unit (IMU) was able to infer visual attention from gaze shift characteristics in pigeons during homing flights (Kano et al., 2018). The key finding was that head movements were reduced when approaching prominent visual landmarks such as roads and railways, and during paired flight, indicating a change in visual attention. The authors also found that head movements precede turns, which confirmed laboratory findings in pigeons (Ros and Biewener, 2017) and findings from onboard video data in steppe eagles (Ozawa, 2007). These findings suggest a role for head movements in flight control.

This study aims to further our understanding of the role of gaze shifts and gaze direction in flying birds. We achieve this by tracking homing pigeons flying within visually complex

natural environments using GPS loggers and the same head-mounted sensors described by Kano et al. (2018) and in Chapter 3. In this chapter, we extend previous work using head orientation to: (i) further explore the relationship between head and body movements by identifying the delay between these signals, (ii) develop a model to help understand the factors underlying shifts in gaze, and (iii) attempt to identify the visual features attended to by homing pigeons during short-range navigation. The saccade model (ii) includes comparisons of flying against grounded birds, grounded birds inside against outside the loft building, body turn rate and whether the birds flew solo or with a group. Both (i) and (iii) require an estimation of the absolute orientation of the bird's head during flight in an inertial reference frame (relative to gravity and magnetic north) which is achieved here by building on the method used by Kano et al. (2018). To achieve (iii), we develop a novel and exploratory approach to landmark identification by inferring the focus of visual attention in pigeons using their gaze orientation. This allows us, for the first time, to identify regions of interest that do not lie on the bird's flight path.

5.3 Methods

This chapter uses the same data as that collected in Chapter 4 and therefore the subjects, instrumentation, release sites and experimental protocol are identical and are not repeated here.

5.3.1 Additional testing procedures

Wind data were recorded using a WS2083 Professional Wireless Weather Station (Aercus Instruments, UK) installed at the loft. The anemometer was located 5 m above ground level and logged average wind direction and wind speed every minute. Wind data were only used

to estimate the bird's air velocity vector as a reference for interpreting body angle relative to head angle.

5.3.2 Data processing and analysis

5.3.2.1 Track analysis

GPS data were overlaid onto satellite images using Google Maps API (Bar-Yehuda, 2015) in MATLAB for initial inspection. These data were subsequently screened using an internal validation method for loss of precision by comparing the highly accurate Doppler shift groundspeed estimate against the noisier differenced groundspeed estimate using methods described by Brighton et al. (2017). Latitude and longitude were converted to meters using a Universal Transverse Mercator projection. The GPS data were cropped using different procedures for the saccade model and fovea heatmap, detailed in sections 5.3.2.4 and 5.3.2.5 respectively. The track angle was defined using the vector pointing from each GPS point to the next. A moving average with a span of 10 points (1 s) was taken to smooth the data. When comparing head and body angles during flight, it is important to note that the track angle (derived from the GPS) does not equal the bird's heading as this will be offset due to the effect of wind. Wind data recorded at the loft was used to illustrate this point by estimating the air velocity vector against which to compare the head and ground track orientation. See Chapter 2 for a full discussion of the effect of wind on track orientation.

5.3.2.2 Head orientation using inertial measurements

Raw IMU data were post-processed using custom-written MATLAB code and then fused to give estimates of the head-mounted board's orientation (in the form of Euler angles – Figure 5.1). This was achieved using open-source code adapted from Barton (2012) and Reynolds (2016); see Chapter 3 for details. This post-processing approach to board state

estimation has distinct advantages over previous attempts to study head orientation in pigeons using the same equipment; Kano et al. (2018) relied on the board's internal real-time sensor fusion algorithm which resulted in half the orientation data being discarded due to low accuracy. For a validation of the method used here, see Chapter 3. The sensor board yaw angle (measured relative to magnetic north) was used as an estimate of the pigeon's primary gaze angle, defined as the direction of the head-fixed vector in the mid-sagittal head plane (Figure 5.1). This indicates where the bird is directing the binocular region of its visual field.

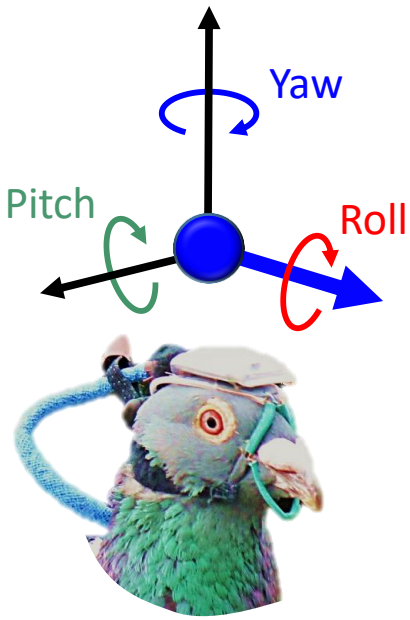

Figure 5.1 – Head-mounted sensor with Euler angles representing the board state, estimated using the Inertial Measurement Unit (IMU). The large blue arrow indicates the board's yaw angle relative to magnetic north and is assumed to align with the pigeon's mid-sagittal head plane in this and subsequent figures.

We determined the delay between bird track angle and head yaw angle for each flight by correlating the rate of change in GPS track angle, as a proxy for body turn rate, against change in head orientation allowing the delay to vary between -5 and 5 s. For each flight,

we identified the delay that maximised the squared correlation coefficient between the rate of head and body movement.

5.3.2.3 Saccade analysis

Head saccades were identified using data from the head-mounted gyroscope, described in detail in Chapter 4, enabling us to determine the start and end times of each saccade for subsequent analysis. Saccades were defined as head rotations exceeding 100 deg/s for a duration of over 30 ms. Start and end points of each saccade were defined as the first point before and after the saccade peak angular velocity where the derivative of the angular rate was zero, i.e. where the angular acceleration changes direction.

5.3.2.4 Saccade logistic model

To test how the head movements of pigeons are related to their visual environment, we used model selection techniques to investigate the statistical relationship between saccade occurrence and several environmental predictors. We used a logistic mixed effects model with a binary response variable indicating whether the bird was saccading at any given timepoint. The response variable was generated by designating every timepoint between each saccade start and end time as 1, and the remaining points as 0. GPS and IMU data from all 100 flights were resampled using quintic spline interpolation to 100 Hz and used to generate predictor variables where each time point is considered as a data point in the model. The predictor variables used are shown in Table 5.1 and explained in detail in the main text below. Random effects were added with a random intercept and fixed mean. Statistical tests were conducted in R (v3.5.1) using ‘lme4’ and ‘cAIC4’ packages to conduct Akaike's information criterion (AIC) model selection (Säfken et al., 2018). We used the conditional AIC (cAIC) to rank models as opposed to AIC, as recommended for

mixed effect models (Blanchard and Blanchard, 2005). For all top models, we checked the assumptions of linearity, normality and homoscedasticity by visual inspection of plotted residuals.

Fixed effects	
Edge (Over edge vs not edge)	*E*
Flight status (Flying vs grounded)	*G*
Loft (Inside loft vs outside)	*O*
Body turn rate (deg/sec)	*T*
Release type (solo, pair or group)	*R*
Release number	*N*
Random effects	
Bird ID	*B*
Flight ID	*F*
Release site	*S*

Table 5.1 – Predictor variables used in the saccade logistic model selection to predict saccade likelihood

Landscape edge density is an indicator of the visual information content of a geographical region (Mann et al., 2014) where hedgerows, forest edges, roads, rivers and villages, for example, would lead to surrounding regions having high edge density values. Given that one of the primary functions of gaze shifts is thought to be extracting salient navigational cues (Kano et al., 2018), we hypothesised that information content of the landscape below the track during flight would correlate with saccade characteristics. Instead of using edge density, we generated a binary edge parameter (*E*). The methods used to calculate binary edge values are summarised here but described in detail in Chapter 2 with associated figures. A binary edge image was produced by running a Canny edge detection on an aerial image covering the region of interest, using similar methods to Lau et al. (2006). The resulting binary image was scaled so that each pixel represented 1 m^2 with a value of 1

over edges or 0 between edges. Each GPS point was overlaid on top of the binary image and each categorised as either over an edge (if an edge occurred within the 3 m^2 area around the point, to account for GPS error), or as not over an edge. This resulted in a binary predictor variable for every data point for the duration of each flight.

The role of visual information for birds in flight is likely to be different from that for birds on the ground, and therefore we expect to see different saccade characteristics between flying and grounded birds. In support of this, Kano et al. (2018) found that pigeons showed less frequent, but larger, saccades when grounded compared to when flying. Therefore, we include ground (*G*) as a factor in our model, defined as sections of the data log with velocities below 1 m/s for more than 1 min with lateral accelerations less than 3 m/s^2. This excluded landing and walking when grounded. Track sections were classified as flight when the differenced GPS velocity was above 3 m/s. Additionally, we found that it was possible to determine when the bird entered the loft building which produced a characteristic spike in differenced GPS velocity above 50 m/s. This likely relates to the loss of satellites when the loft walls occlude the GPS antenna from direct line-of-sight with global positioning satellites. A loft variable (inside/outside the loft) was, therefore, included as a binary variable in the model (*O*). Body turn rate (*T*, deg/sec) is likely linked to flight control which may require feedback from shifts in head orientation as a control input (Ros and Biewener, 2017). It was added as a continuous variable to the full model, calculated as the change in track angle. Kano et al. (2018) found that when birds were released in pairs, their saccade frequency decreased, and therefore we added release type (*R*) into the model with three factors: solo, pair and group. Despite the familiarity of the birds used in this study with the surrounding landscape, we included release number (*N*) as

a variable as Kano et al., (2018) found that saccade frequency and amplitude increased in the learning phases of flights. This is the flight number for each bird at each site.

5.3.2.5 Fovea heatmap generation

To better understand what pigeons are attending to during periods of fixation, head yaw orientation (Figure 5.1) was used to generate heatmaps of geographical regions aligning with assumed fovea angles as a proxy for visual attention. Given that pigeons have multiple foveae, alignment with a fovea does not necessarily imply that a point along a geographical line extending from the bird's eye is the focus of visual attention. However, if a landmark or geographical region is consistently attended to using the fovea by the same or multiple birds across the same or multiple flights, it is likely that this region will align with the fovea more than expected by chance. All solo flight trajectories from Wytham Hill and Swinford release sites (n = 76) were cropped to only include sections where the bird's groundspeed (the Doppler speed derived from the GPS) was greater than 5 m/s, therefore excluding take-off. The tracks were also cropped at the end when the birds were within 50 m from the loft. We then identified the geographical location associated with the endpoint of each saccade (the start of each fixation) along the bird's GPS track. At each gaze fixation location, two lines of points were generated at ± 72 deg relative to the board yaw angle (Figure 5.2A). This is the angle of the central fovea relative to the mid-sagittal head plane based on anatomical measurements (Clarke and Whitteridge, 1976; Westheimer, 1965). These lines extended 3 km with points at 1 m intervals to generate a matrix of density values associated with each location within the vicinity of the track (Figure 5.3A). Fovea lines were chosen up to this distance as pigeons are known to be attracted to landmarks on a previously learned route up to 1.5 - 3 km away, but likely not beyond (Biro et al., 2004, 2006). An additional heatmap was generated for each site using a fovea angle of 0 deg (the board yaw

angle), the convergence point of the temporal fovea and the area of binocular overlap. In the resulting heatmaps, pixels with large fovea alignment values are associated with greater visual attention.

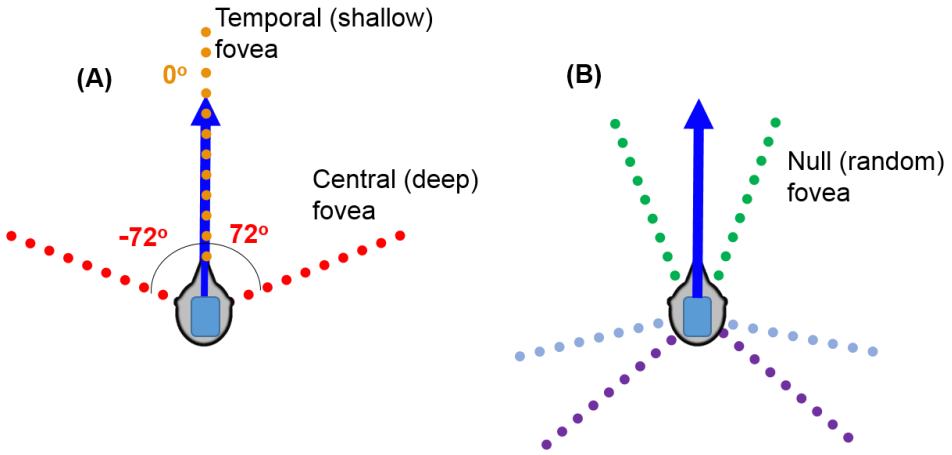

Figure 5.2 – Visual field of a pigeon demonstrating the generation of the fovea heatmap by (A) extending lines from the board yaw vector (blue arrow) at either ± 72 deg (red) for the central fovea or 0 deg for the temporal fovea (orange), and (B) selecting random fovea angles for each saccade between 0 and 180 deg (and the symmetrical equivalent) to generate the null model (3 random angles shown).

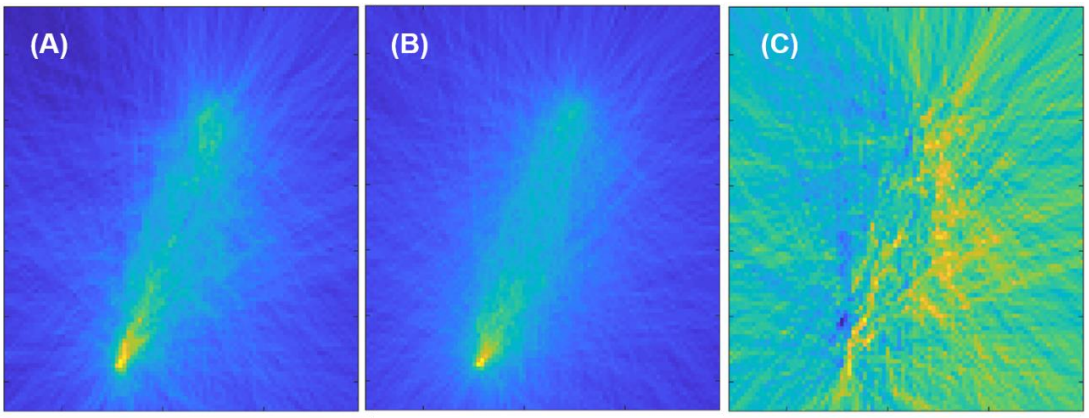

Figure 5.3 – Example of fovea heatmap generation from Wytham Hill based on 39 solo flights from 12 birds. (A) Heatmap generated using fovea angles of ± 72 deg. (B) Heatmap of null model generated using random symmetrical fovea angles for each saccade. (C) Heatmap of 72 deg model matrix after subtracting the null model matrix [A-B]. Bright yellow regions show areas of high fovea alignment after null subtraction.

Fovea lines are likely to converge on certain locations for reasons other than visual attention. For example, the temporal fovea lines are likely to align with the track given that the average head orientation will align with the body. The central fovea points on the inside of a turn will tend to converge on an area close to the centre of the turn. To reduce the noise generated by these incidental alignment points, we subtracted a null heatmap of the points that we expected to identify by chance given the track structure. This null model heatmap was then generated (Figure 5.3B) for the central fovea by drawing two fovea lines from the bird's position at each saccade point – one at a random angle between 0 and 180 deg, and one at the symmetrical angle on the other side of the bird's visual field (Figure 5.2B). The null model for the temporal fovea consisted of only one random fovea line for each saccade. The null model heatmap matrix was subtracted from the 72 deg fovea angle model matrix to generate a fovea alignment matrix (Figure 5.3C). To identify the geographical areas that converged with fovea lines more than expected by chance, pixels were identified containing values greater than the 99.9^{th} percentile and overlaid onto satellite images.

Once these regions had been identified, we wanted to know whether the points align with specific landscape features, or specific types of landscape features. We used satellite images to objectively classify the information content of the area of interest using Canny edge detection on satellite images using previously established methods (Lau et al. 2006; Mann et al. 2011) . To objectively assess whether these points had a greater tendency to fall over edge features than expected by chance, we compared the proportion of points that lay over edges against a null distribution. The null point distribution was produced by randomly generating the same number of points identified as fovea alignment points within a polygon whose vertices are defined by the previously identified points. These null distributions, of the proportion of points overlaying edges, were found to be approximately

normal. Note that these null point distributions are not related to the null fovea heatmap. The distributions were used to find the percentile of the actual proportion over edges relative to the null distribution for each site and fovea.

5.4 Results

5.4.1 Head and body coordination

The analysis of ground track angle against head orientation found that pigeons pre-emptively turn their heads in the direction of a turn before the manoeuvre. This confirms the previous findings of Ros & Biewener (2017) in a laboratory setting and Kano et al. (2018) in free-flying pigeons but using a different method to derive sensor board yaw angle. Figure 5.4A demonstrates this for a 6 s sample of circling flight with the head yaw angle plotted as blue arrows onto the GPS-derived track. A direct comparison of track angle, head yaw angle and air heading for this section of flight is shown in Figure 5.4B. The addition of the estimated air heading to this figure (red line) illustrates the effect of wind on body orientation, demonstrating the difficulty in directly comparing head and body orientation in an inertial reference frame using this setup. In order to compare the timing of these signals, therefore, we compared the head and body turn rates, rather than the estimated absolute head and body orientation in an inertial reference frame. This enabled us to estimate the delay between changes in head yaw angle and GPS track orientation for all 68 solo flights for which we have reliable head yaw data. We found, when averaged across all flights, that changes in body orientation lagged 0.51 ± 0.21 s (mean ± sd) behind changes in head orientation. The delay that maximised the correlation between head and body turn for each flight never had an R^2 value greater than 0.1 which strongly suggests that, although

head saccades proceed body turns, changes in gaze serve other functions, as explored in the model below.

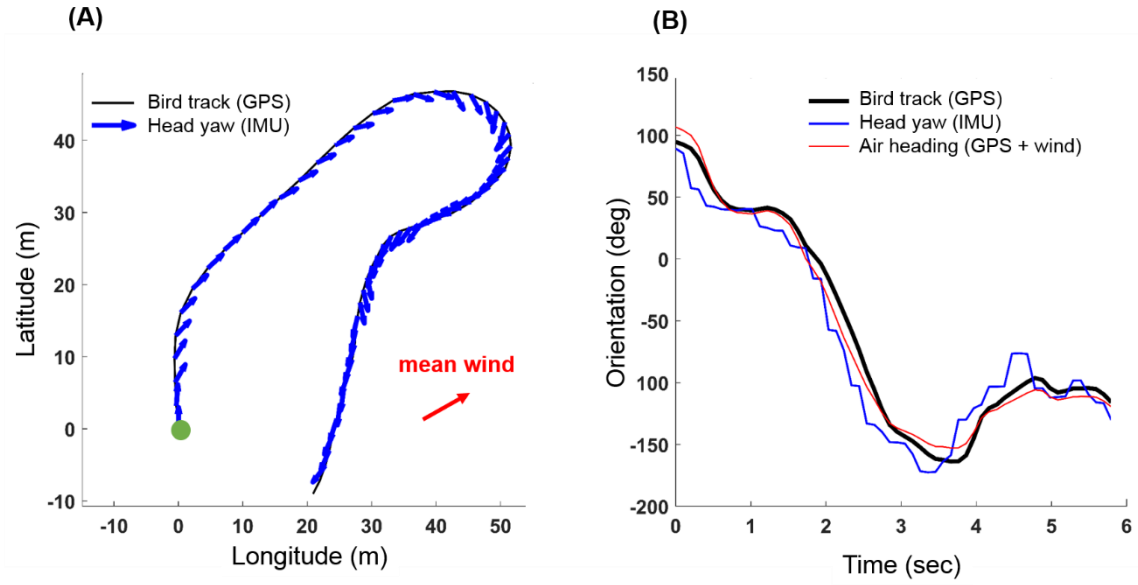

Figure 5.4 – Example of 6 s of circling flight around the loft. (A) 10 Hz GPS-derived ground track starting at green dot with blue arrow indicating head sensor yaw orientation (Figure 5.1) as a proxy for primary gaze direction. Mean wind direction, measured at the loft, is shown using the red arrow (mean wind speed 5.3 m/s). (B) Bird ground track angle plotted for the same flight against head orientation, both sampled at 10 Hz so that each point corresponds to an arrow in (A). Note the offset between track and head angle and the saccadic nature of head movements. The estimated air heading, calculated by subtracting the wind vector from the ground vector, is shown in red as a comparison.

5.4.2 Saccade logistic model

Model selection techniques with linear mixed effects models were used to investigate the statistical relationship between saccade likelihood, as a binary response variable, and the predictor variables summarised in Table 5.1, to better understand the factors affecting gaze shifts. The predictor variables used were edge (*E* — over/not over edge), flight status (*G* — flying/grounded), loft (*O* — inside/outside loft), body turn rate (*T*), release type (*R* – solo/ pair/ group), and release number (*N*) with bird ID (*B*), flight ID (F) and release site (*S*) as random effects. A candidate set of mixed effects linear models were created from all

possible linear combinations of random and fixed effects. The conditional Akaike information criterion (cAIC) was used to assess the performance of the competing candidate models (Burnham and Anderson, 2002). cAIC selects the most parsimonious models with high predictive power while minimising the number of parameters included in the model.

We found flight status (*G*) and body turn rate (*T*) to be the most important factors affecting saccade likelihood. We found that grounded birds are 40.1% less likely to saccade ($e^{-0.520} = 0.599$) than flying birds (χ^2 (1) = 32.5,$p < 0.001$). In flight, birds are 6.89% more likely to saccade ($e^{-0.0664} = 1.07$) for every additional deg/s increase in body turning rate ($\chi^2(1) = 52.3$, $p < 0.001$). Table 5.2 shows the best performing models ranked by the difference (Δ_i) between each model's cAIC value and that of the best model. The six models shown represent the 95% confidence set based on Akaike weights (w_i), i.e. we are 95% confident that one of the models within this credibility set is the best approximating model. The top model for these data is shown on the first row of Table 5.2 and includes flight status (*G*), and body turn rate (*T*) with flight ID (*F*) as a random factor. The estimated regression coefficients for the fixed effects in this model, and their associated standard errors, are shown in Table 5.3. The coefficients of a logistic regression ($\log_e$ odds) were converted to the odds using the exponential function and are referenced above. P-values for each parameter were obtained using likelihood ratio tests of the full top model with the effect in question against the model with the effect in question removed.

Model parameters	Δ_i cAIC	w_i
G, T, (F)	0.000	0.467
T, O,R,(F)	3.124	0.211
T, R, O, (F)	4.123	0.102
E,R, (F)	4.435	0.076
G,T,R, (B)	5.123	0.065
O,E, (F)	7.234	0.025

Table 5.2 – Best performing logistic mixed effect models predicting saccade likelihood with model parameters ordered by Δ_i cAIC values. Random effect parameters are shown in brackets. Shown is the 95% confidence set, defined as the smallest set of models whose Akaike weights (w_i) sum to 0.95. Parameters detailed in Table 5.1.

Parameter	Intercept	Flight status *(G) (1 or 0)*	Body turn rate *(T) (deg/s)*
Regression coefficient	1.19	-0.520	0.0664
Standard error	0.0245	0.231	0.00235

Table 5.3 – Fixed effect parameter estimates for the best candidate model predicting likelihood. Regression coefficients and standard errors are shown for each term in the model.

5.4.3 Fovea alignment heatmap

Using the sensor board yaw angle (Figure 5.1) from the IMU at the start of every period of fixation (inter-saccadic interval), we were able to generate a heatmap to identify geographical regions that aligned with fovea angles from 68 solo flights. The distribution of identified points varies depending on the fovea angle used (temporal vs central fovea). Figure 5.5 and Figure 5.6 show the fovea alignment points for Wytham Hill and Swinford release sites, along with the flight trajectories used to identify them, plotted on a satellite image of the underlying landscape. These are plotted separately for the central (Figure 5.5A & Figure 5.6A) and temporal (Figure 5.5B & Figure 5.6B) foveae. For the temporal fovea, many of the fovea alignment points are located off the bird's tracks. They show a strong bias towards the right for the Wytham Hill release site and a strong bias towards the left

for the Swinford release site. From both sites, the buildings surrounding the loft are identified as points of alignment with the central fovea. At the Swinford release site, many of the birds initially circled around the village of Swinford before making their way around the edge of Wytham Woods (bottom centre of satellite image in Figure 5.6) to the loft. A large number of points are identified both around Swinford and around the village of Cassington to the north of the tracks. However, few points were identified directly over Wytham woods.

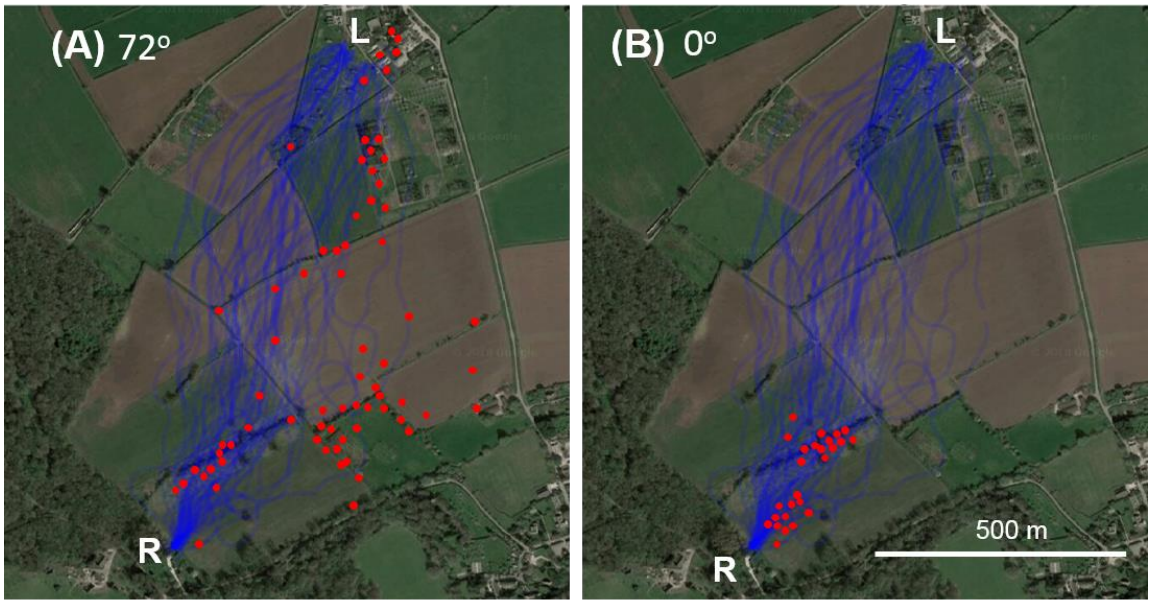

Figure 5.5 – Fovea alignment points from 39 solo flights by 12 birds from Wytham Hill. Satellite image with GPS tracks overlaid in blue shown between release site [R] and loft [L] with points from the subtraction heatmap (Figure 5.3C) containing fovea alignment values above the 99.9th percentile shown as red dots. (A) Fovea angles: ± 72 deg (central fovea). (B) Fovea angles: 0 deg (temporal fovea, i.e. binocular region).

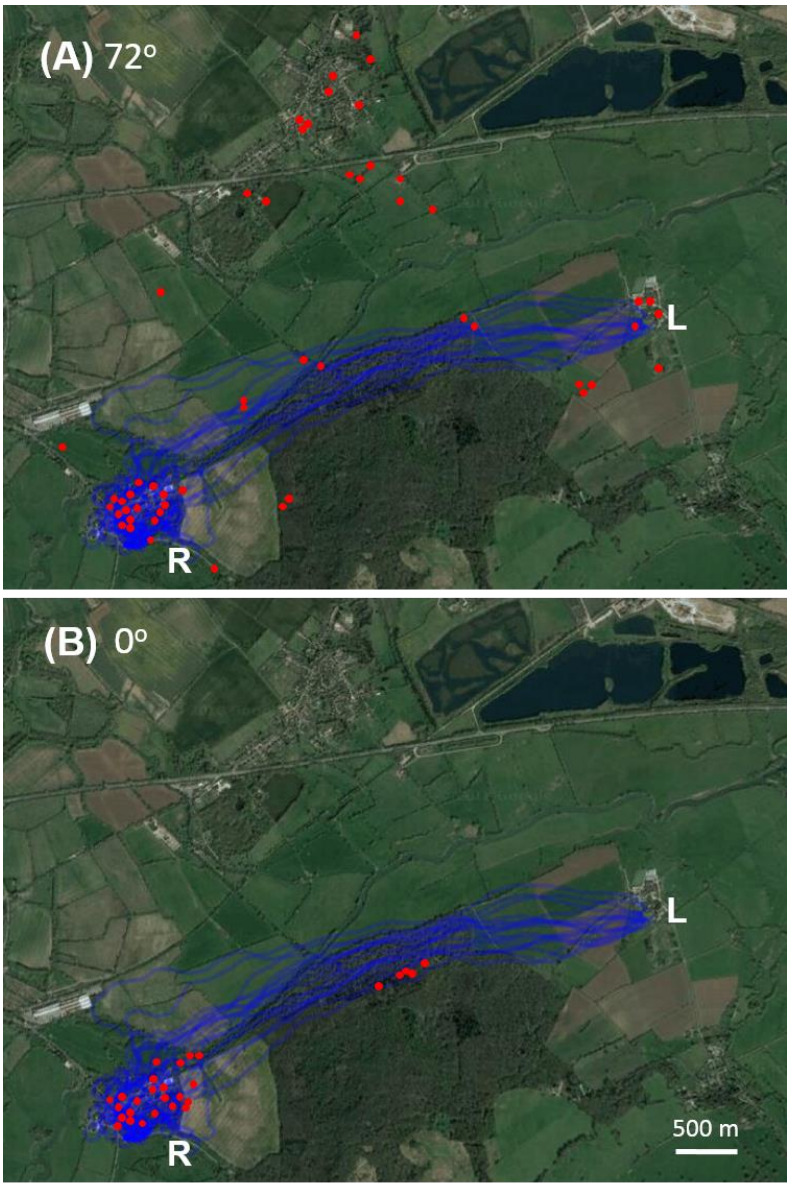

Figure 5.6 — Fovea alignment points from 29 solo flights by 12 birds from Swinford. Satellite image with GPS tracks overlaid in blue shown between release site [R] and loft [L] with points from the subtraction heatmap (Figure 5.3C) containing fovea alignment values above the 99.9th percentile shown as red dots. (A) Fovea angles: ± 72 deg (central fovea). (B) Fovea angles: 0 deg (temporal fovea, i.e. binocular region).

To determine whether these points had a greater tendency to fall on certain types of landscape features than expected by chance, we overlaid them onto a binary edge image generated from satellite imagery to find the proportion that lay over edges (Table 5.4). We

found that for the central fovea at both sites, the proportion of points that lay over edges was greater than 88% and 93% of the null distributions for Wytham Hill and Swinford respectively. These values refer to where the proportion of points lying on edges sits as a percentile of the randomly generated null edge proportion distribution. While the identified points are more likely to fall on edges than expected by chance using this method, we highlight the same caution for the similar analysis in Chapter 2 that the null distributions do not necessarily represent a reasonable sampling distribution of visual attention. We found the temporal fovea alignment points to be less likely to fall over edges compared with the null expectation (28% and 46% — see Table 5.4), however, this could relate to the highly restricted sampling distribution against which the edge proportions were compared.

Fovea		Wytham Hill	Swinford
Central (72 deg)	% over edges	46	51
	percentile	88	93
Temporal (0 deg)	% over edges	37	42
	percentile	28	46

Table 5.4 — Edge comparison of fovea alignment points against a null distribution. Proportion of identified points over edges and percentile relative to a null distribution of randomly selected points (see 5.3.2.5) generated for each release site and for both foveae.

5.5 Discussion

Our results demonstrate that it is possible to infer the visual attention of free-flying pigeons both through their pattern of gaze shifts and the resulting orientation of their gaze during periods of fixation.

5.5.1 Head and body orientation

In accordance with previous findings (Kano et al., 2018), we found that pigeons pre-emptively orient their head in the direction of turns with a delay of just over half a second (0.51 s). This phase delay is longer than that found by Ros & Biewener (2017) for pigeons during sharp turning manoeuvres in a laboratory, where they observed that the delay between body yaw rotations and head offset occurred in the second wingbeat following the corresponding saccade (~0.3 s). The authors defined head offset as the angle between the body vector and head orientation (defined in Chapter 6 as head skew). The difference in observed time between changes in head and body orientation in the laboratory and in the field could be explained by the difference in magnitude of body turns being studied or the distance to points of visual attention. The flight trajectories studied here were predominantly straight flights with shallow turns whereas Ros & Biewener (2017) studied pigeons during sharp 90 deg turns. In addition, the GPS devices used here, with a relative positioning accuracy to within a few meters (50% CEP: 3.0 m), can only detect gross changes in body orientation and may not be able to detect smaller bounding turns. For future experiments, the addition of an IMU on the bird's body would allow a direct assessment of the phasing of body and head orientation in an inertial frame without relying on GPS measurements. This could then be compared against laboratory findings and used to develop a model of flight control using head motion to provide visual feedback to control the bird's flight trajectory. Additionally, future analyses should separate out sections of circling flight from straight flight to determine whether this affects the head and body yaw lag.

5.5.2 Predictors of saccade likelihood

Using model selection techniques to identify factors influencing saccadic behaviour, we found that body turn rate (*T*) and flight status (*G*) both consistently occur in the best performing models. This suggests that they are both important factors determining the frequency of gaze shifts. As discussed in Chapter 4, saccadic head movement may be closely linked to the control of flight with feedback from cervical sensors used to change flight trajectory (Ros and Biewener, 2017). Therefore, it follows that birds may spend more time shifting gaze when they are turning more steeply. In support of this, Kano et al., (2018) showed that birds made larger saccades preceding sharper turns. The sections of flight included in our model with the greatest body turn rate are circling flight around the release site for birds released at Swinford (Figure 5.6). Our finding that birds have a lower saccade likelihood when grounded corroborates the findings of Kano et al., (2018) that pigeons make less frequent but larger saccades when not flying. This could be linked to the saccadic control of flight discussed above which may restrict the range of head yaw but requires frequent movement to guide each turn. In addition, when grounded, the birds may use head movements for behaviours such as preening that are not visually controlled but may be detected by the sensor as head saccades.

We found that loft position (i.e. whether a grounded bird is inside vs outside of the loft - *O*) appeared in the in the 95% confidence set, although it did not appear in the top performing model. The model including this factor suggests that the birds have a lower saccade likelihood inside the loft. Release type (solo, pair or group) appears in multiple models in the 95% confidence set, but not in the top model. This may reflect a lack of statistical power as only six birds were released in pairs and six in groups. The effect of edges (*E*) directly below the track only appeared in one of the top selected models

suggesting that this factor may be only weakly associated with saccade (and hence fixation) likelihood. This could be explained by the method used here to quantify edges not fully accounting for the navigational features used by the birds. Additionally, instead of attending to features directly below to aid navigation, the birds may pay greater visual attention to navigational features that lie ahead or to the side of the track as indicated by the fovea alignment heatmap. We aim to develop the saccade logistic analysis using edge density as a continuous variable across the track using methods developed by Mann et al., (2014) which may prove more informative than the binary edge variable used here. These authors found that pigeon route fidelity varies quadratically with edge density, where the optimal edge density for route learning is intermediate. The same may also be true for saccade likelihood if birds attend to more things in environments that contain enough, but not too much, visual information.

In sum, the model selection technique used here to analyse saccade likelihood had advantages over previous methods used to assess gaze shift characteristics during flight (Kano et al., 2018) in that it allowed us to test the effect of multiple variables simultaneously and objectively identify models using the likelihood of each model given the data. However, the use of saccade likelihood as a response variable discards information on the size of saccades (saccade amplitude) which may provide further information regarding visual attention.

5.5.3 Fovea alignment heatmap

The fovea heatmap generated using head orientation shows that there are regions of the landscape with high fovea alignment across birds. Although many of the identified shifts in gaze may be driven by the requirements of flight control, or anti-predator vigilance, the

convergence may suggest that birds are attending to these regions as common, salient "points of interest", potentially for navigation purposes. Without understanding all the factors important to homing pigeons, the interpretation of the visual features identified here must be treated with caution for reasons discussed below. However, it is tempting to attribute possible explanations to some of the identified geographical locations.

5.5.3.1 Putative points of interest

Despite the fact that flights were cropped to exclude the track within 50 m of the loft, the loft was identified from both release sites using the central fovea model. This provides reassurance that the technique is indeed identifying regions of visual attention as opposed to regions of incidental fovea alignment. The finding that a large number of central fovea alignment points appear over Cassington village accords with previous findings that pigeons show a directional bias towards villages (Wallraff, 1994; Guilford, 1993) and often use the edges of villages as waypoints on their habitual route (Mann et al. 2011) . However, the village does not lie on the track of any bird between the release site and loft, suggesting that distant landmarks could be used for navigation, or at least attract some visual attention, without the waypoint being incorporated into the route.

The bias in distribution of central fovea alignment points (to the right for Wytham Hill — Figure 5.5A, and to the left for Swinford Figure 5.6A) could in principle have related to the lateralisation of pigeon's visual system (Prior et al., 2004), in which the left hemisphere (which receives input from the right eye) is thought to be superior at processing large-scale spatial tasks (Prior et al., 2004) while the right hemisphere (receiving input from the left eye) processes social input (Nagy et al., 2010). However, given that we find a bias in different directions for the two different release sites, this suggests instead that the bias

may be related to the saliency of the landscape. There are very few points over Wytham Wood, suggesting that this area of the landscape has few specific landmarks that attract visual attention. This offers an alternative possible explanation for the observation that pigeons tend to avoid forested areas as a means to reduce the risk of predation (Wallraff, 1994). When the distribution of points was evaluated, we found that identified central fovea points have a greater tendency than expected by chance to fall on features of the landscape identified as edges at both release sites (albeit not to a statistically significant degree). This is in accordance with the psychology literature where it is consistently found that areas of high visual contrast attract most visual attention (Li and Yu, 2015). Specifically, Canny edge detection algorithms, similar to the technique adopted here, are used in studies of human visual attention to characterize models of perception and visual information retrieval (Feng et al., 2010). This attraction to edges may be a cognitive bias or 'behavioural rule of thumb' rather than relating directly to some visual function (Mathews et al., 2015).

5.5.3.2 Limitations and future developments

The technique described here to study visual attention for birds navigating in complex natural environments offers a distinct advantage over existing techniques used to infer visual attention in pigeons (Mann et al. 2011; Kano et al. 2018; Mann et al. 2014) as it allows regions to be identified that do not lie on the flight trajectory. As has been done for studies of visual attention in humans and primates (Kano and Call, 2014), regions of fovea alignment throughout a flight could act as a behavioural index of ongoing visual and cognitive processing, opening up avenues for future research using this system beyond navigation. However, the technique is still in its early stages of development and there are a number of future developments for deeper analysis, improved study design and improved

instrumentation that could advance the utility and accuracy of this technique. Each of these categories of developments are discussed in detail below.

For future analysis, the method used to assess the association between visual attention and landscape features could be refined in a number of ways. For example, overlaying edge density data directly onto the null subtraction heatmap would allow for a simpler visual comparison. This would make full use of the fovea alignment data, as opposed to selecting locations exceeding an arbitrary value, and would allow a better assessment of landscape complexity rather than using a binary edge variable. This could be examined statistically by analysing the spatial correlation between a continuous edge density variable (Mann et al., 2014) against the matrix of fovea alignment values after null subtraction (Figure 5.3C). In addition, if a particular visual landmark, such as the loft, is consistently identified, it would be possible to determine where along the track that landmark tends to be fixated from. It would then also be possible to test the angle of the assumed fovea locations by finding the fovea angles that maximised the fovea alignment density values surrounding the landmark location, as was done for the peregrine falcons in Chapter 6.

In this study, we have pooled the data from 12 birds to make inferences generalised across individuals. However, individuals are known to develop their own idiosyncratic routes (Meade et al. 2005) and therefore presumably rely on their own unique set of landmark features to guide their trajectories. Therefore, future studies should conduct a larger number of releases per bird to identify salient landmarks for each bird individually. In addition, the analysis of data from flocks of birds using this technique may provide further evidence for visual lateralisation, and offer additional insight to the large body of work on flock hierarchies and dynamics (Sasaki et al., 2018; Flack et al., 2013; Nagy et al., 2010). For

example, comparing the difference in fovea alignment points identified by leaders and followers in a flock. Evidence for lateralisation may only emerge from a much larger dataset, with a larger range of landscapes that the birds fly over, that isn't masked by landscape biases such as woods on one side. In addition, undertaking releases from a wider range of release sites further from the loft, including unfamiliar locations, could prove highly informative allowing the generality of this result to be tested.

A number of methodological factors will contribute to uncertainty in identified fovea alignment regions. These include GPS error, sensor board misalignment with the head axis and sensor fusion error. Although the angular error will be the same at any distance from the track, the effect of these errors on the heatmap generation is larger the further the points of visual attention are from the track. Therefore, identifying specific pinpoint features more than a few hundred meters from the track, rather than general regions of interest such as a village is unlikely to be possible. The precision of this technique could be considerably improved with the incorporation of altitude and head pitch data allowing one specific point to be identified for each saccade rather than assuming a line of possible points. However, GPS-derived altitude data are extremely error-prone (Reynolds 2016) and therefore this would require the addition of a barometric altimeter or differential GPS module (also requiring a ground station) to the instrumentation. Another possible future development is the use of head-mounted video cameras to verify the focus of visual attention. Existing miniature commercially available lenses lack the resolution and wide field of view required to capture the broad but detailed visual scene available to navigating pigeons. However, future iterations are likely to play an important role in elucidating the focus of visual attention in birds flying in their natural environments, possibly used in combination with

head mounted IMUs. Such techniques could revolutionise our understanding of large-scale spatial cognition in a paradigmatic avian model.

Chapter 6. Gaze strategy during pursuit in a visually guided predator

6.1 Abstract

Peregrine falcons (*Falco peregrinus)* rely on aerial attack behaviours for predation using visual information to guide their trajectory to target interception. To understand how peregrines implement the underlying feedback law governing pursuit, it is important to determine their gaze strategy both in relation to the visual environment and to the target. There are at least three possible gaze strategies: (i) fixing the head relative to the body, (ii) continuous tracking of the target with smooth head movements, and (iii) fixing the head relative to the visual environment using nystagmic head movements to keep the target in field of view. To differentiate between these mechanisms, we released peregrines trained to pursue and intercept a falconer's lure towed by a small remotely controlled aircraft. The birds were fitted with a head-mounted inertial measurement unit (IMU) to track gaze direction and a GPS logger to track the peregrine's position during flight. We found that in the final phase of pursuit, rather than stabilising their gaze against the background, peregrines continuously track the target position using either their frontally or laterally facing fovea, depending on the angle of their approach. While the birds show a preference for approach angles that allow them to align their head with their body, making them more streamlined, the head also makes some saccadic movement independent of the body. Our findings led us to hypothesise that peregrines' heads behave much like the seeker of a

guided missile, where information gathered from the tracking movements of the head when locked onto the target is fed back into the guidance law used to intercept the target.

6.2 Introduction

Many birds rely on aerial attack behaviours for predation using visual information on their target to guide their trajectory to interception. Previous research has characterised these behaviours by describing the geometry of pursuit trajectories between the pursuer and its target (Tucker et al., 2000; Kane & Zamani, 2014). Recent research using GPS loggers to study peregrine falcons (*Falco peregrinus*) attacking manoeuvring targets revealed that the terminal attack trajectories of these predators can be described using the same guidance law (proportional navigation) used by visually guided missiles (Brighton et al., 2017). Physics-based simulations of aerial attacks by peregrines have corroborated these findings, demonstrating that the tuning of this feedback loop requires highly precise visual feedback (Mills et al., 2018). This chapter aims to build on previous work by measuring the head movements of peregrines when in pursuit of prey to further understand the mechanism used to implement proportional navigation.

Stabilising and directing their visual system using head movements is critical to enable birds of prey to extract the visual information required to guide their trajectory to target interception. While both head and eye movements can be used by animals to direct their visual systems and extract salient visual cues, compared with many mammals, birds exhibit only limited eye mobility. Therefore, birds tend to rely on head movement when shifting gaze, which is aided by their light heads and highly flexible necks (Land 2014; O'Rourke et al. 2010). During pursuit of a target, birds' eyes are thought to show an even greater tendency to be fixed in the primary gaze direction in order to reduce the processing required

to translate between head and eye coordinate systems (Ohayon et al., 2006; Wallman and Letelier, 1993).

Like pigeons, discussed in Chapters 4 and 5, the visual field of peregrines contains two regions of high visual acuity: the temporal (shallow) and central (deep) foveae. Anatomical measurements in a closely related species, the American kestrel (O'Rourke, Hall, et al., 2010), show that the temporal fovea meets the mid-sagittal head plane at 10 deg creating a 30 deg region of binocular overlap, while the central fovea is directed laterally at 45 deg in each eye. Bifoveate birds typically use their forward-facing temporal fovea when inspecting nearby targets, and the laterally directed central fovea to focus on more distant visual cues (Frost et al., 1990). The way in which peregrines direct these acute regions of their visual field in relation to the target during pursuit is essential to understanding the mechanisation of the guidance law used to intercept their target, proportional navigation. Proportional navigation commands the body turning at a rate ($\dot{\gamma}$) proportional to the rotation rate of the line-of-sight (i.e., LOS rate, $\dot{\lambda}$), such that

$$\dot{\gamma} = N\dot{\lambda}(t)$$

where N is the navigation constant that can be tuned to produce different pursuit geometries. Therefore, to command its body turn rate using proportional navigation, a peregrine must have some measure of the LOS rate – the change in angular rate between pursuer and target, determined relative to an inertial reference frame (Shneydor 1998). At least three possible visual strategies exist for extracting the information required for pursuit: (i) fixing the head relative to the body to reduce aerodynamic drag (like the strap down seeker of some guided missiles; Tucker et al. 2000); (ii) continuous tracking of the

target with smooth head movements (like the seeker of a guided missile), and (iii) fixing the head relative to the visual environment using nystagmic head movements (like an image-stabilised camera) and measuring the drift of the target across their retina. These strategies are discussed below.

(i) Given the high speed at which peregrines pursue their prey, often exceeding 50 m/s, aerodynamic efficiency is a key performance objective for natural selection acting on this predator. This observation led Tucker et al. (2000) to suggest that peregrines keep their body in line with their head during pursuit to reduce drag while keeping their central fovea (angled at 45 deg relative to the head axis) pointed sideways at the prey. The authors suggest that when the prey is close enough to be seen directly ahead using binocular vision, the falcon flies straight towards the prey. This strategy does not require the measurement of the LOS rate but instead gives rise to a pursuit geometry known as deviated pursuit. In this geometric rule, the pursuer directs its velocity at a non-zero lead angle ahead of the LOS angle (in this case 45 deg), producing a deviated pursuit course. However, Brighton et al. (2017) found that GPS-derived falcon pursuit trajectories cannot be described by a single geometric rule, such as deviated pursuit, suggesting that the trajectories are not simply an emergent property of the falcon's visual anatomy.

(ii) Guided missiles use a gimballed seeker to continuously track their target using onboard gyroscopes, which minimise the tracking error (ε) between the seeker centreline and LOS to the target (Figure 6.1). The dish rate ($\dot{\vartheta}$), the rate at which the seeker is turning to track the target, can then be used as an estimate of the LOS rate ($\dot{\lambda}$) and fed back into the guidance law (Palumbo et al., 2010). The head of a peregrine falcon is analogous to the seeker on a guided missile, as it is free to move independently of the body, and the fovea is equivalent

to the seeker boresight. If a bird is using its head like a missile seeker in tracking mode — attempting to minimise the tracking error with the target held on a fovea — it could theoretically be using its head turn rate (equivalent to the dish rate) as an estimate of the LOS rate. Kane & Zamani (2014) provided evidence to support this gaze strategy using head-mounted video data which suggested that during pursuit, gyrfalcons maintain their prey's image at constant visual angles on their retina coinciding with the location of their temporal fovea.

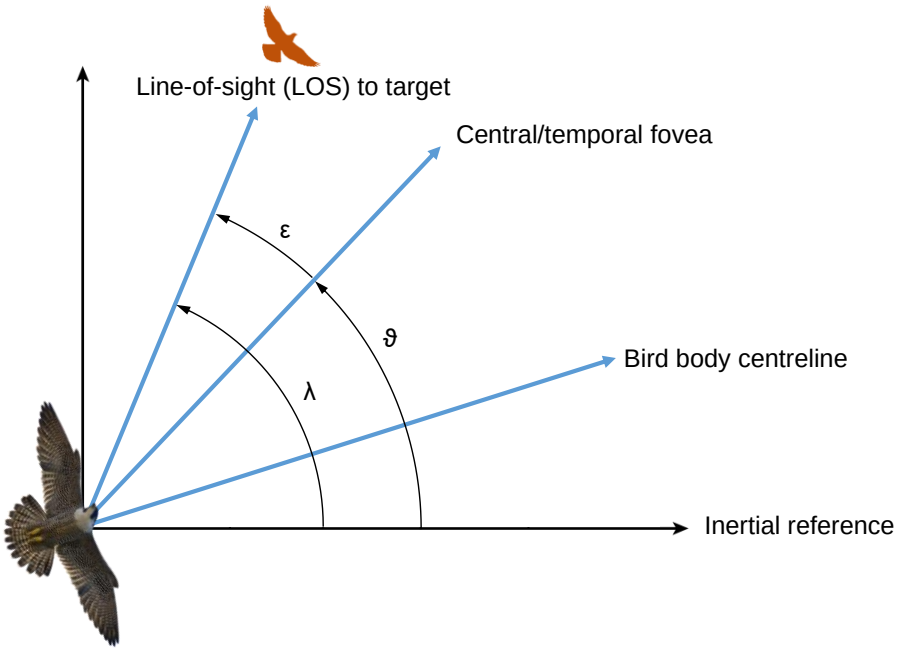

Figure 6.1 — Angles used to analyse the mechanisation of proportional navigation. Proportional navigation requires knowledge of the LOS rate $\dot{\lambda}$ to command the bird's body turn rate. The prey target is shown in orange.

(iii) Predatory birds often use rapid saccades to shift gaze between periods of fixation, as evidenced by head-mounted video cameras (Brighton et al., 2017; Kane et al., 2015). By

fixating on the background, birds can use the drift of the target across their retina to estimate the LOS rate, performing head saccades to keep the target at the centre of their field of view. This head stabilisation strategy has been observed in both dragonflies (Olberg et al., 2007) and bats (Ghose, 2006) during pursuit.

Here, we aim to differentiate between these gaze strategies using novel onboard instrumentation to track peregrines during pursuit. Although the use of GPS loggers and head-mounted cameras has gone some way to differentiate between these alternative gaze strategies, a detailed understanding of precisely how peregrines direct their gaze in relation to the target position is currently lacking. We address this knowledge gap using a custom-built head-mounted inertial measurement unit (IMU), capable of tracking head orientation at high frequency, synchronised with a GPS logger to track peregrine and target position during pursuit. This device allowed us, for the first time, to directly measure the angular quantities used to analyse the mechanisation of proportional navigation, enabling us to explicitly test the hypotheses detailed above. This chapter reports the results of these flight tests and discusses the findings in the context of both the engineering guidance literature and the visual ecology of peregrines.

6.3 Methods

6.3.1 Subjects

Three captive-bred peregrine falcons ("Robyn": ♀; "Robina": ♀; "Mo" ♂) aged <1 y were trained to fly at a falconer's lure towed by a small remote-controlled aircraft. The birds had flying maeeses in the range 745 – 950 g.

6.3.2 Experimental protocol

The main experimental procedure involved methods first developed by Brighton (2015), who released falcons to pursue a food lure resembling a winged prey item, which was towed on a 5 m kite line by a small remote-controlled aircraft (Figure 6.2). The falcon was allowed to gain height before the aircraft was launched and the pilot was instructed to perform manoeuvres that caused the lure to move unpredictably. Upon interception, the lure was released from the aircraft on a parachute, which allowed the bird to ground the target for it to be retrieved by the falconer. This protocol was reviewed and approved by the Animal Welfare and Ethical Review Board of the University of Oxford's Department of Zoology. Flight tests were carried out in August and September 2016 at Gelligaer Common (51.723520 N, -3.303710 W) in Monmouthshire (Wales, UK), at locations chosen daily according to local wind conditions (Figure 6.3).

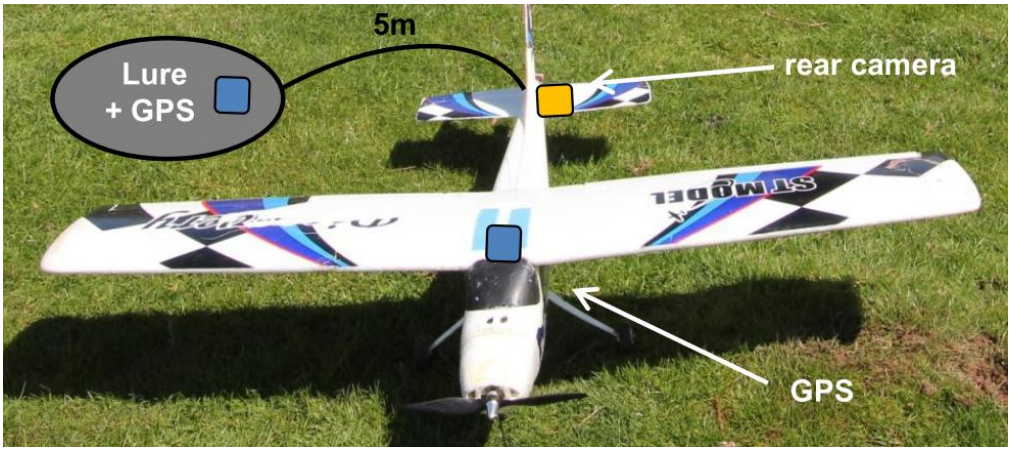

Figure 6.2 — Remote controlled airplane used in experiments, showing positions of the GPS units and camera, and attachment point of the lure line. Reproduced from Brighton (2015).

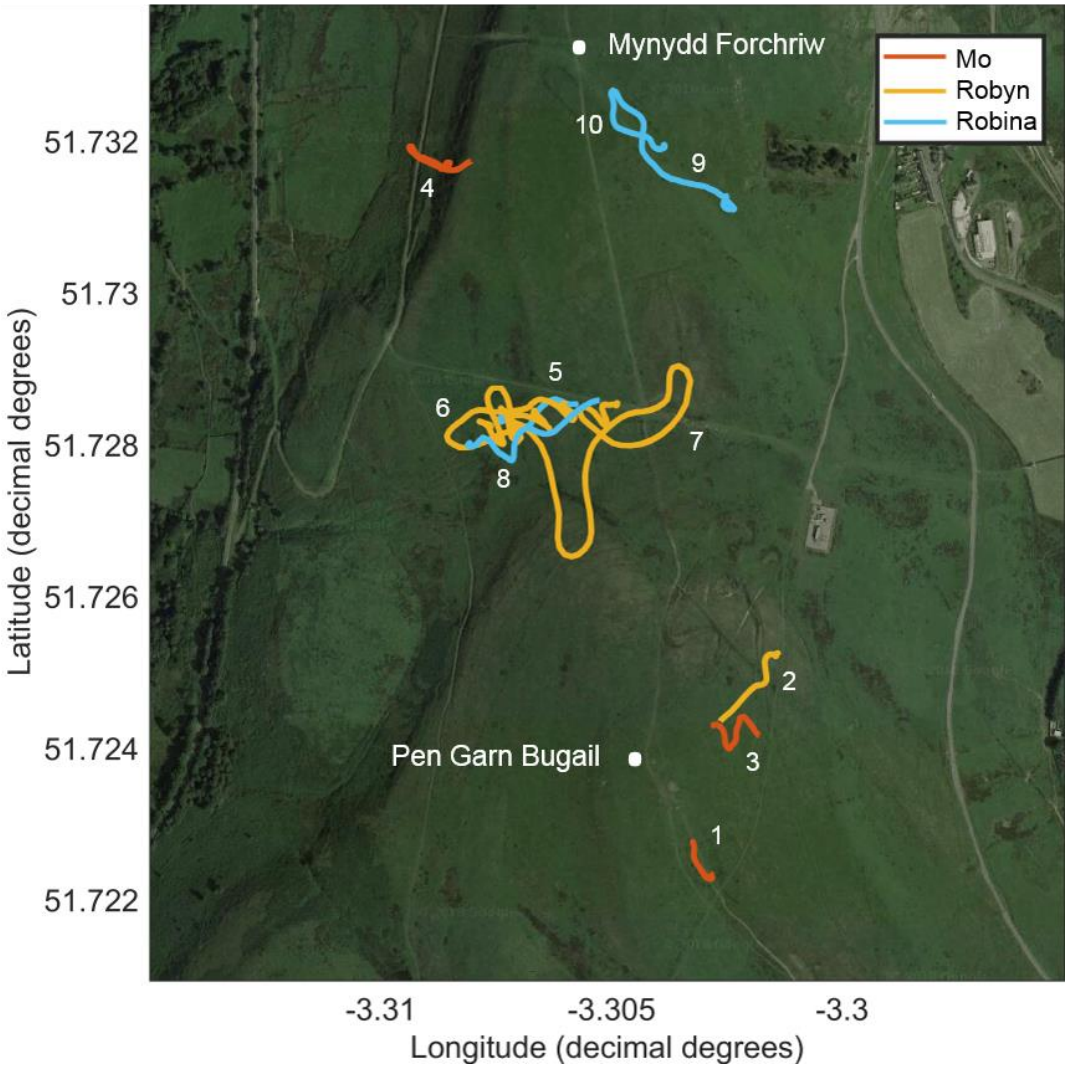

Figure 6.3 — Satellite image of Gelligaer Common with all 10 flights overlaid coloured by bird, see also Table 1.1. The two peaks are marked in white.

6.3.3 Instrumentation

Each bird carried a custom-made inertial measurement unit (IMU, Adafruit BNO055) with logger and GPS receiver (Adafruit MTK3339) to simultaneously record peregrine head movement and position during aerial attacks. The development of this device is detailed in Chapter 3. The device recorded synchronised GPS data at 10 Hz and IMU data (three-axis gyroscope, accelerometer, and magnetometer) at 60 Hz. See Chapter 3 for an experimental

validation of its measurement accuracy during flight. The IMU was mounted on a custom-made eye-less leather hood (designed and built with Martin Cray) using double-sided tape and strapped to the bird's head (Figure 6.4). The GPS logger, SD card, battery and microcomputer were worn dorsally on a falconry harness (TrackPack; Marshall Radio Telemetry) attached using a 3D printed fitting (designed and printed by Malcolm Beard). The birds were initially habituated to wearing the eye-less hood and instrumentation when sitting on a perch for 20 mins on two consecutive days prior to flight-testing. Prior to each flight, the IMU was calibrated using a 3D printed cuboid (see Chapter 3 for the detailed procedure). The instrumentation, mask and harness had a mass of 32.8 g and constituted 4.4% of the body mass of the smallest bird at its lowest flight mass (745 g). For two flights using one bird (Mo), a high definition video camera (HD720P Mini DV, 30 fps, resolution: 1280 x 720 pixels) was mounted on the bird, instead of the GPS and IMU. The battery and logging unit was mounted dorsally and the lens was mounted on the hood attached via an extension ribbon cable. The total camera mass was 18.6 g, giving a combined mass of camera, mask and harness of 29.5 g. At least seven test flights were carried out with each bird without any instrumentation to familiarise it with the pursuit setup, followed by three to six flights with only a back-mounted GPS, before introducing the birds to the hood.

The target (the falconer's lure) was fitted with two GPS devices (Qstarz BT-Q1300; Qstarz International Co. Ltd, Taipei, Taiwan) logging at 5 Hz and attached to the kite line with their patch antenna facing outwards (Figure 6.2). The plane was also fitted with two GPS Qstarz GPS devices and an HD720P Mini DV camera that was fixed beneath the aircraft facing backwards towards the towed lure. All GPS devices were allowed to settle for at least five min prior to the flight to ensure an accurate fix. Wind data were recorded for each

flight using a 10 Hz 3D sonic anemometer (Windmaster, Gill Instruments, Hampshire, UK) located 1.8 m above the ground within 50 m of the bird's take-off position.

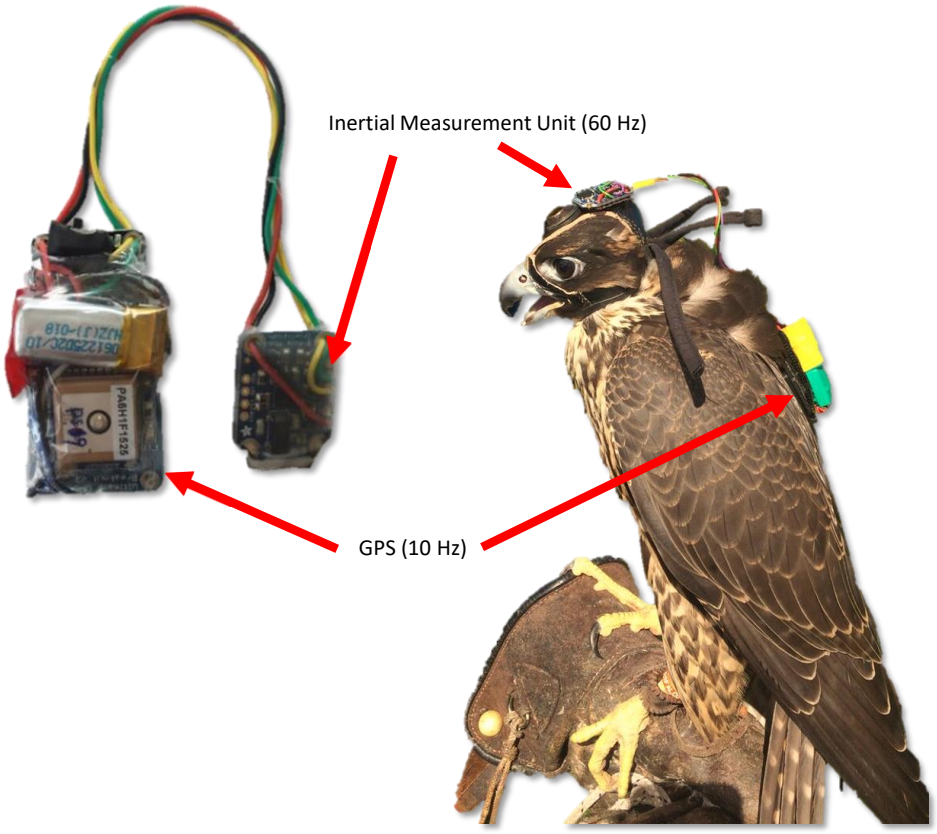

Figure 6.4 — Peregrine falcon wearing custom-made eye-less leather hood with head-mounted sensor attached via wires to back-mounted unit containing GPS and logger.

6.3.4 Data processing and analysis

All raw IMU data were plotted in MATLAB (R2017b, Mathworks) for visual inspection each day after importing from the SD card. GPS data were overlaid onto satellite images using Google Maps API (Bar-Yehuda, 2015) in MATLAB for inspection before being converted to meters using a Universal Transverse Mercator projection. These data were screened using an internal validation method for loss of precision by comparing the highly accurate Doppler shift groundspeed estimate against the noisier differenced groundspeed

estimate, see methods described in Brighton et al. (2017). From a total of 16 flights from three birds, nine flights met all of the quality criteria described above with accurate data from the head-mounted IMU, bird GPS and lure GPS, and were therefore used in subsequent analysis. An additional two flights were recorded using a head-mounted camera, which was not quantitatively analysed, but instead used to validate and help interpret the results from the IMU.

6.3.4.1 Track analysis and synchronisation

We identified the start time of each flight, along with the time the bird intercepted the lure, using the onboard plane camera to the nearest frame. The start point of the flight was then identified using the groundspeed from the bird GPS, and the bird GPS interception point was calculated using the time interval between the flight start and interception point identified from the video. The position estimates from the two GPS devices on the target were averaged to improve positioning accuracy (Schrader et al., 2016). We then used quintic spline interpolation of the bird and target GPS data to reduce the effect of sudden jumps in position. Bird GPS data were down-sampled to 5 Hz to match the target GPS for subsequent analysis. The timestamp from the bird GPS intercept was matched with the target GPS to identify the lure intercept, and both tracks were translated so that the coordinates of the target and bird both lay at the origin. This translation allowed us to remove discrepancies arising from the inaccuracy associated with absolute GPS measurements. The LOS vector from the bird to the target was calculated between each bird GPS point and the corresponding time-matched target GPS point. Flights with two passes at the target (flights 6, 8, 9 and 10 — judged by plane camera footage and GPS data) were partitioned into two sections and both used to contribute to subsequent figures, as has been done previously for the treatment of similar data (Brighton et al., 2017). This inclusion

of multiple passes within multiple flights of multiple birds leads to inherent problems of pseudoreplication if the datapoints are treated as being statistically independent, and they are therefore not treated in this way here.

6.3.4.2 Retinal coordinate estimation

Raw IMU data were post-processed using custom-written MATLAB code. The data were fused to give estimates of the sensor board's orientation in inertial space relative to magnetic north and gravity (in the form of Euler angles, Figure 6.5B). This was achieved using open-source code adapted from Barton (2012) and Reynolds (2016), see Chapter 3 for details. The sensor board yaw angle was used as an estimate of the peregrine's gaze angle, which indicates where the bird is directing the binocular region of its visual field. The retinal coordinate was calculated for each GPS point as the angle between the board yaw vector (blue arrow Figure 6.5) and the line of sight vector between the bird and the target. This value gives an estimate of the location of the target on the peregrine's visual field, where zero is directly ahead and 180 is directly behind the bird's head (Figure 6.5A). For the retinal coordinate analysis, we excluded GPS points of the bird and lure that lay within the device 50% Circular Error Probability (50% CEP) range as these points were found to result in spurious retinal coordinate angles. Given that 50% CEP is 3 m for each device — meaning that 50% of readings will be within 3 m of the true position – this led to points within 4.2 m of each other being excluded.

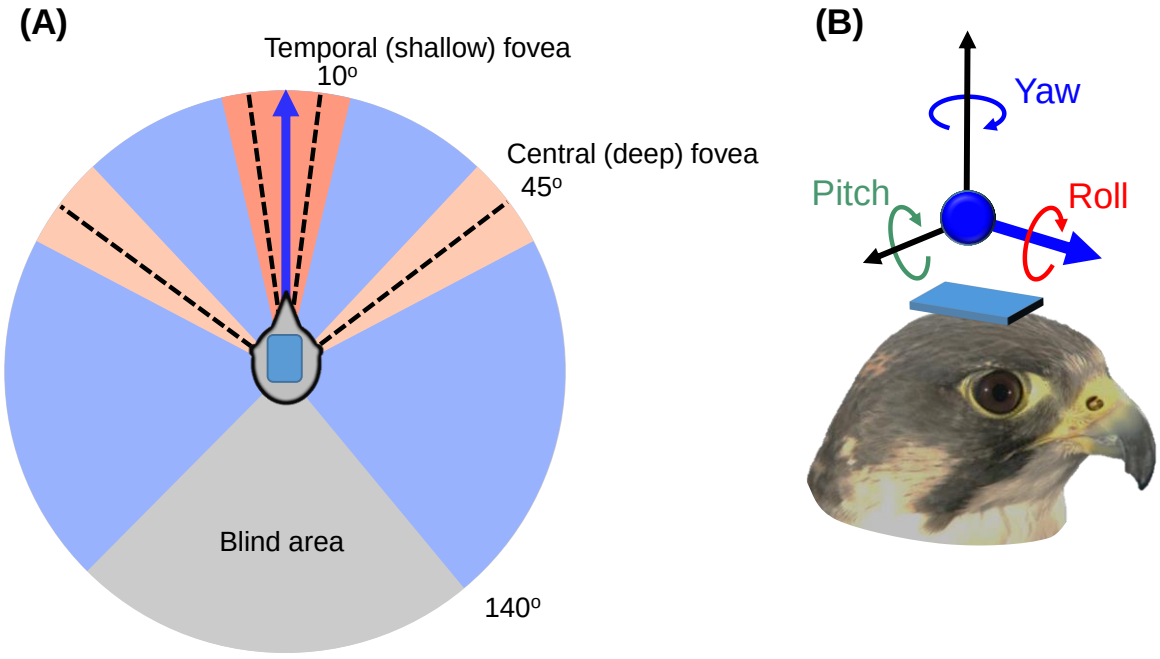

Figure 6.5 — Visual field and sensor board axes on peregrine's head. (A) Visual field of a peregrine falcon with the two fovea angles of each eye drawn relative to the head axis (blue arrow) assumed here to be aligned with the sensor board yaw axis. Angles taken from O'Rourke et al. (2010) and Tucker (2000) and subsequently referred to as retinal coordinates. 5 deg either side of central fovea shown in orange accounting for uncertainty in fovea position and sensor fusion error. Region of binocular overlap shown in red and blind area in grey. (B) Axes of sensor board mounted on the peregrine's head with rotational axes of the bird's head labelled. Yaw angle (blue arrow), measured by the sensor relative to magnetic north and assumed to be aligned with the mid-sagittal head plane.

6.3.4.3 Target tracking analysis

To test predictions on the mechanisation of proportional navigation, the relationship between tracking error (ε — Figure 6.1) and both head turn rate and body turn rates was determined for each flight. The tracking error is referred to in the missile guidance literature as the angular difference between the line-of-sight to the target and the seeker (the bird's head) centreline. However, given that peregrines have three acute regions across their visual field (Figure 6.5A: 0 deg, +45 deg,-45 deg), we chose the seeker centreline angle

that minimised the tracking error (the angle between the fovea and target) for each timepoint throughout the flight. Head turn rate was determined in the body reference frame as the rate of change of the angle between the air velocity vector and the IMU-derived inertial head-yaw angle. The air velocity vector is used as an estimate of the body orientation and calculated by subtracting the wind vector (wind direction and speed, averaged across the flight) from the GPS-derived ground vector (track angle and groundspeed). This vector is plotted as black lines extending from each GPS point in Section 6.6 (Appendix A). The head turn rate was regressed against tracking error incorporating a range of delays between 0.0 and 0.2 s to account for the difference in frequency of gyroscope (60 Hz) and boresight error (5 Hz) measurements. Body turn rate was calculated as the change in angle of trajectory between successive GPS points. The deviation angle, the angle between the peregrine's velocity vector and the instantaneous line-of-sight to target, was calculated using successive peregrine and target GPS points.

6.4 Results

The head-mounted sensor was successfully used to record 10 flights of the three birds (summarised in Table 6.1, Figure 6.7 and Section 6.6 — Appendix A). As with pigeons discussed in previous chapters, we found that peregrines change the direction of their gaze via saccades (rapid motions of the head) between periods of visual fixation, see blue line in Figure 6.6. However, peregrines had longer periods of fixation than pigeons. During short sections of non-pursuit flight (when the bird was airborne but the target was still on the ground – flights 6 & 7) we observed that, like pigeons, peregrines pre-emptively turn their head in the direction of a change in flight direction. We found no obvious differences between individual birds in terms of their maximum flight speed, approach direction, or

catch success. Given that the birds were naive hunters, the flight distance and maximum speed tended to increase over the testing period as they became more experienced.

Flight number	Bird	Date	Flight distance (m)	Max speed (m/s)	Discrepancy at intercept (m)
1	Mo	23 Aug 2016	190	9.4	14.3
2	Robyn	24 Aug 2016	493	12.2	16.2
3	Mo	24 Aug 2016	449	14.7	5.4
4	Mo	31 Aug 2016	651	16.7	25.4
5	Robina	1 Sept 2016	571	17.8	14.2
6	Robyn	1 Sept 2016	2177	23.6	6.7
7	Robyn	6 Sept 2016	1283	34.4	21.3
8	Robina	6 Sept 2016	940	18.3	34.3
9	Robina	7 Sept 2016	1109	25.8	25.0
10	Robina	7 Sept 2016	526	14.4	45.6

Table 6.1 — Summary of flights recorded with bird ID, distance flow, maximum flight speed and the discrepancy between bird and lure GPS's at interception (i.e. the distance that the trajectories were shifted in order to align interception points).

6.4.1 Peregrine saccade characteristics differ from pigeons

The use of the same instrumentation to study peregrines in this Chapter and to study pigeons in Chapter 4 and 5 allows a unique opportunity to directly compare the saccade characteristics between a predator and its prey. The pattern of head movement in peregrine falcons was found to be less saccadic than that of pigeons, showing smoother, less frequent head movement. Figure 6.6 shows a time series of the LOS angle, the bird track angle from the GPS and the head yaw angle (blue arrow, Figure 6.5) for an example flight (flight 4, see Appendix B for track plot). This flight was selected because it illustrates the saccadic behaviour of the bird during a 180 deg turn followed by a period of fixation from ~3.5 s before intercept where the head (blue arrow) is fixed in inertial space. During the turn, the bird shows punctuated changes in primary gaze angle that precede the turn (compare bird

track angle and head yaw), as was found in pigeons, see Chapter 5. However, as discussed in Chapter 5, although the GPS track angle is an estimate of the body orientation throughout the flight, the air velocity vector will be offset from the GPS velocity vector due to the wind (see Chapter 2 for full discussion of this effect), and body axis may not be aligned with the air velocity vector. Nevertheless, the difference between the bird track and the head yaw angle provides an estimate of the bird's head skew throughout the flight.

The retinal coordinate (Figure 6.5B) is the difference between the LOS (Figure 6.6 – green line) and head yaw (Figure 6.6 – blue line). If the bird is using the temporal fovea to fixate the target, then this is also equivalent to the tracking error (ε). However, if it the bird is using either the left or right central fovea, then this tracking error will be offset from the head yaw angle by approximately ± 45 deg. Figure 6.6 appears to show that the target is fixated on the left central fovea in the final 3.5 s of pursuit for this flight while the head orientation remains fixed in inertial space. During this period of fixation, the pursuit geometry can be described as parallel navigation (Brighton et al., 2017), where the LOS angle remains relatively constant. It is clear from both Figure 6.7 and Section 6.6 (Appendix A) that sections of pursuit across many of the flights can be described as parallel navigation where the plotted LOS lines between pursuer and target are parallel.

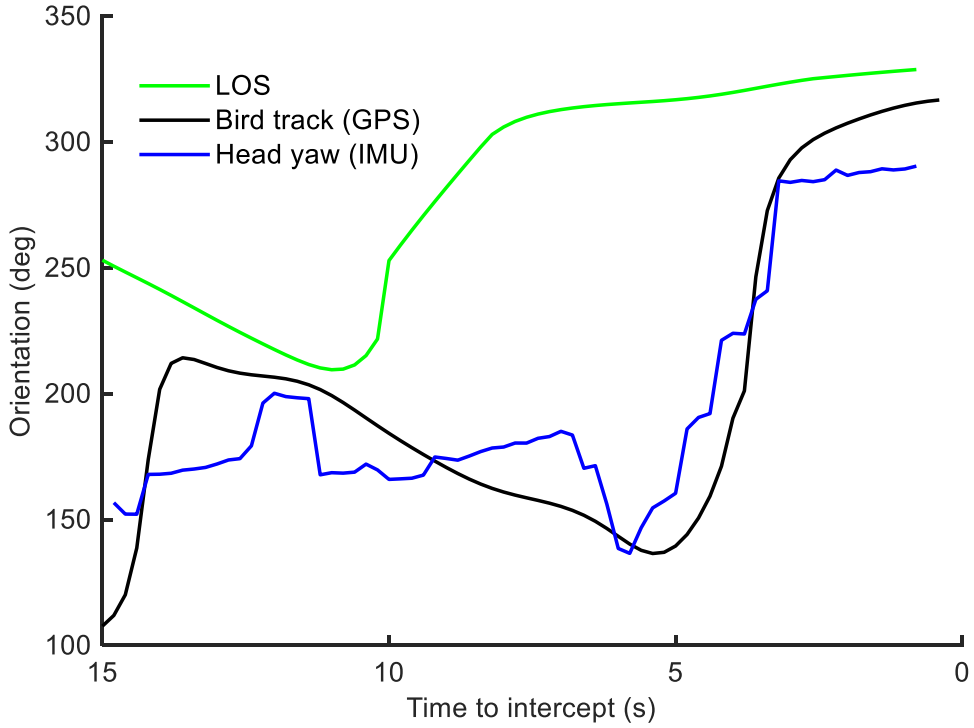

Figure 6.6 – Example flight (flight 4, see Appendix A for GPS track plot) showing the times series of LOS, bird track and head yaw. The retinal coordinate is the difference between the LOS angle and head yaw angle.

Unlike pigeons, we found no significant phase bias of peregrine saccades in relation to the wingbeat timing. The methods described in Chapter 4 were used to identify 880 saccades across 10 peregrine flights from head-mounted gyroscope data and to identify their phase within wingbeats using head-mounted accelerometer data. These data were pooled, treating each saccade as an independent event, as has been done in previous analyses (Kress et al. 2015) . In contrast to pigeons, the Omnibus test for circular uniformity found no significant departure from randomness in the saccade-start wingbeat phase ($m = 94$, $df = 879$, $p = 0.12$) or saccade-end wingbeat phase ($m = 50$, $df = 879$, $p = 0.19$) relative to vertical velocity peaks caused by the wingbeat. *C* values were calculated using methods described in Chapter 4 and found to be 0.17 and 0.11 for start and end timings respectively (where higher values represent a greater departure from circular uniformity). However, note that

this effect size is not adjusted for sample size. The lack of significant departure from circular uniformity could be explained by the small sample size; however circular histograms did not indicate a bias in any particular wingbeat phase.

We compared peregrine saccade timing characteristics against pigeons and previous studies in raptors, which indicate a different gaze strategy to pigeons but show similarities to other raptors during pursuit. Median within flight saccade latency (the time between successive head saccades) was 0.93 ± 0.42 s (mean ± sd) compared with 0.59 ± 0.21 s for pigeons. The distribution of saccade latencies pooled across all birds and flights was found to follow a log-normal distribution (Lilliefors goodness of fit test: $k = 1.32$, $df = 879$, $p = 0.0012$) consistent with the findings of previous studies of gaze shifts in raptors during pursuit using head-mounted video (Ochs et al., 2017). The authors attribute this result to the stochastic change in gaze direction on the basis of accumulated environmental information rather than a constant probability of gaze redirection over time. The median saccade latency for peregrines in this study was found to be remarkably similar to that of a Northern goshawk (*Accipiter gentilis*) during aerial prey pursuit (0.87 s) which may suggest similar underlying neural processes (Ochs et al., 2017).

6.4.2 Peregrines use both foveae to fixate their target during pursuit

We found that in the final phase of pursuit, peregrines continuously track the target position using either their frontally or laterally facing fovea, depending on the angle of their approach. The sensor board yaw angle and GPS data were used to estimate the retinal coordinate of the target on the peregrine's retina throughout the flight (Figure 6.5A). Figure 6.7 shows the pursuit trajectories of the bird and target with the bird trajectory coloured by the visual field region occupied by the target (the retinal coordinate). This plot shows that

when the bird approaches the target head-on or from directly behind (intercept of flights 2, 3, & 7 and first pass of flights 8-10), there is a tendency to focus the target on its region of binocular overlap (red). However, when the bird approaches the target from the side (intercepts of flights 1, 5, 8, 9, & 10), in the majority of cases it focuses the target on the central fovea at 45 deg (orange). Figure 6.8 shows a time series of retinal coordinates for all intercepts and near misses across the 10 flights. The time at which the target begins to be foveated is variable but in the final 3-4 s before intercept, peregrines appear to foveate the target using either the temporal (~0 deg) or central (~45 deg) fovea. Head-mounted video footage for two additional flights corroborated these findings, showing that the target is held at a fixed position on the camera's field of view to within a couple of degrees in the 3 s before intercept.

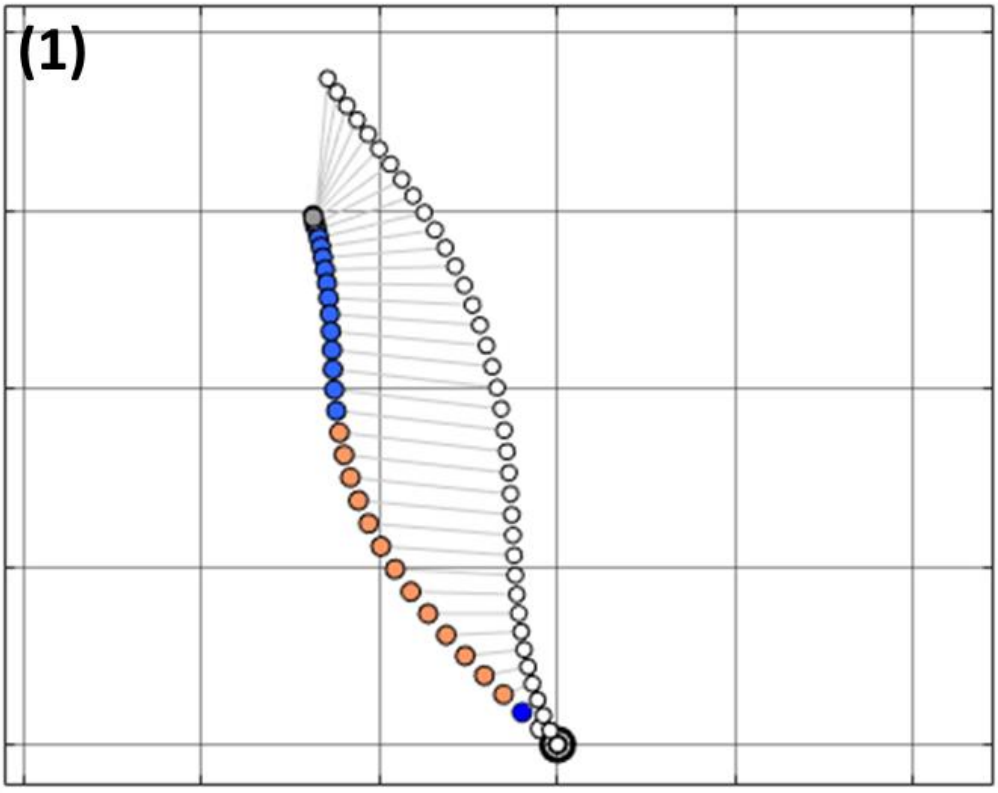
(1)

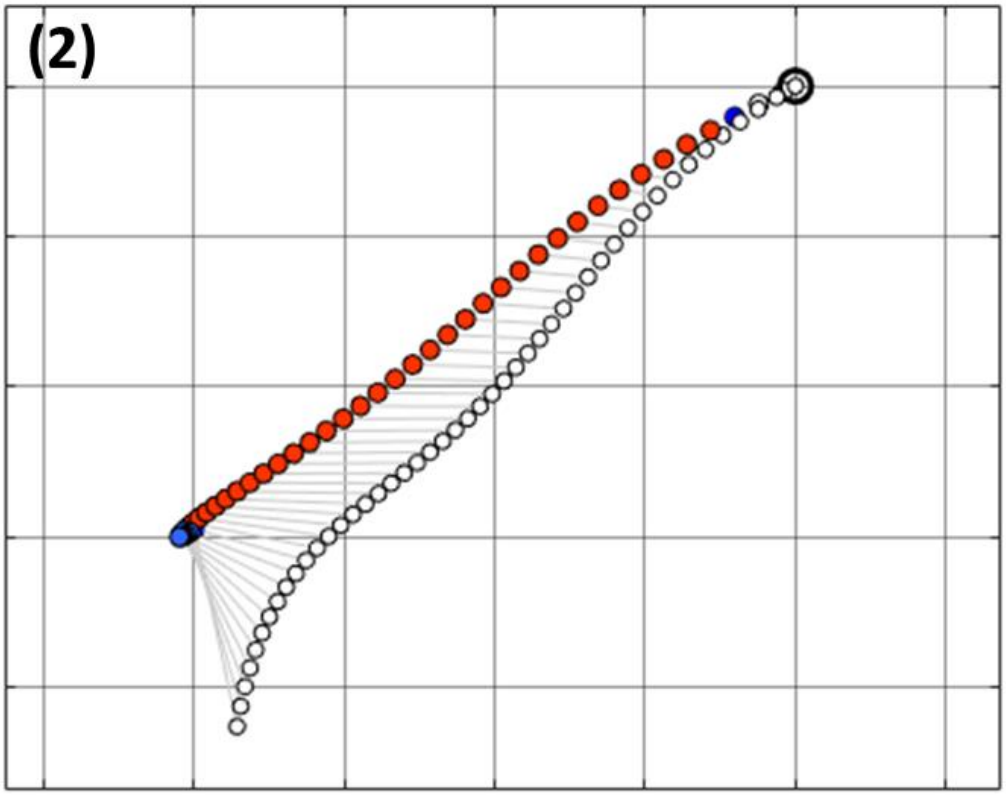
(2)

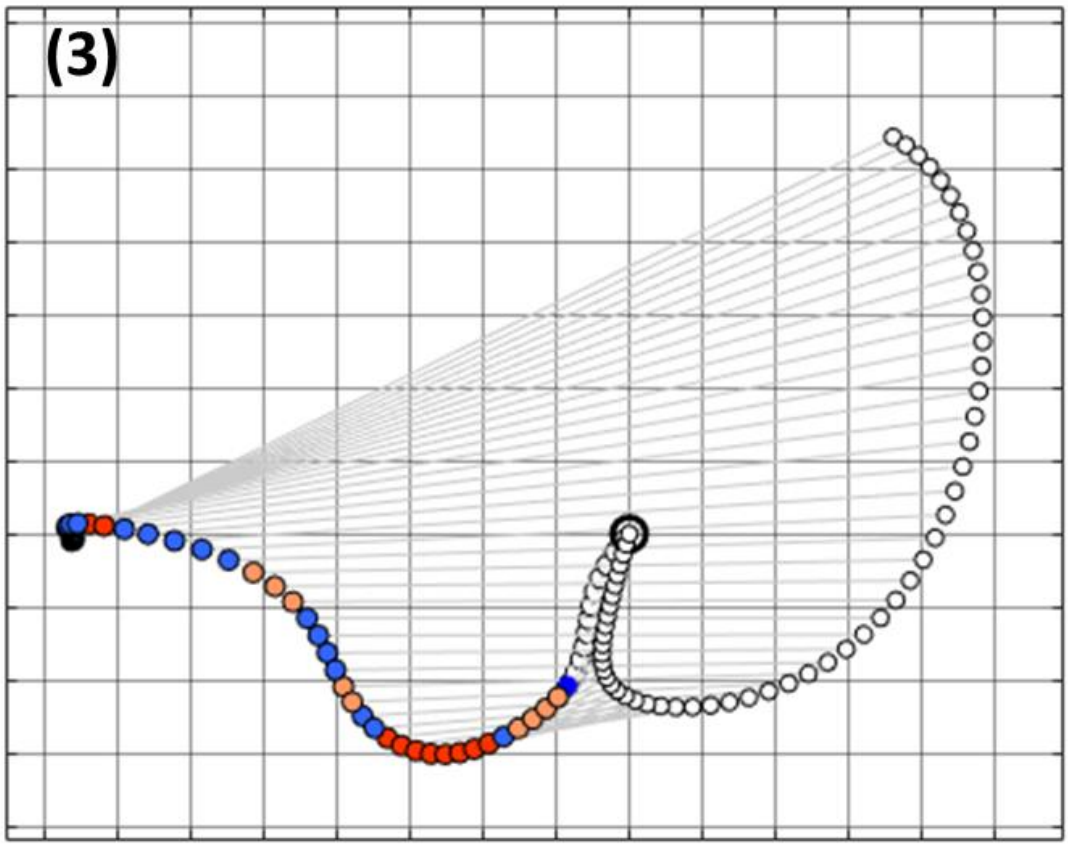
(3)

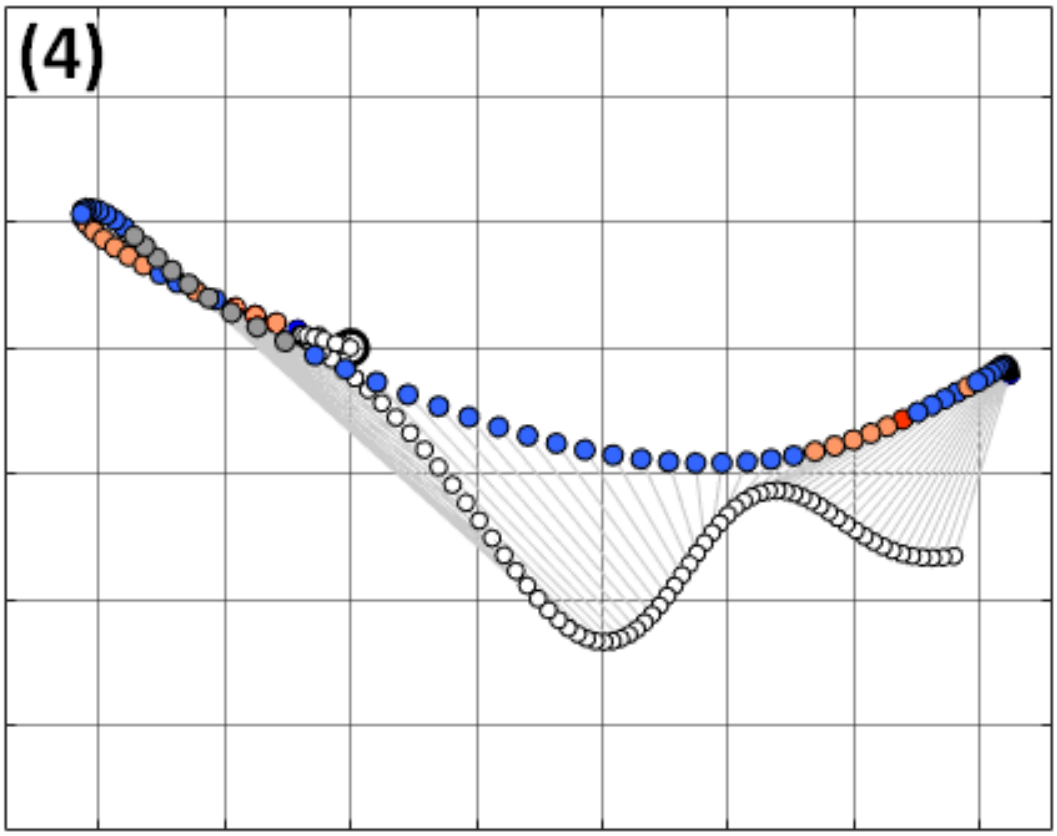
(4)

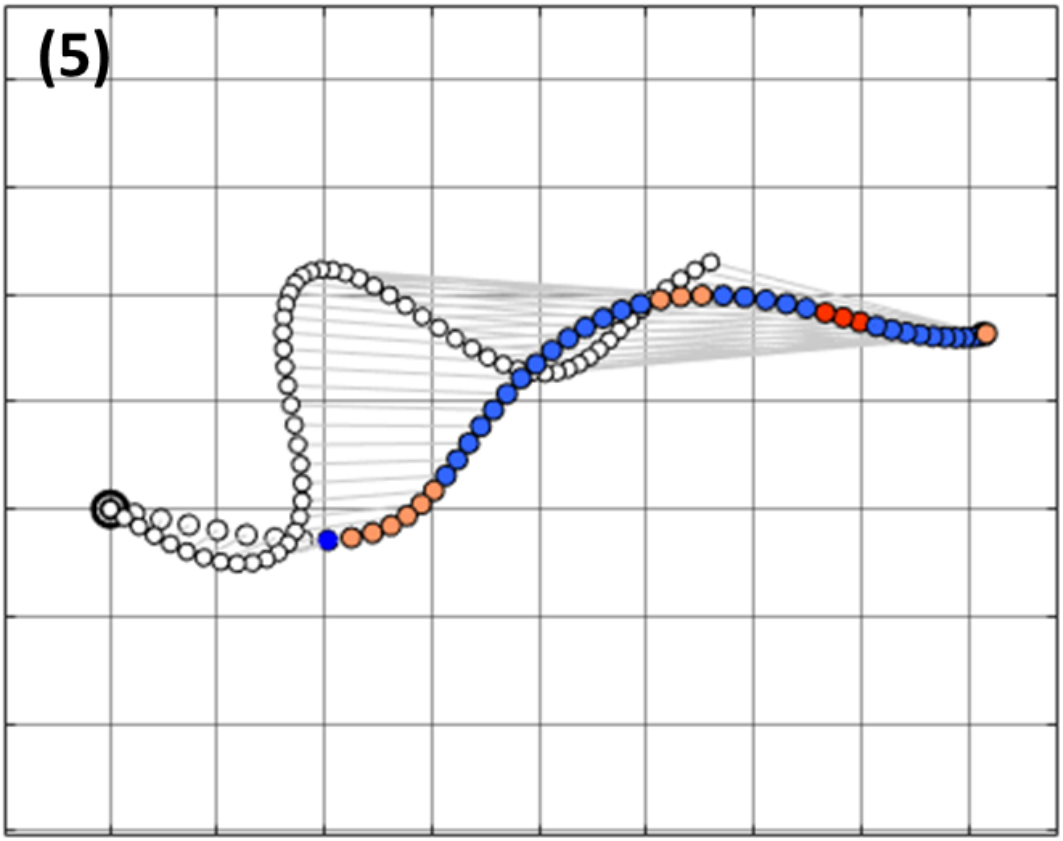
(5)

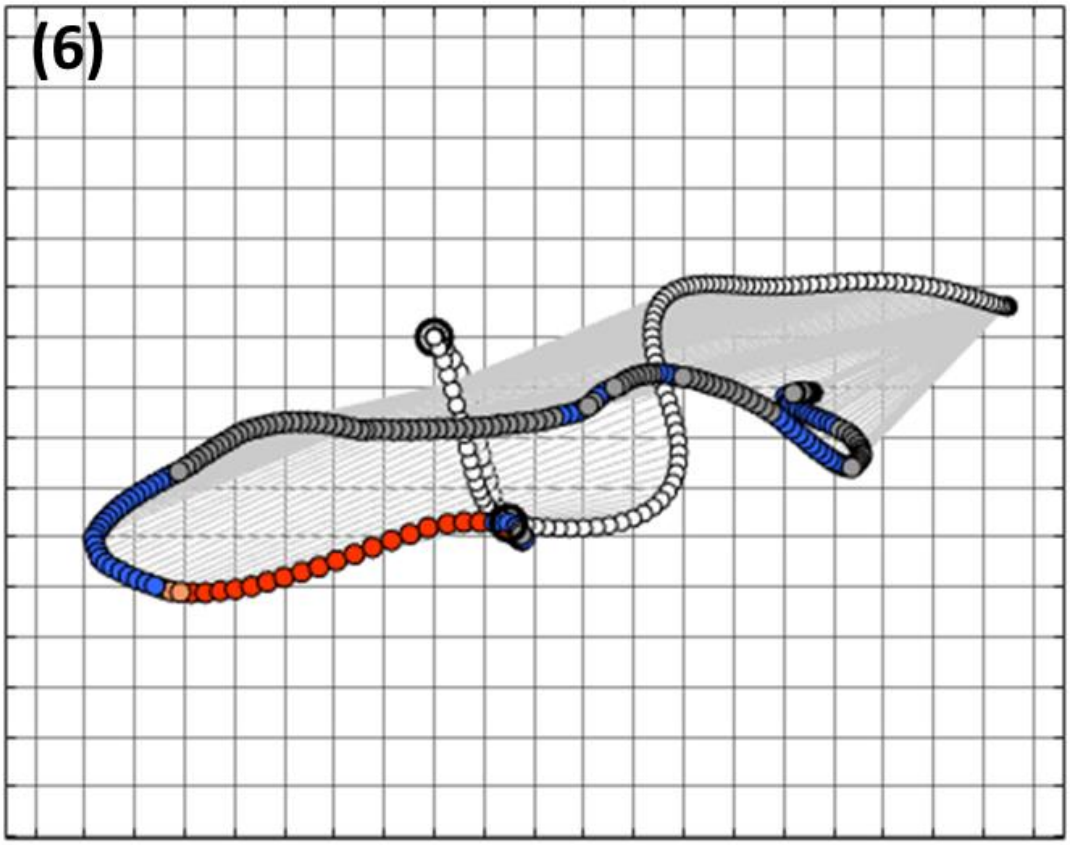
(6)

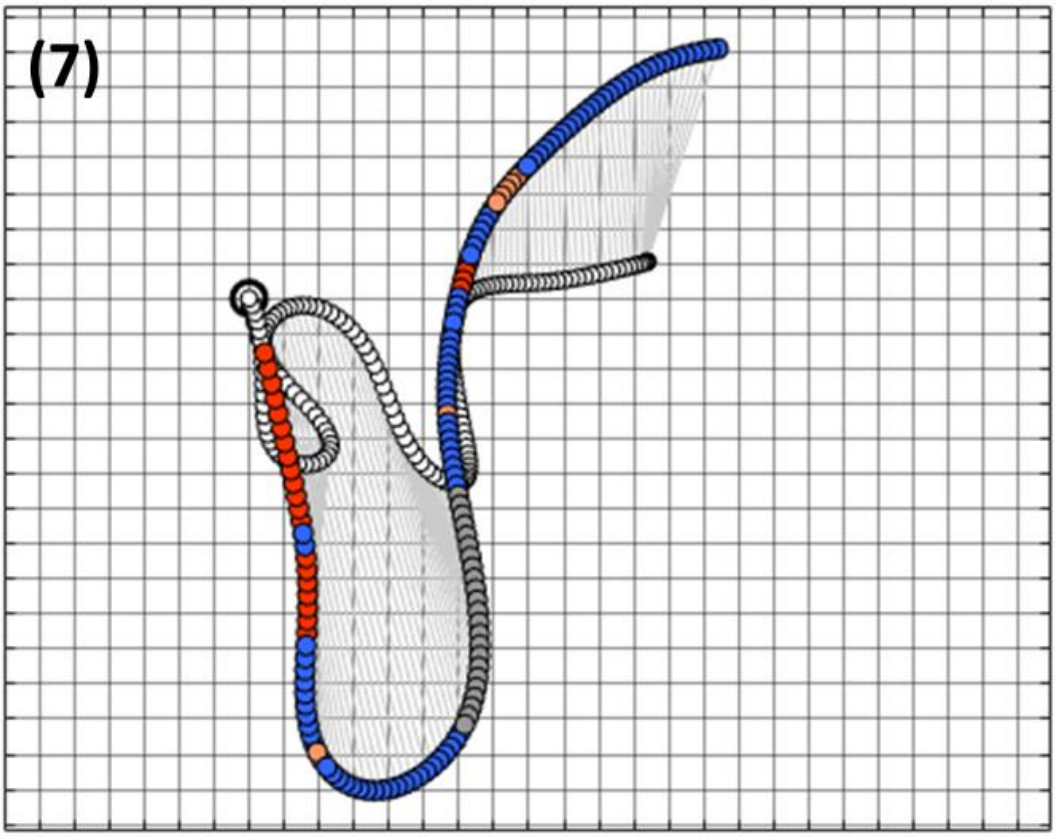
(7)

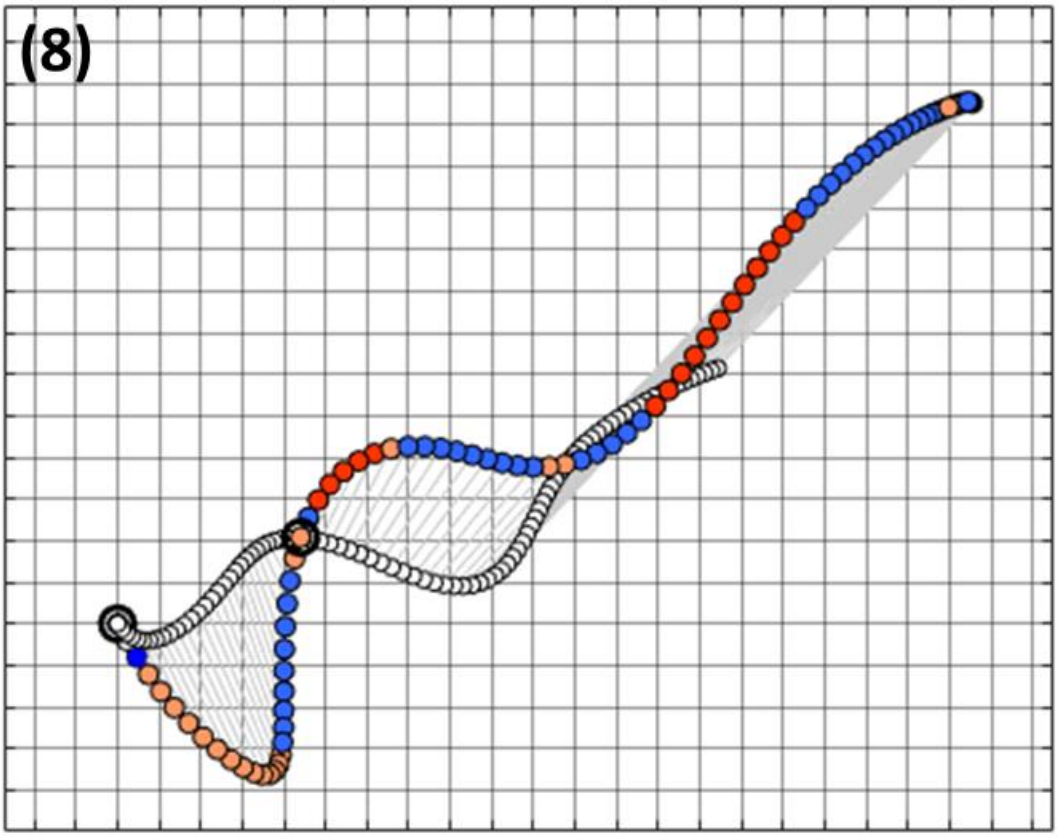
(8)

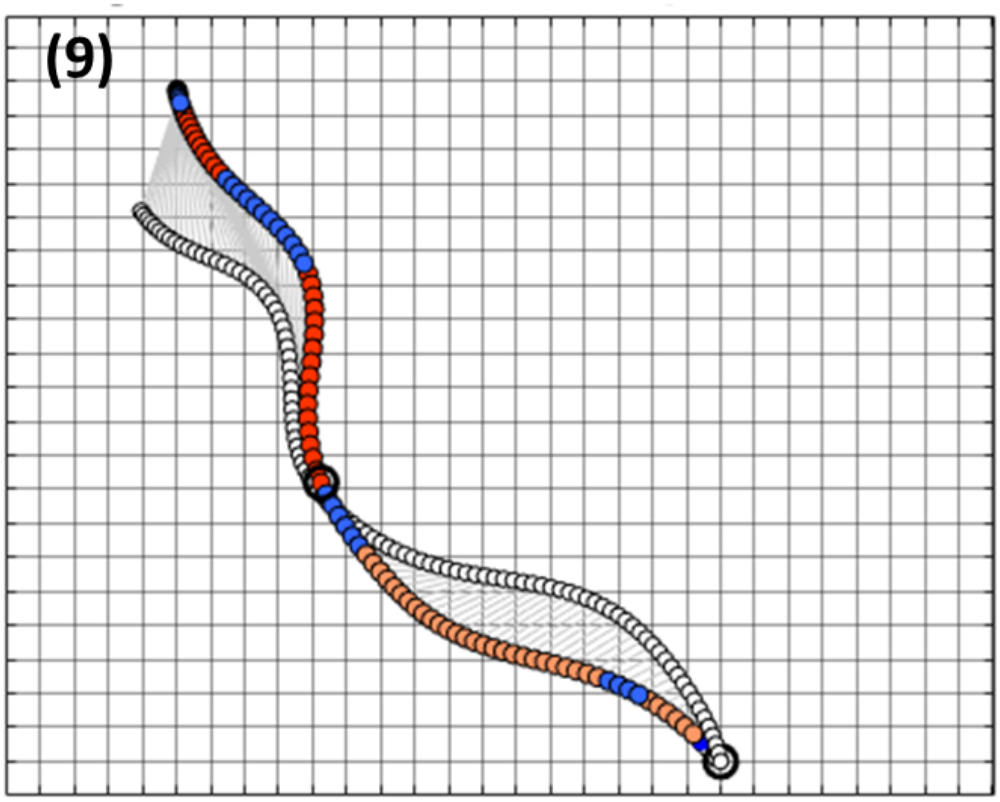
(9)

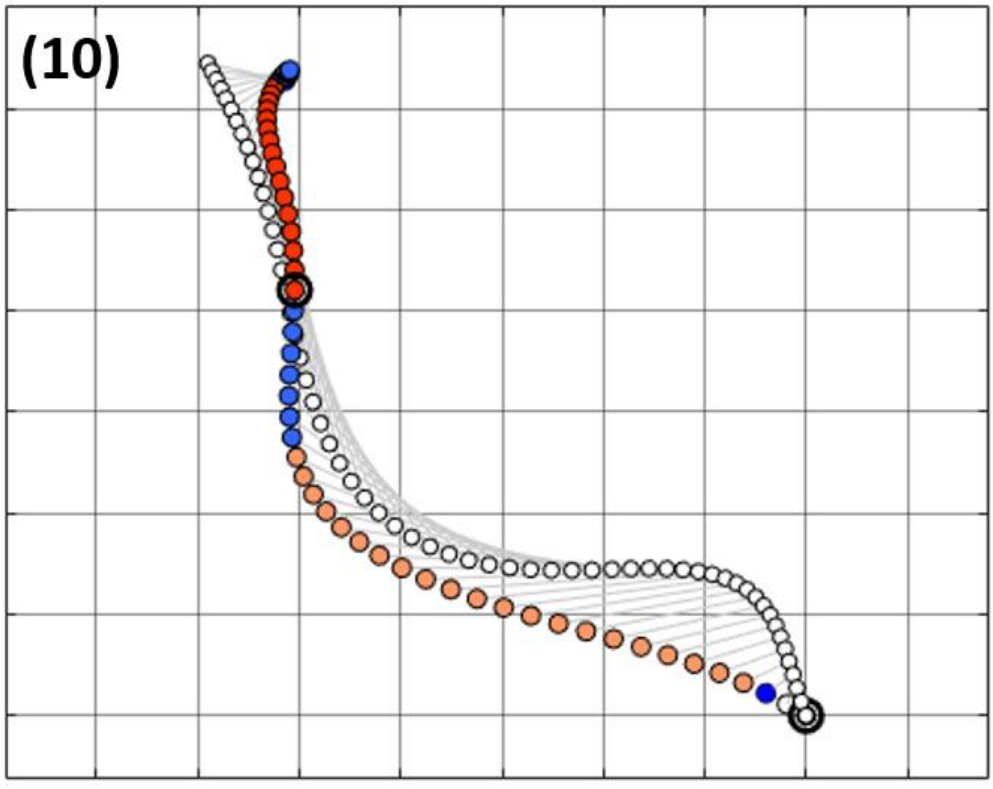
(10)

Figure 6.7 — GPS-derived trajectories of 10 pursuit flights (see Table 6.1) from three peregrines (coloured by the visual field region retinal coordinate on which the target is located – Figure 6.5A) and moving target in white. Intercepts or close flight passes indicated with a black circle, note the additional pass for flights 8-10. Bird GPS points that lie within 4.2 m of the target are within range of GPS error and are coloured white and removed from retinal coordinate analysis. The instantaneous lines-of-sight between bird and lure are shown in grey. Grid lines are at 10 m spacing.

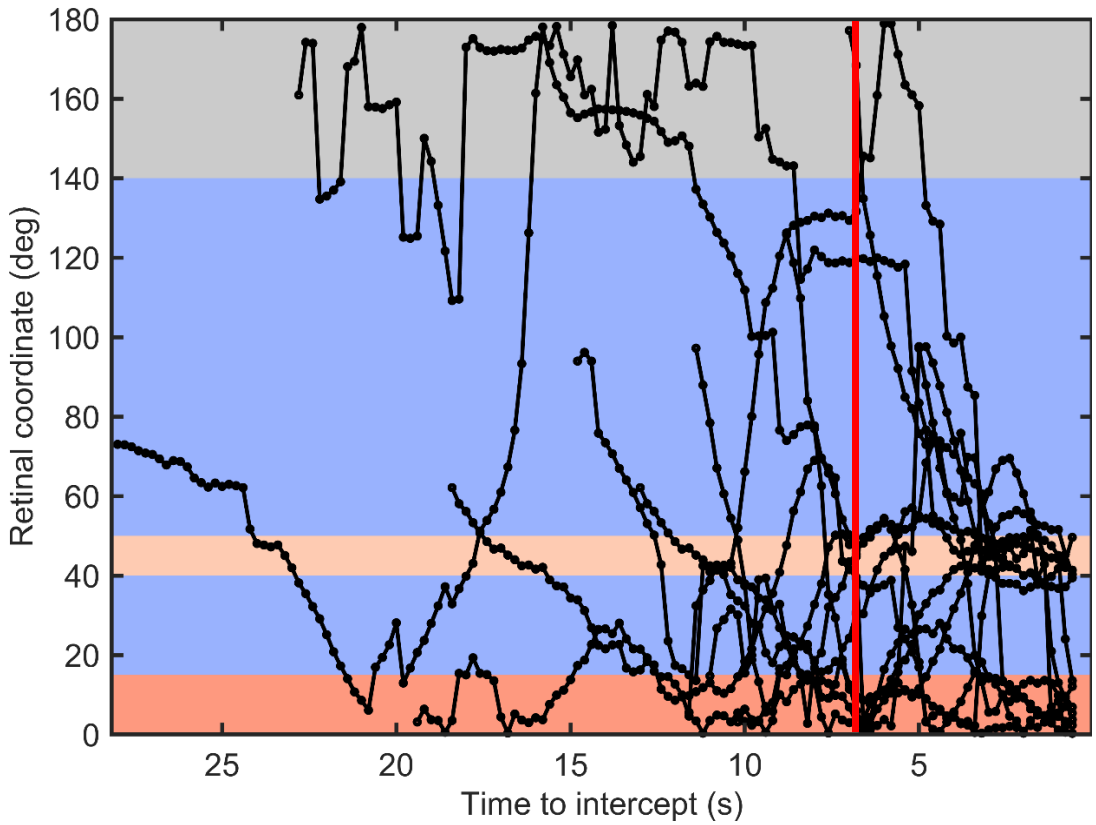

Figure 6.8 — Retinal coordinate (Figure 6.5) of target on peregrine visual field across 10 flights cropped to the time when both target and bird are airborne. Flights 8-10 containing one close pass at the target and one intercept (Figure 6.7) were split and plotted as separate lines aligning the pass and intercept with zero. Points where the bird and GPS lay within the range of GPS error (4.2 m) at the end of the flight were removed. The vertical red line indicates the point at which flights were cropped for subsequent analysis to include only the final stage of the pursuit.

The finding detailed above, that peregrines fixate the target using either their central or temporal fovea in the final few seconds before intercept, is demonstrated even more clearly in the histogram in Figure 6.9A. This shows distinct peaks aligning with assumed fovea angles from anatomical studies at 0 deg and 45 deg. Figure 6.9B illustrates the importance of applying GPS endpoint correction to each flight at intercept (detailed in Table 6.1) by displaying the distribution of retinal coordinates when the correction is not applied, which shows no clear bias towards certain retinal regions. The distribution of deviation angles between the peregrine's GPS velocity vector and the instantaneous LOS to the target (Figure 6.9C) highlights a weak tendency for peregrines to choose pursuit trajectories that allow them to keep their head aligned with their body while fixing the target on either central or temporal fovea. However, a scatter plot of retinal coordinate against deviation angle did not reveal clear point clusters at (0,0) and (45,45) suggesting that the peregrines are showing some degree of head movement relative to their body.

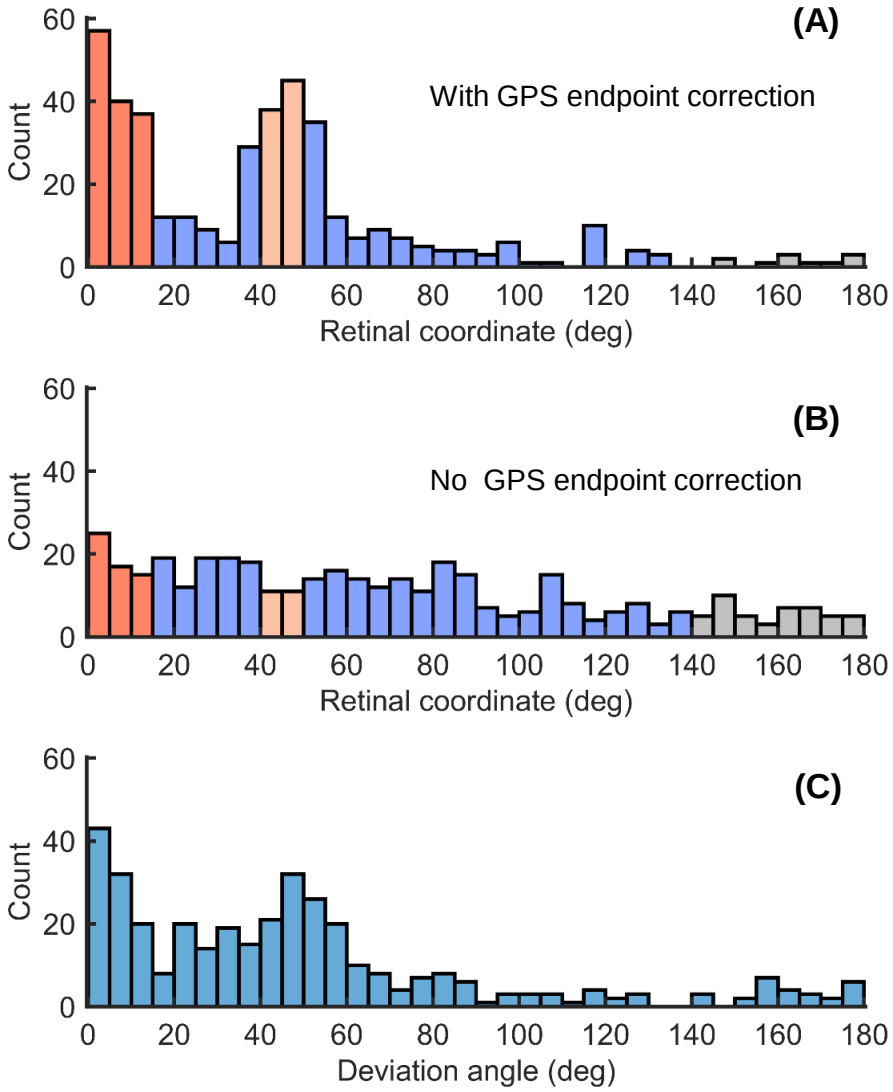

Figure 6.9 — Histograms of 5 Hz timepoints with 5 deg bin widths of retinal coordinate (A & B, coloured as Figure 6.5A) and deviation angle (C) for all flights cropped to the final 7 s before intercept including three additional close passes at the target (13 passes total, Figure 6.7). (A) Retinal coordinates from shifted trajectory to align the coordinates of the target and the bird at the known point of intercept, so as to remove any discrepancies arising from inaccuracy in the GPS position estimates. (B) Retinal coordinate from uncorrected trajectories. (C) Deviation angle between the peregrine's GPS velocity vector and the instantaneous line-of-sight to target.

6.4.3 Fovea selection with distance to the target

We found that peregrines use both temporal and central foveae to fixate the target when it is less than 50 m away. This does not support Tucker et al.'s (2000) hypothesis that the the central fovea is only used to foveate the target at long range while the temporal fovea is used when in close range. This was determined by plotting the distribution of distances to the target for each point that lay within the temporal fovea region of retinal coordinate space (0-15 deg) and comparing it with the distribution of distances for all points with a retinal coordinate near the central fovea (40-50 deg), Figure 6.10. This shows that although the birds in this study use both foveae within 50 m of the target, the temporal fovea only appears to be used within 50 m of the target whereas the target is foveated on the central fovea at a larger range of distances. Figure 6.7 and Figure 6.8 show that the peregrines rarely switch between fovea and instead that the birds tend to fixate the target until interception.

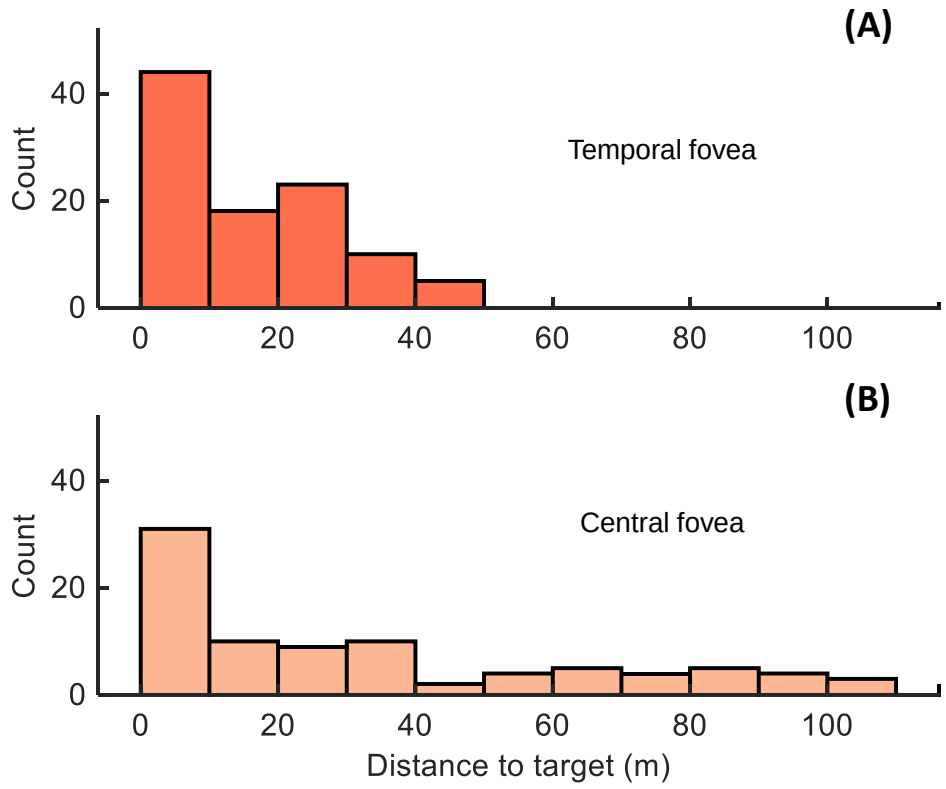

Figure 6.10 – Distance to the target for all points pooled from all 13 intercepts across 10 flights that had retinal coordinates corresponding to the temporal (A: 0 – 15 deg) fovea and central (B: 40 deg – 50 deg) fovea. Bin widths selected at 10 m.

In contrast to the predictions from the missile guidance literature, no relationship was found between tracking error and either inertial body rate or head turn rate (with respect to the body) across any of the flights. Linear regression models were fitted to both these variables for all flights for delays between 0.0 and 0.2 s between data streams. This returned R^2 values lower than 0.2 for all flights and delays.

6.5 Discussion

This chapter has detailed the successful use of a custom-built head-mounted sensor to measure the gaze direction of falcons during pursuit. We found that peregrines

preferentially fixate the target on either their temporal or central fovea in the final 2-3 seconds of pursuit like the seeker of a guided missile (Figure 6.8) but make small saccadic head movements to shift their gaze in the early phases of pursuit. The parallel LOS lines of the pursuit trajectories (Figure 6.7 and Section 6.6 — Appendix A) clearly show that the birds are not using deviated pursuit as suggested by Tucker et al. (2000) and that the trajectory shapes cannot be explained away as an emergent property of the bird's visual anatomy. This supports earlier findings that peregrines use a guidance law, proportional navigation, that can give rise to multiple pursuit geometries (Brighton et al., 2017). In addition, our results do not support Tucker et al.'s (2000) hypothesis that peregrines switch from the central to temporal fovea as they approach their target as both foveae were used at close range (Figure 6.7), but note that we find no evidence for use of the temporal fovea at >50 m range to the target. Instead, our results suggest that peregrines select their fovea based on the angle with which they approach the target. The birds show a weak preference to approach the target at deviation angles around 0 deg and 50 deg (Figure 6.9C), presumably to minimise head skew (the angle between body and head centrelines) to reduce aerodynamic drag. The use of the central fovea (at 45 deg to the head axis) to fixate the target will generally lead to a less optimal deviated pursuit trajectory than fixating the target using the binocular region as it will result in a longer curved trajectory. However, if the peregrine is attempting to limit head skew, it affords the bird the flexibility to approach at different angles. These conclusions demonstrate the importance of an understanding of the guidance law used to govern pursuit in order to understand the functional significance of the peregrine's visual anatomy.

Although peregrines are clearly foveating their target like the seeker of a guided missile, the finding that neither inertial body turn rate or their head turn rate are correlated with

tracking error suggests that they are extracting information on the LOS rate of the target using a different mechanism to that adopted by homing missiles. One possibility is that peregrines measure the rate of background drift with the target fixed by measuring the net rate of optic flow over the image. This strategy would work well over richly featured visual backdrops, but would not work at high altitude. In contrast to the seeker of a guided missile, birds' heads are roll stabilised for flight control and have inertial sensors that detect angular acceleration rather than angular velocity (Warrick, 2002; Money et al., 1971). However, it is likely that peregrines are able to estimate the rate of change in the head skew angle between the body axis and fovea using angular acceleration sensors, as this is how the oculomotor reflex works.

6.5.1 Limitations and future directions

The conclusions within this study must be treated with some caution when generalising to the pursuit behaviour of experienced falcons — the data presented here represent only 10 short flights from inexperienced birds that reached less than half the maximum flight speeds typically observed in an experienced peregrine. In addition to the small sample size, there will be additional uncertainty due to the precise orientation of the sensor board on the bird's head, the performance of the sensor fusion algorithm in estimating the sensor board orientation and error in the GPS measurements. However, the high degree of precision with which this technique was able to identify the retinal regions of the peregrine visual field used to fixate the target, that correspond to anatomical measurements, suggests that the cumulative effect of these errors is relatively small. This result also gives confidence in the relative GPS positioning accuracy over the short time scales used in this and previous studies (Brighton et al., 2017), but demonstrates the importance of applying an endpoint

correction to reduce errors associated with absolute positioning accuracy. Additionally, it confirms previous assumptions that the range of eye movement in raptors is limited to within a few degrees during flight (Jones et al., 2007). While the addition of eye tracking capabilities may be technologically problematic to implement using onboard sensors during pursuit, it could offer further insights into the precise gaze strategy adopted.

A further significant limitation is that we approximate body angle (used to estimate head turn rate) as the air velocity vector using the track angle from the GPS after removing the mean wind vector. This introduces error due to fluctuating wind throughout the flight and due to differences in wind conditions at flight altitude and at the ground where measurements were taken. In addition, the air velocity vector is unlikely to align with the body during turns due to aerodynamic sideslip. This could contribute to the lack of relationship that was found between head turn rate and tracking error. These limitations could be easily resolved with the addition of an IMU on the bird's body, synchronised with the current head-mounted IMU. This would allow a direct comparison of head and body orientation in order to give a better estimate of the head turn rate and more conclusively tackle Tucker et al.'s (2000) aerodynamic head skew hypothesis. However, given that the instrumentation and hood already weigh 4.4% of the smallest bird's body mass, any future iterations of this technology should first aim to reduce the weight of the current device before adding additional components.

Given the success of this study in using onboard instrumentation to extract retinal information for a predatory bird during pursuit, future studies should aim to explore the generality of these findings by applying the same methodology to a wider range of species. A broader understanding of the precise gaze strategies adopted by a range of predatory bird

species could have important implications for the design of visually-guided autonomous aerial systems that implement similar guidance laws for applications such as swarming, obstacle avoidance and target interception.

6.6 Appendix A — GPS trajectories with head orientation

GPS trajectories of 10 flights plotted individually with lure (orange dots), bird (blue dots) and the line-of-sight between the target and the lure plotted in grey. Blue arrows extending from bird GPS points indicate the head-yaw estimate from the head mounted sensor (Figure 6.4B) while the black lines are an estimate of the air vector based on wind measurements. The Red arrow indicates the mean wind direction.

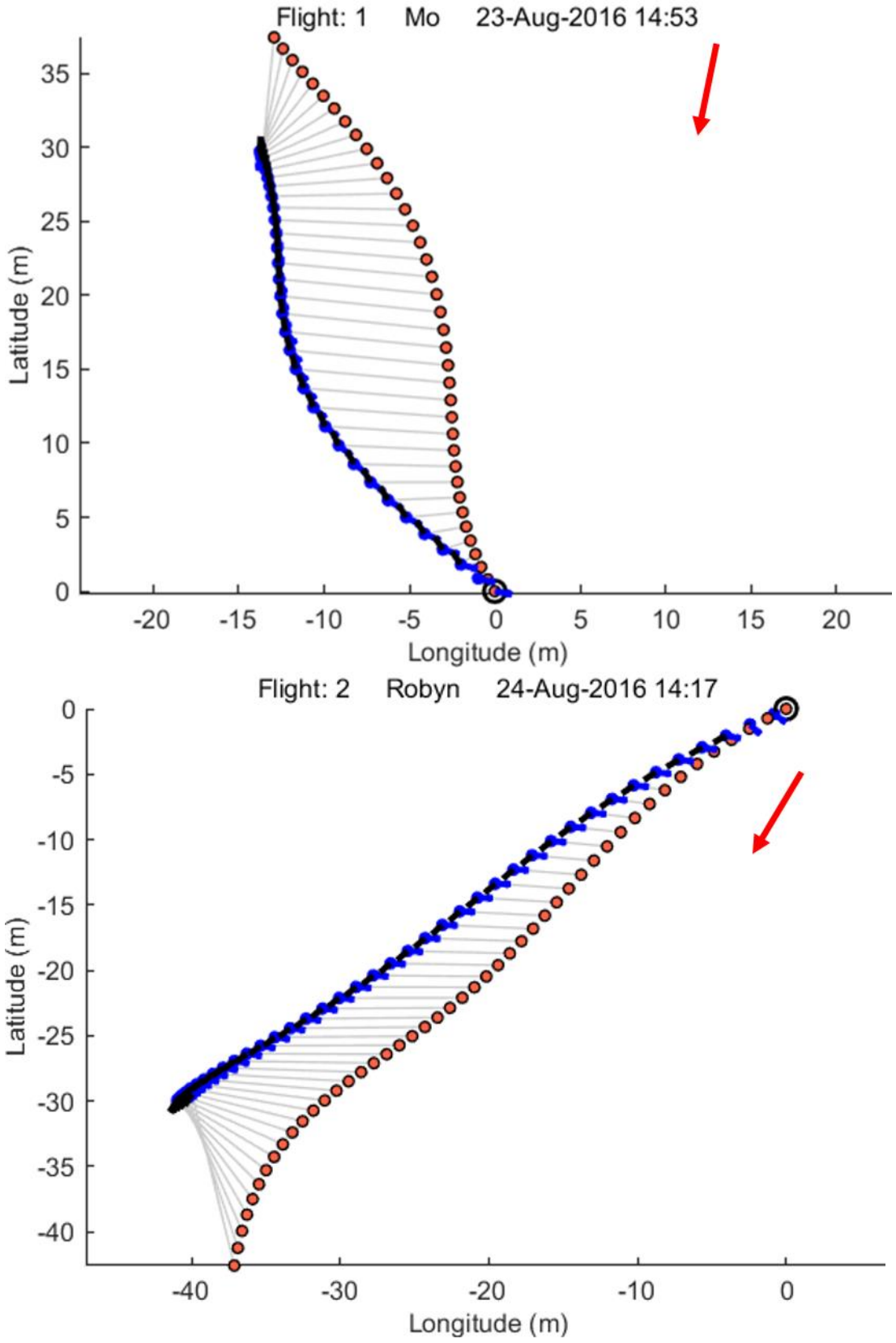
Flight: 1 Mo 23-Aug-2016 14:53
Latitude (m)
Longitude (m)
35
30
25
20
15
10
5
0
-20
-15
-10
-5
0
5
10
15
20
Flight: 2 Robyn 24-Aug-2016 14:17
Latitude (m)
Longitude (m)
0
-5
-10
-15
-20
-25
-30
-35
-40
-40
-30
-20
-10
0

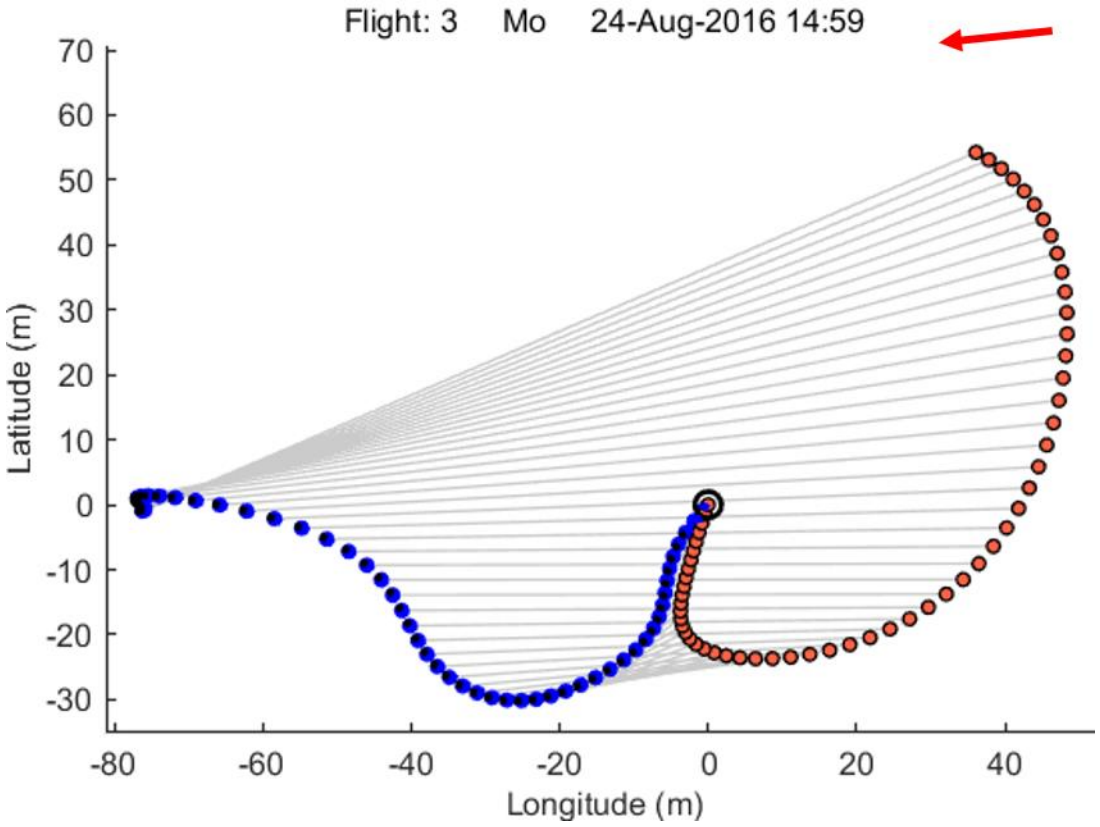
Flight: 3 Mo 24-Aug-2016 14:59
Latitude (m)
Longitude (m)
70
60
50
40
30
20
10
0
-10
-20
-30
-80
-60
-40
-20
0
20
40

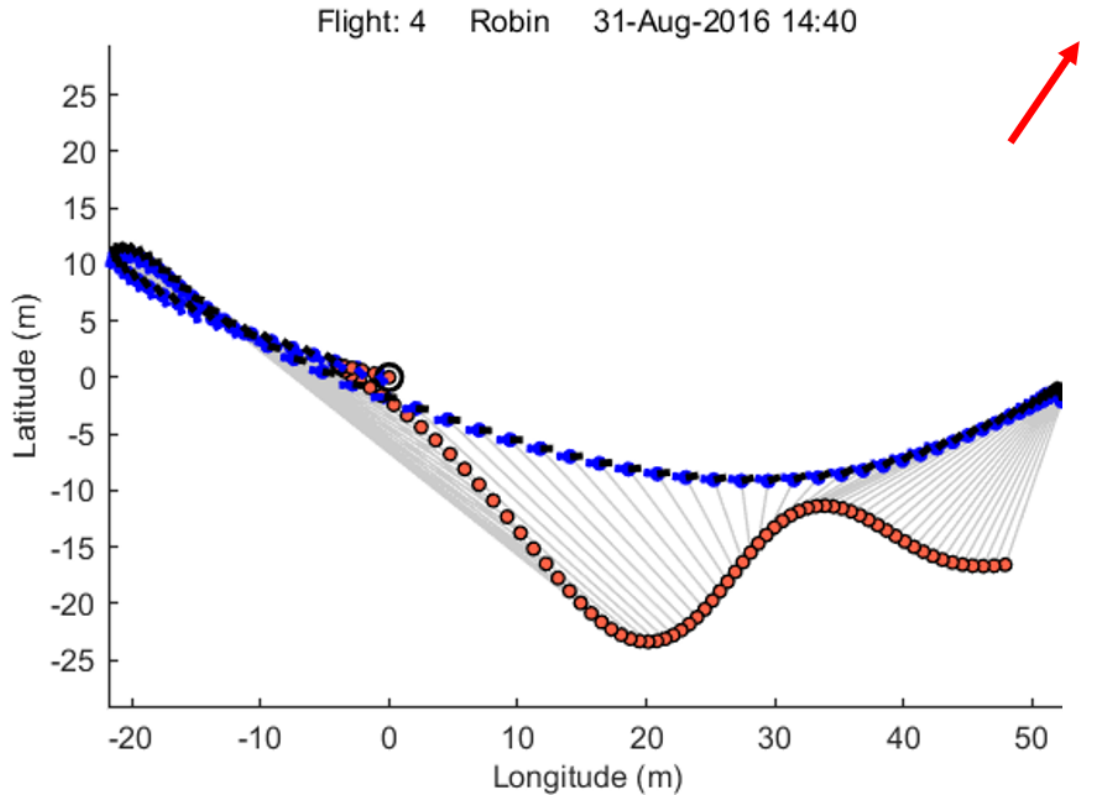
Flight: 4 Robin 31-Aug-2016 14:40
Latitude (m)
Longitude (m)
25
20
15
10
5
0
-5
-10
-15
-20
-25
-20
-10
0
10
20
30
40
50

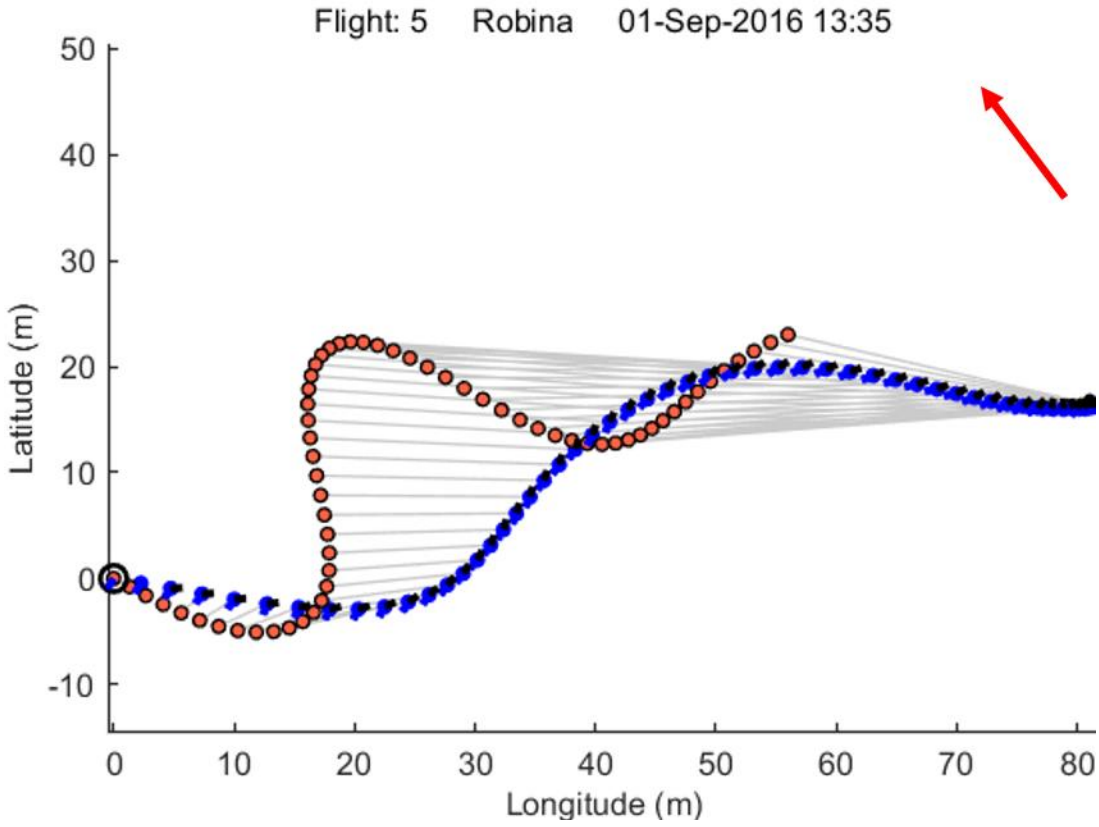
Flight: 5 Robina 01-Sep-2016 13:35
Latitude (m)
Longitude (m)
50
40
30
20
10
0
-10
0
10
20
30
40
50
60
70
80

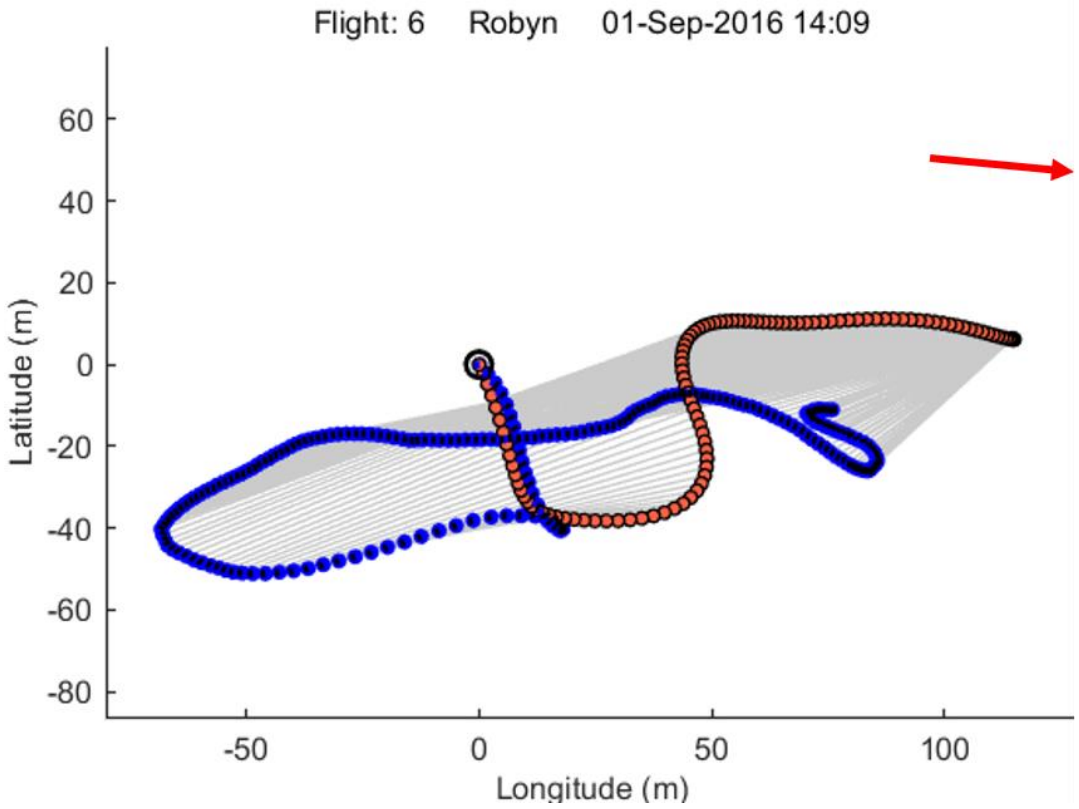
Flight: 6 Robyn 01-Sep-2016 14:09
Latitude (m)
Longitude (m)
60
40
20
0
-20
-40
-60
-80
-50
0
50
100

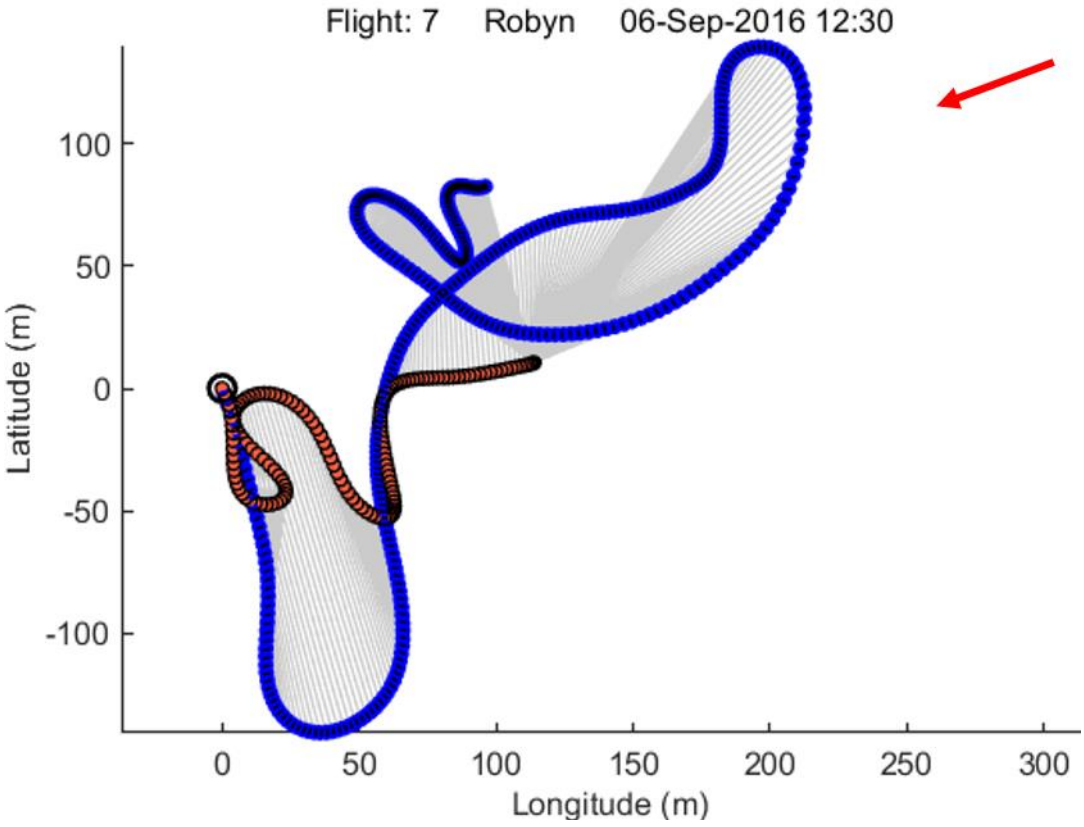
Flight: 7 Robyn 06-Sep-2016 12:30
Latitude (m)
Longitude (m)
100
50
0
-50
-100
0
50
100
150
200
250
300

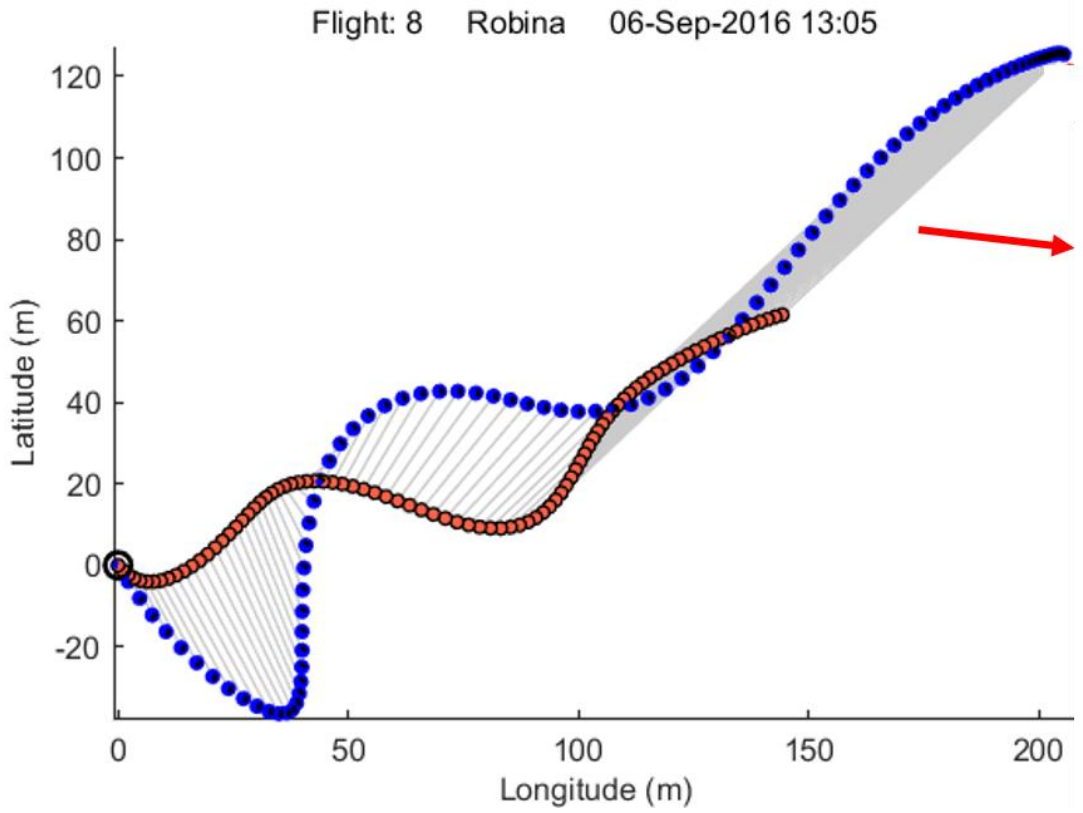
Flight: 8 Robina 06-Sep-2016 13:05
Latitude (m)
Longitude (m)
120
100
80
60
40
20
0
-20
0
50
100
150
200

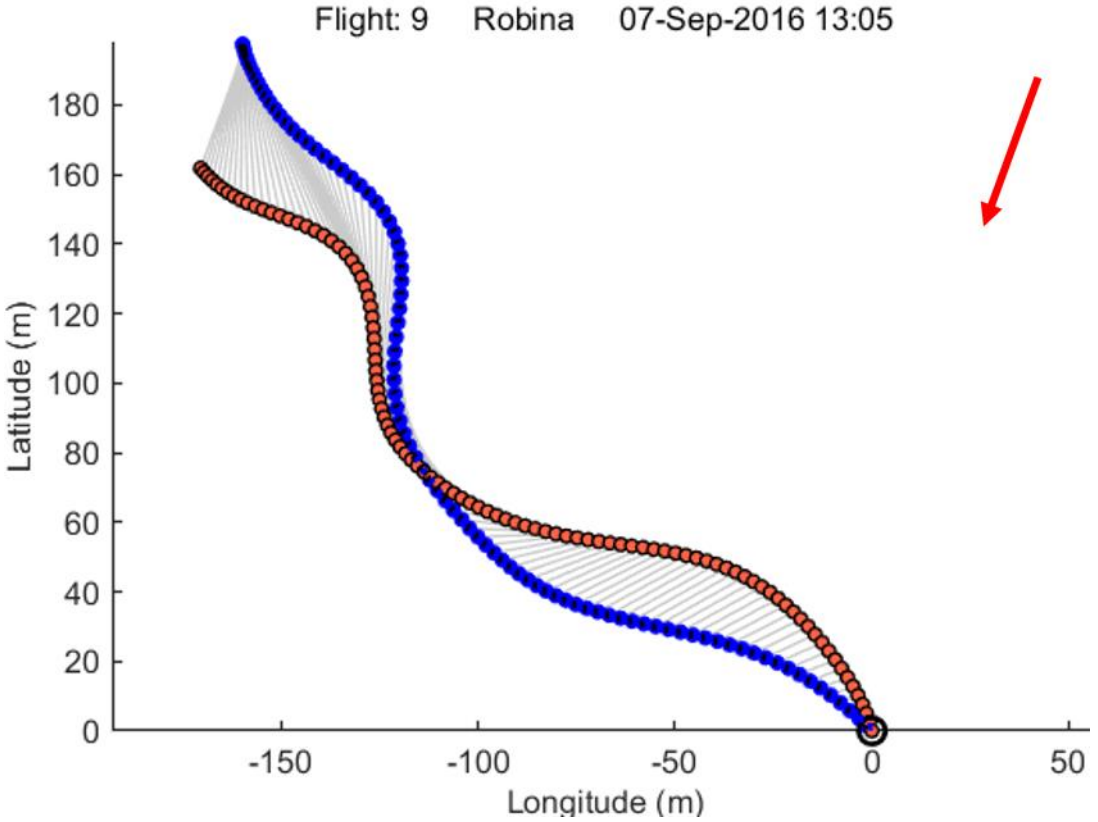
Flight: 9 Robina 07-Sep-2016 13:05
Latitude (m)
Longitude (m)
180
160
140
120
100
80
60
40
20
0
-150
-100
-50
0
50

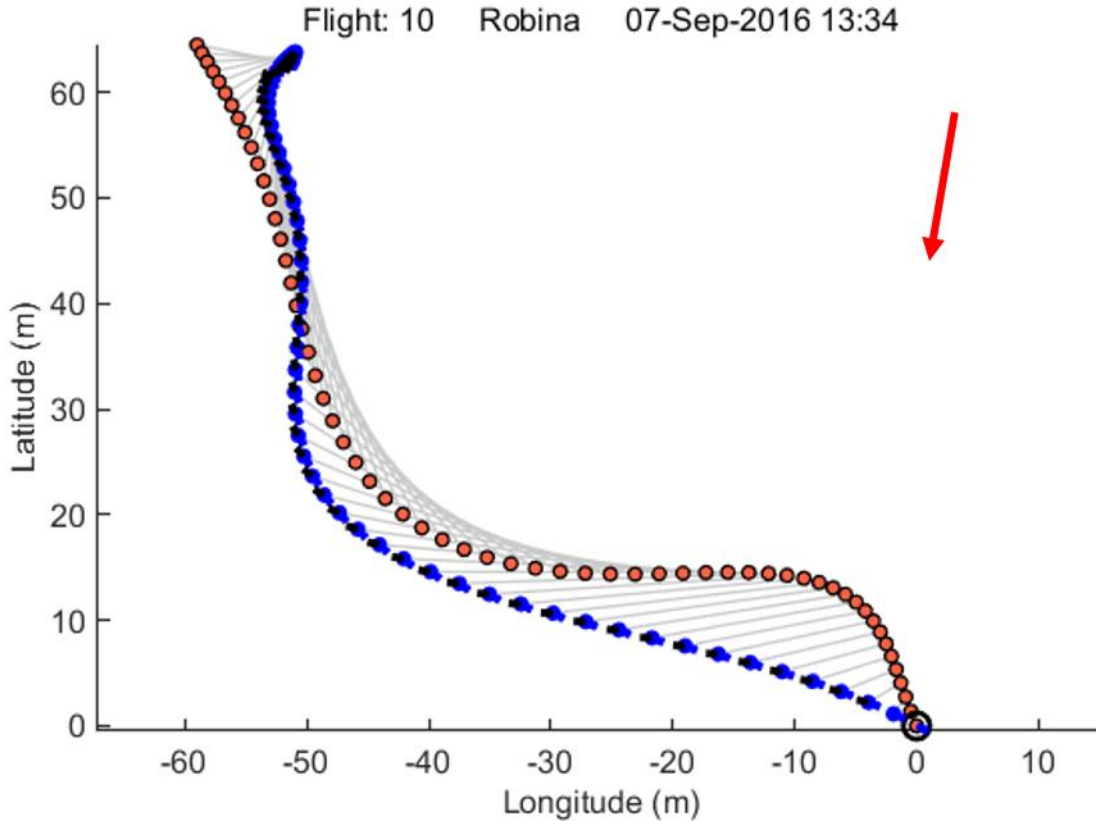
Flight: 10 Robina 07-Sep-2016 13:34
Latitude (m)
Longitude (m)
60
50
40
30
20
10
0
-60
-50
-40
-30
-20
-10
0
10

Chapter 7. General discussion

7.1 Summary

This thesis set out to investigate the mechanisms underlying the visual guidance of target-directed flight in birds, and the way in which birds stabilise and direct their visual system to extract the information required to implement these mechanisms. Previous studies of visually guided flight behaviours of birds in their natural environments have been limited to inferences based on GPS-derived flight trajectories (Brighton et al. 2017; T. Guilford & Biro 2014; Mann et al. 2011) or head mounted cameras (Kane et al., 2015), while laboratory studies have been limited to short-range flight behaviours (Ros and Biewener, 2017; Kress and Lentink, 2015). This thesis has successfully demonstrated the use of custom-built onboard instrumentation to precisely measure gaze stabilisation and visual attention during goal-directed tasks in homing pigeons (*Columba livia*) and peregrine falcons (*Falco peregrinus*) in their natural environments. It therefore represents an important step in linking the study of guidance and short-range navigation in birds, and in developing a better understanding of how birds perceive and respond to their environment. Each of the chapters contained within this thesis includes its own discussion. Therefore, here, I briefly summarise the general conclusions and consider the limitations of each chapter and comment on the broader significance of this work. I conclude by highlighting avenues for future research.

7.2 Conclusions and limitations

In Chapter 2, I analysed GPS-derived tracks from homing pigeons released within sight of their home loft to investigate the visual mechanisms used by birds to compensate for wind

drift. A key finding was that pigeons are able to compensate for wind drift, but do so imperfectly, leading their tracks to be displaced in the direction of the crosswind experienced. Guidance model simulations indicated that the pigeons performed better than a naive drift compensation strategy requiring no knowledge of the wind vector, but performed worse than a model that assumed full knowledge of the wind field. These models assume that the bird adjusts its heading vector using visual information on the target position: their home loft. However, the fovea alignment heatmap from the same release site (Wytham Hill) in Chapter 5 demonstrates that although the loft is a focus of visual attention, pigeons direct their visual attention widely around the track vicinity, focussing on a range of landscape features throughout the flight. This, when combined with the findings from Chapter 2, highlights the complex nature of homing navigation and drift compensation and suggests that pigeons may flexibly be using a range of visual cues to navigation in the face of wind. The analysis in Chapter 2 also highlights the limitations of inferring visual mechanisms using only data on the bird's ground track.

Chapter 3 addresses this limitation by describing the development and implementation of a novel head-mounted sensor capable of recording the head movement and position of birds during flight. By measuring head movement, I showed that it was possible to record both the saccade characteristics and the primary gaze direction of birds during homing navigation and pursuit. This technology has built on previous iterations of onboard inertial sensors in avian research (Reynolds 2016; Gillies et al. 2011; Portugal et al. 2014) but is among the first to adopt a head-mounted inertial measurement unit (IMU) and GPS receiver for birds flying in their natural environments. The key insights gained from the use of this sensor are outlined below.

In Chapter 4, I used the head-mounted sensor to find that pigeons coordinate their angular head saccades with the timing of their wingbeats. However, the onboard accelerometers were only able to provide information on the wingbeat phase and not precise timing of wingbeat kinematics. Therefore, while it is likely that the coordination of wingbeat and saccade timing provides some functional benefit, the interpretation of this result is not possible without additional technology, as discussed in the future directions below. I also found that translational head stabilisation is enhanced when flying with conspecifics and that this is largely achieved through an increase in wingbeat frequency. Our finding that stabilisation is enhanced when flying with conspecifics is likely because the birds are required to keep their heads translationally stabilised when flying near conspecifics to coordinate flocking behaviour, but may also only be possible when close visual stimuli is provided by their flock companions.

In Chapter 5, I used the head-mounted sensor to investigate how pigeons direct their visual attention during homing flights. This enabled me to identify points of interest in the landscape that aligned with lines projected from the birds' foveae throughout their flight. This technique represents a significant methodological advancement, allowing, for the first time, features such as villages that attract visual attention to be identified that do not lie on the bird's ground track. Prior to this thesis, to my knowledge, no study had directly recorded the focus of visual attention of pigeons during free flight in their natural environment, with previous attempts relying instead on inferences from GPS trajectories (Mann et al. 2011) or the analysis of video footage (Ozawa, 2010). This technique is in its early stages of development and therefore is limited in its current scope. However, refined iterations have the potential to revolutionise our understanding of large-scale spatial cognition in a paradigmatic avian model.

In Chapter 6, I used the head-mounted sensor to investigate peregrine falcon gaze strategy during pursuit. I took the reverse approach to that adopted in Chapter 5 by assuming that the target was the focus of visual attention and using head orientation, as well as bird and target positions, to determine the regions of the visual field used to fixate the target. This revealed that in the final phase of pursuit, rather than stabilising their gaze against the background, peregrines continuously track the target position using either their frontally or laterally facing fovea, depending on the angle of their approach to the target. This work provides significant insight beyond that of previous studies of pursuit using only GPS trajectories (Brighton et al., 2017) or head-mounted video (Kane et al., 2015).

A corollary finding from both Chapters 5 and 6 was that head-saccades precede body turns during flight in pigeons and peregrines. This confirms findings from onboard video footage (Ozawa, 2010) and high-speed video in a laboratory (Ros and Biewener, 2017). However, this was not investigated within this thesis in detail and, therefore, precise coupling between head and body movements during flight in natural environments has important implications for flight control and warrants further attention.

While the head-mounted instrumentation offers the potential to provide a range of insights into visual guidance and spatial cognition, there are three primary limitations with the technology. Firstly, the extent to which the bird's behaviour is altered through the attachment of a head-mounted sensor is uncertain. As discussed in Chapter 3, the sensor could have an effect on the bird's senses, aerodynamics and motivation to perform certain tasks which could lead to differences in flight path selection and head movement characteristics. Although I found no detectable difference in a range of flight performance metrics, it is unclear whether the attachment of the sensor affects some of the key variables

of interest in this thesis such as saccade characteristics or the coordination of wingbeats and saccades. Secondly, the extent of eye movement during flight in birds is unclear. While there is some (unpublished) evidence from an experiment tracking both head and eye movements that pigeons keep their eyes fixed to within a 5 deg diameter during flight (Ivo Ros, pers. comm.), the extent of eye movement is thought to vary considerably between species (O'Rourke, Hall, et al., 2010) and no such data exists for peregrines during flight.

Thirdly, the performance of the sensor fusion algorithm in calculating absolute yaw orientation from raw magnetometer, accelerometer and gyroscope data throughout long flights is hard to quantify. The sensor validation experiments using the phantom drone in Chapter 3 demonstrate a close correspondence in the yaw axis between fused data from the sensor and the built-in drone IMU giving confidence in the accuracy of the fusion algorithm. The findings from Chapter 6 go some way to addressing the second and third limitations, given the high degree of precision with which information from the head- yaw angle is used to assess the retinal coordinate used to fixate the target to within a few degrees of anatomical predictions. This provides internal validation, not only that the sensor fusion algorithm is accurately calculating the board yaw angle, but also that eye movement is limited to within a few degrees in the head reference frame. Further recommendations for validation are discussed below.

7.3 Future directions

The instrumentation developed here represents a significant advancement in the data available to researchers studying visually guided flight in birds. However, it is clear from the limitations highlighted above that there are improvements that could further enhance this technology. Here, I discuss ways in which the existing technology could be used to

answer further research questions and developments for future iterations of the instrumentation.

The wind experiments in Chapter 2 were conducted before the head-mounted instrumentation was developed and therefore did not include any data on head movement. The experiments were not repeated using the head-mounted units due to concerns over releasing birds in high wind conditions fitted with unfamiliar instrumentation. However, the experiments detailed in Chapters 3 – 5 resulted in no bird losses indicating that it is relatively safe. Therefore, future studies should consider repeating the wind experiments using the head-mounted sensor. This could provide additional insight into the drift compensation mechanism adopted by enabling the focus of visual attention to be determined throughout flight. It would also enable the primary assumption of the guidance models to be tested — that the birds are paying attention to the target throughout their flight. However, given the saccadic nature of gaze shifts in pigeons, it may be hard to clearly relate head gaze direction to possible visual mechanisms adopted by pigeons to compensate for wind. It would, at the very least, allow a comparison of saccade characteristics between different wind conditions.

Given the success with which the instrumentation was able to reliably capture the visual gaze strategies in two different species undertaking very different flight tasks, I expect this technology to provide valuable insight into the visual gaze strategies of other bird species. Indeed, the technology developed here is currently being adapted to study Harris' hawks pursuing moving ground targets by researchers from the Oxford Flight Group. However, prior to these experiments, I recommend that further validation of the technology is undertaken using a motion capture system. This system is capable of tracking the 3D

position of retroreflective markers at high frequency. With markers on the sensor board and on the bird's head it would be possible to compare absolute orientation from board markers with orientation from the board sensor fusion algorithm. A comparison of saccade characteristics of the birds with and without the head sensor would also be possible. In addition, validation experiments that fly pigeons in a motion capture system while wearing the head-mounted sensor would also allow the precise phasing of wingbeat timing with head movements to be determined. This would enable a clearer interpretation of the wingbeat-head movement phasing results from Chapter 4 during long range flight. To develop a more complete understanding of the role of gaze during flight, it will be necessary to measure eye movements in addition to head movements. Eye tracking during flight remains a significant technical challenge but recent developments in miniature cameras with a $1mm^2$ lens offer a minimally invasive solution if mounted on a stalk or on the bird's beak.

Future developments of onboard sensors, particularly head-mounted devices, should have animal welfare as their primary concern. The often cited 5% of body mass instrumentation weight limit should not be seen as a target for sensor development but instead as an absolute upper bound that should be reduced as technology allows (Portugal & White 2018). Recent rapid developments in mobile phone and aerial robotics technologies are likely to result in continued miniaturisation of sensor boards, microprocessors and batteries enabling further miniaturisation of this technology. This should make it possible to mount units with similar capacities on birds during longer flights while reducing the effect it may have on the bird's flight performance. As discussed in Chapters 4, 5, and 6, the addition of a second IMU on the back-mounted unit, synchronised with the head mounted IMU, would allow a direct comparison of head and body dynamics. The accelerometers would allow the coupling of

flap-induced head and body displacement to be directly measured and compared against previous studies. Orientation data, fused using data from both IMUs, would also allow the precise timing of head and body movements to be assessed without the reliance on GPS to estimate the air velocity vector from the bird's ground track. This would allow direct measurements of the head-body angles which will likely act as an important input for flight control (Ros and Biewener, 2017) and pursuit guidance strategy (Palumbo et al., 2010).

To conclude, the findings presented in this thesis represent an important step in the use of state of the art technology to better understand one of nature's most impressive feats: flight. I hope that, in turn, inspiration from this work will feed back into the development of more advanced aerial robotic systems.

References

Alerstam, T. (1979) ‘Wind as Selective Agent in Bird Migration’, *Ornis Scandinavica*, WileyNordic Society Oikos, vol. 10, no. 1, p. 76 [Online]. DOI: 10.2307/3676347.

Altshuler, D. L. and Srinivasan, M. V. (2018) ‘Comparison of visually guided flight in insects and birds’, *Frontiers in Neuroscience*, vol. 12, no. MAR [Online]. DOI: 10.3389/fnins.2018.00157.

Bar-Yehuda, Z. (2015) ‘Plot Google Earth MATLAB’,.

Barton, J. D. (2012) ‘Fundamentals of Small Unmanned Aircraft Flight’, *Johns Hopkins Apl Technical Digest*, vol. 31, no. 2, pp. 132–149.

Bates, D., Mächler, M., Bolker, B. and Walker, S. (2014) ‘Fitting Linear Mixed-Effects Models using lme4’, *Journal of Statistical Software*, vol. 67, no. 1, pp. 1–48 [Online]. DOI: 10.18637/jss.v067.i01.

Benson, R. B. J., Starmer-Jones, E., Close, R. A. and Walsh, S. A. (2017) ‘Comparative analysis of vestibular ecomorphology in birds’, *Journal of Anatomy*, vol. 231, no. 6, pp. 990–1018 [Online]. DOI: 10.1111/joa.12726.

Berens, P., Baclawski, K., Berens, P. and Baclawski, K. (2009) ‘CircStat: A MATLAB Toolbox for Circular Statistics’, *Journal of Statistical Software*, vol. 30, no. April, pp. 1–3 [Online]. DOI: 10.1002/wics.10.

Bhagavatula, P. S., Claudianos, C., Ibbotson, M. R. and Srinivasan, M. V. (2011) ‘Optic flow cues guide flight in birds’, *Current Biology*, Elsevier, vol. 21, no. 21, pp. 1794–1799 [Online]. DOI: 10.1016/j.cub.2011.09.009.

Bilo, D., Bilo, A., Müller, M., Theis, B. and Wedekind, F. (1985) ‘Neurophysiological-cybernetic analysis of course-control in the pigeon’, *Biona report*, vol. 3, pp. 445–477.

Bingman, V. P., Able, K. P. and Kerlinger, P. (1982) ‘Wind drift, compensation, and the use of landmarks by nocturnal bird migrants’, *Animal Behaviour*, Academic Press, vol. 30, no. 1, pp. 49–53 [Online]. DOI: 10.1016/S0003-3472(82)80236-4.

Biro, D. (2002) ‘The Role of Visual Landmarks in The Homing Pigeon’s Familiar Area Map.’, University of Oxford.

Biro, D., Guilford, T. and Dawkins, M. S. (2003) ‘Mechanisms of visually mediated site recognition by the homing pigeon’, *Animal Behaviour*, vol. 65, no. 1, pp. 115–122 [Online]. DOI: 10.1006/anbe.2002.2014.

Biro, D., Guilford, T., Dell’Omo, G. and Lipp, H.-P. (2002) ‘How the viewing of familiar landscapes prior to release allows pigeons to home faster: evidence from GPS tracking’, *The Journal of Experimental Biology*, vol. 205, no. Pt 24, pp. 3833–3844.

Biro, D., Meade, J. and Guilford, T. (2004) ‘Familiar route loyalty implies visual pilotage in the homing pigeon’, *Proceedings of the National Academy of Sciences*, vol. 101, no. 50, pp. 17440–17443 [Online]. DOI: 10.1073/pnas.0406984101.

Biro, D., Meade, J. and Guilford, T. (2006) ‘Route recapitulation and route loyalty in homing pigeons: Pilotage from 25 km?’, *Journal of Navigation*, vol. 59, no. 1, pp. 43–53

[Online]. DOI: 10.1017/S0373463305003541.

Blanchard, S. and Blanchard, S. (2005) ‘Conditional Akaike information for mixed-e ects models’, *Biometrika*, pp. 351–370.

Bohrer, G., Brandes, D., Mandel, J. T., Bildstein, K. L., Miller, T. A., Lanzone, M., Katzner, T., Maisonneuve, C. and Tremblay, J. A. (2012) ‘Estimating updraft velocity components over large spatial scales: contrasting migration strategies of golden eagles and turkey vultures’, *Ecology Letters*, vol. 15, no. 2, pp. 96–103 [Online]. DOI: 10.1111/j.1461-0248.2011.01713.x.

Brighton, C. H. (2015) ‘Attack strategies in birds of prey’, University of Oxford, DPhil Thesis.

Brighton, C. H., Thomas, A. L. R. and Taylor, G. K. (2017) ‘Terminal attack trajectories of peregrine falcons are described by the proportional navigation guidance law of missiles.’, *Proceedings of the National Academy of Sciences of the United States of America*, National Academy of Sciences, vol. 114, no. 51, pp. 13495–13500 [Online]. DOI: 10.1073/pnas.1714532114.

Brown, R. E. and Fedde, M. R. (1993) ‘Airflow sensors in the avian wing, *Journal of Experimental Biology*, vol. 179, no. 1.

Bruderer, B. (1978) ‘Effects of alpine topography and winds on migrating birds’, in Springer, Berlin, Heidelberg, pp. 252–265 [Online]. DOI: 10.1007/978-3-662-11147-5_24.

Burnham, K. P. and Anderson, D. R. (2002) *Model Selection and Multimodel Inference: A Practical Information-Theoretic Approach (2nd ed), Ecological Modelling*, New York, Springer-Verlag, vol. 172 [Online]. DOI: 10.1016/j.ecolmodel.2003.11.004.

Burt, T., Holland, R. and Guilford, T. (1997) ‘Further evidence for visual landmark involvement in the pigeon’s familiar area map’, *Animal Behaviour*, vol. 53, no. 6, pp. 1203–1209 [Online]. DOI: 10.1006/anbe.1996.0389.

Caruso, M. J. (2000) ‘Applications of magnetic sensors for low cost compass systems’, *IEEE 2000. Position Location and Navigation Symposium (Cat. No.00CH37062)*, IEEE, pp. 177–184 [Online]. DOI: 10.1109/PLANS.2000.838300.

Chapman, J. W., Klaassen, R. H. G., Drake, V. A., Fossette, S., Hays, G. C., Metcalfe, J. D., Reynolds, A. M., Reynolds, D. R. and Alerstam, T. (2011) ‘Animal orientation strategies for movement in flows.’, *Current biology : CB*, Elsevier, vol. 21, no. 20, pp. R861-70 [Online]. DOI: 10.1016/j.cub.2011.08.014.

Chapman, J. W., Reynolds, D. R., Mouritsen, H., Hill, J. K., Riley, J. R., Sivell, D., Smith, A. D. and Woiwod, I. P. (2008) ‘Wind Selection and Drift Compensation Optimize Migratory Pathways in a High-Flying Moth’, *Current Biology*, vol. 18, no. 7, pp. 514–518 [Online]. DOI: 10.1016/j.cub.2008.02.080.

Clarke, G. . and Whitteridge, D. (1976) ‘The projection of the retina, including the “red area”, on to the optic tectum of the pigeon.’, *Quarterly Journal of Experimental Physiology*, no. 1976, pp. 351–358.

Davies, M. N. O. and Green, P. R. (1988) ‘Head-bobbing during walking, running and flying: relative motion perception in the pigeon’, *Journal of Experimental Biology*, vol. 91, no. 1, pp. 71–91.

Davies, M. N. O. and Green, P. R. (1990) ‘Optic flow-field variables trigger landing in hawk but not in pigeons’, *Naturwissenschaften*, vol. 77, no. 3, pp. 142–144 [Online]. DOI:

10.1007/BF01134481.

Davis, M. and Green, P. (1988) ‘Head-bobbing during walking, running and flying: relative motion perception in the pigeon’, *Journal of experimental biology*, vol. 1, no. 138, pp. 71–91.

Eckmeier, D., Geurten, B. R. H., Kress, D., Mertes, M., Kern, R., Egelhaaf, M. and Bischof, H. J. (2008) ‘Gaze strategy in the free flying zebra finch (Taeniopygia guttata)’, *PLoS ONE*, Public Library of Science, vol. 3, no. 12, p. e3956 [Online]. DOI: 10.1371/journal.pone.0003956.

Erichsen, J. T., Hodos, W., Evinger, C., Bessette, B. B. and Phillips, S. J. (1989) ‘Head orientation in pigeons: Postural, locomotor and visual determinants’, *Brain, Behavior and Evolution*, Karger Publishers, vol. 33, no. 5, pp. 268–278 [Online]. DOI: 10.1159/000115935.

Feng, S., Xu, D. and Yang, X. (2010) ‘Attention-driven salient edge(s) and region(s) extraction with application to CBIR’, *Signal Processing*, Elsevier, vol. 90, no. 1, pp. 1–15 [Online]. DOI: 10.1016/j.sigpro.2009.05.017.

Fite, K. V. and Rosenfield-Wessels, S. (1975) ‘A comparative study of deep avian fovea’, *Brain, Behavior and Evolution*, vol. 12, pp. 97–115.

Flack, A., Ákos, Z., Nagy, M., Vicsek, T. and Biro, D. (2013) ‘Robustness of flight leadership relations in pigeons’, *Animal Behaviour*, vol. 86, no. 4, pp. 723–732 [Online]. DOI: 10.1016/j.anbehav.2013.07.005.

Floryan, D., Van Buren, T. and Smits, A. J. (2018) ‘Efficient cruising for swimming and flying animals is dictated by fluid drag’, *Proceedings of the National Academy of Sciences*, no. 4, p. 201805941 [Online]. DOI: 10.1073/pnas.1805941115.

Freckleton, R. P. and Iossa, G. (2010) ‘Methods in Ecology and Evolution’, *Methods in Ecology and Evolution*, vol. 1, no. 1, pp. 1–2 [Online]. DOI: 10.1111/j.2041-210X.2010.00016.x.

Freeman, R., Mann, R., Guilford, T., Biro, D., Freeman, R. and Mann, R. (2011) ‘Group decisions and individual differences : route fidelity predicts flight leadership in homing pigeons (Columba livia)’, *Biology Letters*, vol. 7, no. September 2010, pp. 63–66 [Online]. DOI: 10.1098/rsbl.2010.0627.

Friedman, M. B. (1975) ‘Visual control of head movements during avian locomotion’, *Nature*, vol. 255, no. 5503, pp. 67–69 [Online]. DOI: 10.1038/255067a0.

Frost, B. J. (2009) ‘Bird head stabilization’, *CURBIO*, vol. 19, pp. R315–R316 [Online]. DOI: 10.1016/j.cub.2009.02.002.

Frost, B. J., Wise, L. Z., Morgan, B. and Bird, D. (1990) ‘Retinotopic representation of the bifoveate eye of the kestrel (Falco spraverius) on the optic tectum.’, *Visual neuroscience*, vol. 5, no. 3, pp. 231–9.

Fux, M. and Eilam, D. (2009) ‘How barn owls (Tyto alba) visually follow moving voles (Microtus socialis) before attacking them’, *Physiology and Behavior*, Elsevier Inc., vol. 98, no. 3, pp. 359–366 [Online]. DOI: 10.1016/j.physbeh.2009.06.016.

Ghose, K. (2006) ‘Steering by hearing: A bat’s acoustic gaze is linked to its flight motor output by a delayed, adaptive linear law’, *Journal of Neuroscience*, vol. 26, no. 6, pp. 1704–1710 [Online]. DOI: 10.1523/JNEUROSCI.4315-05.2006.

Gillies, J. A., Bacic, M., Yuan, F. G., Thomas, A. L. R., Taylor, G. K., Road, S. P., Road, P. and Carolina, N. (2008) 'Modeling and Identification of Steppe Eagle (Aquila nipalensis) dynamics', *AIAA Modeling and Simulation Technologies Conference and Exhibit*, no. August, pp. 1–10 [Online]. DOI: 10.2514/6.2008-7096.

Gillies, J. A., Thomas, A. L. R. and Taylor, G. K. (2011) 'Soaring and manoeuvring flight of a steppe eagle Aquila nipalensis', *Journal of Avian Biology*, vol. 42, no. 5, pp. 377–386 [Online]. DOI: 10.1111/j.1600-048X.2011.05105.x.

Gioanni, H. (1988a) 'Stabilizing gaze reflexes in the pigeon (Columba livia) - II. Vestibulo-ocular (VOR) and vestibulo-collic (closed-loop VCR) reflexes', *Experimental Brain Research*, vol. 69, no. 3, pp. 583–593 [Online]. DOI: 10.1007/BF00247311.

Gioanni, H. (1988b) 'Stabilizing gaze reflexes in the pigeon (Columba livia) - I. Horizontbal and vertical optokinetic eye (OKN) and head (OCR) reflexes', *Experimental Brain Research*, vol. 69, no. 3, pp. 567–582 [Online]. DOI: 10.1007/BF00247310.

Gioanni, H. (1988c) 'Stabilizing gaze reflexes in the pigeon (Columba livia) - I. Horizontbal and vertical optokinetic eye (OKN) and head (OCR) reflexes', *Experimental Brain Research*, Springer-Verlag, vol. 69, no. 3, pp. 567–582 [Online]. DOI: 10.1007/BF00247310.

Gioanni, H. and Vidal, P.-P. (2012) 'Possible cues driving context-specific adaptation of optocollic reflex in pigeons (*Columba livia*)', *Journal of Neurophysiology*, vol. 107, no. 2, pp. 704–717 [Online]. DOI: 10.1152/jn.00684.2011.

Green, M. and Alerstam, T. (2002) 'The problem of estimating wind drift in migrating birds', *Journal of Theoretical Biology*, vol. 218, no. 4, pp. 485–496 [Online]. DOI: 10.1016/S0022-5193(02)93094-8.

Green, M., Alerstam, T., Gudmundsson, G. A., Hedenström, A. and Piersma, T. (2004) 'Do Arctic waders use adaptive wind drift?', *Journal of Avian Biology*, Wiley/Blackwell (10.1111), vol. 35, no. 4, pp. 305–315 [Online]. DOI: 10.1111/j.0908-8857.2004.03181.x.

Green, P. R., Davies, M. N. O. and Thorpe, P. H. (1994) 'Head-bobbing and head orientation during landing flights of pigeons', *Journal of Comparative Physiology A*, Springer-Verlag, vol. 174, no. 2, pp. 249–256 [Online]. DOI: 10.1007/BF00193791.

Grillner, S. (2006) 'Biological Pattern Generation : The Cellular and Computational Logic of Networks in Motion', pp. 751–766 [Online]. DOI: 10.1016/j.neuron.2006.11.008.

Guilford, T. (1993) 'Homing mechanisms in sight', *Nature*, Nature Publishing Group, vol. 340, pp. 91–93.

Guilford, T. and Biro, D. (2014) 'Route following and the pigeon's familiar area map', *Journal of Experimental Biology*, vol. 217, no. 2, pp. 169–179 [Online]. DOI: 10.1242/jeb.092908.

Guilford, Tim and Biro, D. (2014) 'Route following and the pigeon's familiar area map.', *The Journal of experimental biology*, The Company of Biologists Ltd, vol. 217, no. Pt 2, pp. 169–79 [Online]. DOI: 10.1242/jeb.092908.

Guilford, T. and de Perera, T. B. (2017) 'An associative account of avian navigation', *Journal of Avian Biology*, Blackwell Publishing Ltd, vol. 48, no. 1, pp. 191–195 [Online]. DOI: 10.1111/jav.01355.

Guilford, T., Roberts, S., Biro, D. and Rezek, I. (2004) 'Positional entropy during pigeon homing II: navigational interpretation of Bayesian latent state models', *Journal of*

Theoretical Biology, vol. 227, no. 1, pp. 25–38 [Online]. DOI: 10.1016/j.jtbi.2003.07.003.

Guilford, T. and Taylor, G. K. (2014) 'The sun compass revisited', *Animal Behaviour*, vol. 97, pp. 135–143 [Online]. DOI: 10.1016/j.anbehav.2014.09.005.

Haque, A. (2004) 'Vestibular Gaze Stabilization: Different Behavioral Strategies for Arboreal and Terrestrial Avians', *Journal of Neurophysiology*, vol. 93, no. 3, pp. 1165–1173 [Online]. DOI: 10.1152/jn.00966.2004.

Hedenström, A. and Åkesson, S. (2016) 'Ecology of tern flight in relation to wind, topography and aerodynamic theory', *Philosophical Transactions of the Royal Society B: Biological Sciences*, vol. 371, no. 1704, p. 20150396 [Online]. DOI: 10.1098/rstb.2015.0396.

Hedenstrom, A. and Alerstam, T. (1995) 'Optimal Flight Speed of Birds', *Philosophical Transactions of the Royal Society B: Biological Sciences*, The Royal Society, vol. 348, no. 1326, pp. 471–487 [Online]. DOI: 10.1098/rstb.1995.0082.

Hedenström, A., Alerstam, T., Green, M. and Gudmundsson, G. A. (2002) 'Adaptive variation of airspeed in relation to wind, altitude and climb rate by migrating birds in the Arctic', *Behavioral Ecology and Sociobiology*, vol. 52, no. 4, pp. 308–317 [Online]. DOI: 10.1007/s00265-002-0504-0.

Holmqvist, K., Nyström, M., Andersson, R., Dewhurst, R., Jarodzka, H. and Van de Weijer, J. (2011) *Eye-tracking: A comprehensive guide to methods and measures*, OUP Oxford.

von Hünerbein, K., Wiltschko, W. and Rüter, E. (2001) 'Flight Tracks of Homing Pigeons Measured with GPS', *Journal of Navigation*, Cambridge University Press, vol. 54, no. 02, pp. 167–175 [Online]. DOI: 10.1017/S0373463301001345.

Jones, M. P., Pierce, K. E. and Ward, D. (2007) 'Avian Vision: A Review of Form and Function with Special Consideration to Birds of Prey', *Journal of Exotic Pet Medicine*, vol. 16, no. 2, pp. 69–87 [Online]. DOI: 10.1053/j.jepm.2007.03.012.

Kane, S. A., Fulton, A. H. and Rosenthal, L. J. (2015) 'When hawks attack: animal-borne video studies of goshawk pursuit and prey-evasion strategies', *Journal of Experimental Biology*, vol. 218, no. 2, pp. 212–222 [Online]. DOI: 10.1242/jeb.108597.

Kane, S. A. and Zamani, M. (2014) 'Falcons pursue prey using visual motion cues: new perspectives from animal-borne cameras', *Journal of Experimental Biology*, vol. 217, no. 2, pp. 225–234 [Online]. DOI: 10.1242/jeb.092403.

Kano, F. and Call, J. (2014) 'Cross-species variation in gaze following and conspecific preference among great apes, human infants and adults', *Animal Behaviour*, Academic Press, vol. 91, pp. 136–149 [Online]. DOI: 10.1016/j.anbehav.2014.03.011.

Kano, F. and Call, J. (2017) 'Great Ape Social Attention', in *Evolution of the Brain, Cognition, and Emotion in Vertebrates*, Tokyo, Springer Japan, pp. 187–206 [Online]. DOI: 10.1007/978-4-431-56559-8_9.

Kano, F., Walker, J., Sasaki, T. and Biro, D. (2018) 'Head-mounted sensors reveal visual attention of free-flying homing pigeons', *Journal of Experimental Biology*, vol. 221, no. 1 [Online]. DOI: doi:10.1242/jeb.183475.

Katzir, G., Schechtman, E., Carmi, N. and Weihs, D. (2001) 'Head stabilization in herons', *Journal of Comparative Physiology - A Sensory, Neural, and Behavioral Physiology*, vol. 187, no. 6, pp. 423–432 [Online]. DOI: 10.1007/s003590100210.

Kenward, R. (2001) *A manual for wildlife radio tagging*, Academic Press.

Krekelberg, B. (2010) 'Saccadic suppression', *Current Biology*, vol. 20, no. 5 [Online]. DOI: 10.1016/j.cub.2009.12.018.

Kress, D., Van Bokhorst, E. and Lentink, D. (2015a) 'How lovebirds maneuver rapidly using super-fast head saccades and image feature stabilization', *PLoS ONE*, vol. 10, no. 6, p. e0129287 [Online]. DOI: 10.1371/journal.pone.0129287.

Kress, D., Van Bokhorst, E. and Lentink, D. (2015b) 'How lovebirds maneuver rapidly using super-fast head saccades and image feature stabilization', *PLoS ONE*, Public Library of Science, vol. 10, no. 6, p. e0129287 [Online]. DOI: 10.1371/journal.pone.0129287.

Kress, D. and Egelhaaf, M. (2014) 'Gaze characteristics of freely walking blowflies Calliphora vicina in a goal-directed task', *Journal of Experimental Biology*, vol. 217, no. 18, pp. 3209–3220 [Online]. DOI: 10.1242/jeb.097436.

Kress, D. and Lentink, D. (2015) 'How birds change their gaze to accommodate rapid transitions between flight modes', *Integrative and Comparative Biology*, vol. 55, pp. E102–E102.

Lanchester, B. S. and Mark, R. F. (1975) 'Pursuit and prediction in the tracking of moving food by a teleost fish (Acanthaluteres spilomelanurus).', *The Journal of experimental biology*, vol. 63, no. 3, pp. 627–45.

Land, M. F. (1993) 'Chasing and pursuit in the dolichopodid fly Poecilobothrus nobilitatus', *Journal of Comparative Physiology A*, Springer-Verlag, vol. 173, no. 5, pp. 605–613 [Online]. DOI: 10.1007/BF00197768.

Land, M. F. (1999a) 'The roles of head movements in the search and capture strategy of a tern (Aves, Laridae)', *Journal of Comparative Physiology - A Sensory, Neural, and Behavioral Physiology*, vol. 184, no. 3, pp. 265–272 [Online]. DOI: 10.1007/s003590050324.

Land, M. F. (1999b) 'Motion and vision: Why animals move their eyes', *Journal of Comparative Physiology - A Sensory, Neural, and Behavioral Physiology*, vol. 185, no. 4, pp. 341–352 [Online]. DOI: 10.1007/s003590050393.

Land, M. F. (2014a) 'Eye movements of vertebrates and their relation to eye form and function', *Journal of Comparative Physiology A: Neuroethology, Sensory, Neural, and Behavioral Physiology*, vol. 201, no. 2, pp. 195–214 [Online]. DOI: 10.1007/s00359-014-0964-5.

Land, M. F. (2014b) 'Eye movements of vertebrates and their relation to eye form and function', *Journal of Comparative Physiology A: Neuroethology, Sensory, Neural, and Behavioral Physiology*, vol. 201, no. 2, pp. 195–214 [Online]. DOI: 10.1007/s00359-014-0964-5.

Lau, K.-K., Roberts, S., Biro, D., Freeman, R., Meade, J. and Guilford, T. (2006) 'An edge-detection approach to investigating pigeon navigation', *Journal of Theoretical Biology*, vol. 239, pp. 71–78 [Online]. DOI: 10.1016/j.jtbi.2005.07.013.

Lee, D. N., Davies, M. N. O., Green, P. R. and Weel, F. R. R. (1993) 'Visual Control of Velocity of Approach By Pigeons When Landing', *Journal of Experimental Biology*, vol. 180, no. 1, pp. 85–104.

Li, G. and Yu, Y. (2015) 'Visual saliency based on multiscale deep features', *Proceedings of the IEEE Conference on Computer Vision and Pattern Recognition*, pp. 5455–5463.

Liechti, F. (2006) ‘Birds: Blowin’ by the wind?’, *Journal of Ornithology*, vol. 147, no. 2 [Online]. DOI: 10.1007/s10336-006-0061-9.

Liechti, F., Hedenström, A. and Alerstam, T. (1994) ‘Effects of sidewinds on optimal flight speed of birds’, *Journal of Theoretical Biology*, vol. 170, no. 2, pp. 219–225 [Online]. DOI: 10.1006/jtbi.1994.1181.

Lin, H. T., Ros, I. G. and Biewener, A. A. (2014) ‘Through the eyes of a bird: Modelling visually guided obstacle flight’, *Journal of the Royal Society Interface*, vol. 11, no. 96, pp. 20140239–20140239 [Online]. DOI: 10.1098/rsif.2014.0239.

Lipp, H.-P., Vyssotski, A. L., Wolfer, D. P., Renaudineau, S., Savini, M., Tröster, G. and Dell’Omo, G. (2004) ‘Pigeon homing along highways and exits.’, *Current biology : CB*, Elsevier, vol. 14, no. 14, pp. 1239–49 [Online]. DOI: 10.1016/j.cub.2004.07.024.

Loretto, M. C., Schloegl, C. and Bugnyar, T. (2010) ‘Northern bald ibises follow others’ gaze into distant space but not behind barriers’, *Biology Letters*, vol. 6, no. 1, pp. 14–17 [Online]. DOI: 10.1098/rsbl.2009.0510.

Mandel, J. T., Bildstein, K. L., Bohrer, G. and Winkler, D. W. (2008) ‘Movement ecology of migration in turkey vultures.’, *Proceedings of the National Academy of Sciences of the United States of America*, National Academy of Sciences, vol. 105, no. 49, pp. 19102–7 [Online]. DOI: 10.1073/pnas.0801789105.

Mann, R., Freeman, R., Osborne, M., Garnett, R., Armstrong, C., Meade, J., Biro, D., Guilford, T. and Roberts, S. (2011a) ‘Objectively identifying landmark use and predicting flight trajectories of the homing pigeon using Gaussian processes.’, *Journal of the Royal Society, Interface*, The Royal Society, vol. 8, no. 55, pp. 210–9 [Online]. DOI: 10.1098/rsif.2010.0301.

Mann, R., Freeman, R., Osborne, M., Garnett, R., Armstrong, C., Meade, J., Biro, D., Guilford, T. and Roberts, S. (2011b) ‘Objectively identifying landmark use and predicting flight trajectories of the homing pigeon using Gaussian processes’, *Journal of the Royal Society Interface*, vol. 8, no. 55, pp. 210–219 [Online]. DOI: 10.1098/rsif.2010.0301.

Mann, R. P., Armstrong, C., Meade, J., Freeman, R., Biro, D. and Guilford, T. (2014) ‘Landscape complexity influences routememory formation in navigating pigeons’, *Biology Letters*, vol. 10, no. 1, pp. 20130885–20130885 [Online]. DOI: 10.1098/rsbl.2013.0885.

Martin, G. R. (2007) ‘Visual fields and their functions in birds’, *Journal of Ornithology*, vol. 148, no. SUPLL. 2, pp. 547–562 [Online]. DOI: 10.1007/s10336-007-0213-6.

Martin, G. R. (2009) ‘What is binocular vision for? A birds’ eye view’, *Journal of Vision*, The Association for Research in Vision and Ophthalmology, vol. 9, no. 11, pp. 14–14 [Online]. DOI: 10.1167/9.11.14.

Martin, G. R. (2014) ‘The subtlety of simple eyes: The tuning of visual fields to perceptual challenges in birds’, *Philosophical Transactions of the Royal Society B: Biological Sciences*, vol. 369, no. 1636, p. 20130040 [Online]. DOI: 10.1098/rstb.2013.0040.

Mathews, Z., Cetnarski, R. and Verschure, P. F. M. J. (2015) ‘Visual anticipation biases conscious decision making but not bottom-up visual processing’, *Frontiers in Psychology*, Frontiers, vol. 5, p. 1443 [Online]. DOI: 10.3389/fpsyg.2014.01443.

Maurice, M. (2006) ‘Influence of the behavioural context on the optocollic reflex (OCR) in pigeons (Columba livia)’, *Journal of Experimental Biology*, vol. 209, no. 2, pp. 292–301 [Online]. DOI: 10.1242/jeb.02005.

Meade, J. (2005) ‘Tracking Homing Pigeons by GPS Tracking homing pigeons using GPS technology’, University of Oxford, Dphil Thesis.

Meade, J., Biro, D. and Guilford, T. (2005a) ‘Homing pigeons develop local route stereotypy’, *Proceedings of the Royal Society B: Biological Sciences*, The Royal Society, vol. 272, no. 1558, pp. 17–23 [Online]. DOI: 10.1098/rspb.2004.2873.

Meade, J., Biro, D. and Guilford, T. (2005b) ‘Homing pigeons develop local route stereotypy.’, *Proceedings. Biological sciences*, The Royal Society, vol. 272, no. 1558, pp. 17–23 [Online]. DOI: 10.1098/rspb.2004.2873.

Mills, R., Hildenbrandt, H., Taylor, G. K. and Hemelrijk, C. K. (2018) ‘Physics-based simulations of aerial attacks by peregrine falcons reveal that stooping at high speed maximizes catch success against agile prey’, *PLoS Computational Biology*, vol. 14, no. 4, pp. 1–38 [Online]. DOI: 10.1371/journal.pcbi.1006044.

Money, K. E., Bonen, L., Beatty, J. D., Kuehn, L. a, Sokoloff, M. and Weaver, R. S. (1971) ‘Physical properties of fluids and structures of vestibular apparatus of the pigeon.’, *The American journal of physiology*, vol. 220, no. 1, pp. 140–147 [Online]. DOI: 10.1152/ajplegacy.1971.220.1.140.

Mora, C. V., Ross, J. D., Gorsevski, P. V., Chowdhury, B. and Bingman, V. P. (2012) ‘Evidence for discrete landmark use by pigeons during homing’, *Journal of Experimental Biology*, vol. 215, no. 19, pp. 3379–3387 [Online]. DOI: 10.1242/jeb.071225.

Nagy, M., Ákos, Z., Biro, D. and Vicsek, T. (2010) ‘Hierarchical group dynamics in pigeon flocks’, *Nature*, vol. 464, no. 7290, pp. 890–893 [Online]. DOI: 10.1038/nature08891.

Necker, R. (2007) ‘Head-bobbing of walking birds’, *Journal of Comparative Physiology A: Neuroethology, Sensory, Neural, and Behavioral Physiology*, vol. 193, no. 12, pp. 1177–1183 [Online]. DOI: 10.1007/s00359-007-0281-3.

O’Rourke, C. T., Hall, M. I., Pitlik, T. and Fernández-Juricic, E. (2010) ‘Hawk eyes I: Diurnal raptors differ in visual fields and degree of eye movement’, *PLoS ONE*, Public Library of Science, vol. 5, no. 9, pp. 1–8 [Online]. DOI: 10.1371/journal.pone.0012802.

O’Rourke, C. T., Pitlik, T., Hoover, M. and Fernández-Juricic, E. (2010a) ‘Hawk eyes II: Diurnal raptors differ in head movement strategies when scanning from perches’, *PLoS ONE*, Public Library of Science, vol. 5, no. 9, pp. 1–6 [Online]. DOI: 10.1371/journal.pone.0012169.

O’Rourke, C. T., Pitlik, T., Hoover, M. and Fernández-Juricic, E. (2010b) ‘Hawk eyes II: Diurnal raptors differ in head movement strategies when scanning from perches’, *PLoS ONE*, Public Library of Science, vol. 5, no. 9, pp. 1–6 [Online]. DOI: 10.1371/journal.pone.0012169.

Ochs, M. F., Zamani, M., Gomes, G. M. R., de Oliveira Neto, R. C. and Kane, S. A. (2017) ‘Sneak peek: Raptors search for prey using stochastic head turns’, *The Auk*, The American Ornithologists’ Union, vol. 134, no. 1, pp. 104–115 [Online]. DOI: 10.1642/AUK-15-230.1.

Ohayon, S., Van Der Willigen, R. F., Wagner, H., Katsman, I. and Rivlin, E. (2006) ‘On the barn owl’s visual pre-attack behavior: I. Structure of head movements and motion patterns’, *Journal of Comparative Physiology A: Neuroethology, Sensory, Neural, and Behavioral Physiology*, vol. 192, no. 9, pp. 927–940 [Online]. DOI: 10.1007/s00359-006-0130-9.

Olberg, R. M., Seaman, R. C., Coats, M. I. and Henry, A. F. (2007) ‘Eye movements and target fixation during dragonfly prey-interception flights’, *Journal of Comparative Physiology A: Neuroethology, Sensory, Neural, and Behavioral Physiology*, vol. 193, no. 7, pp. 685–693 [Online]. DOI: 10.1007/s00359-007-0223-0.

Paddan, G. S. and Griffin, M. J. (1988) ‘The transmission of translational seat vibration to the head-I. Vertical seat vibration’, *Journal of Biomechanics*, vol. 21, no. 3, pp. 191–197 [Online]. DOI: 10.1016/0021-9290(88)90169-8.

Palumbo, N. F., Blauwkamp, R. A. and Lloyd, J. M. (2010) ‘Basic principles of homing guidance’, *Johns Hopkins APL Technical Digest (Applied Physics Laboratory)*, vol. 29, no. 1, pp. 25–41.

Pennycuick, C. J. (1978) ‘Fifteen Testable Predictions about Bird Flight’, *Oikos*, vol. 30, no. 2, p. 165 [Online]. DOI: 10.2307/3543476.

Pennycuick, C. J., Klaassen, M., Kvist, A. and Lindström, Å. (1996) ‘Wingbeat Frequency and the Body Drag Anomaly: Wind-Tunnel Observations on a Thrush Nightingale (Luscinia luscinia) and a Teal (Anas crecca)’, *Journal of Experimental Biology*, vol. 199, no. Pt 12, pp. 2757–65.

Pete, A. E., Kress, D., Dimitrov, M. A. and Lentink, D. (2015) ‘The role of passive avian head stabilization in flapping flight’, *Journal of the Royal Society Interface*, vol. 12, no. 110, p. 20150508 [Online]. DOI: 10.1098/rsif.2015.0508.

Pettit, B., Ákos, Z., Vicsek, T. and Biro, D. (2015) ‘Speed determines leadership and leadership determines learning during pigeon flocking’, *Current Biology*, Elsevier, vol. 25, no. 23, pp. 3132–3137 [Online]. DOI: 10.1016/j.cub.2015.10.044.

Pio, R. L. (1966) ‘Euler Angle Transformations’, *IEEE Transactions on Automatic Control*, vol. 11, no. 4, pp. 707–715 [Online]. DOI: 10.1109/TAC.1966.1098430.

Portugal, S. J., Hubel, T. Y., Fritz, J., Heese, S., Trobe, D., Voelkl, B., Hailes, S., Wilson, A. M. and Usherwood, J. R. (2014) ‘Upwash exploitation and downwash avoidance by flap phasing in ibis formation flight’, *Nature*, Nature Publishing Group, vol. 505, no. 7483, pp. 399–402 [Online]. DOI: 10.1038/nature12939.

Portugal, S. J. and White, Craig R (2018) ‘Methods in Ecology and Evolution’, *Methods in Ecology and Evolution*, vol. 1, no. 1, pp. 1–2 [Online]. DOI: 10.1111/j.2041-210X.2010.00016.x.

Portugal, S. J. and White, Craig R. (2018) ‘Miniaturization of biologgers is not alleviating the 5% rule’, *Methods in Ecology and Evolution*, vol. 9, no. 7, pp. 1662–1666 [Online]. DOI: 10.1111/2041-210X.13013.

Pozzo, T., Berthoz, A. and Lefort, L. (1990) ‘Head stabilization during various locomotor tasks in humans’, *Experimental Brian Research*, vol. 82, pp. 97–106.

Prior, H., Wiltschko, R., Stapput, K., Güntürkün, O. and Wiltschko, W. (2004) ‘Visual lateralization and homing in pigeons’, *Behavioural Brain Research*, vol. 154, no. 2, pp. 301–310 [Online]. DOI: 10.1016/j.bbr.2004.02.018.

Pycke, J.-R. (2010) ‘Some tests for uniformity of circular distributions powerful against multimodal alternatives’, *Canadian Journal of Statistics*, vol. 38, no. 1, p. n/a-n/a [Online]. DOI: 10.1002/cjs.10048.

Quinn, D. B., Watts, A., Nagle, T. and Lentink, D. (2017) ‘A new low-turbulence wind tunnel for animal and small vehicle flight experiments’, *Royal Society Open Science*, vol.

4, no. 3 [Online]. DOI: 10.1098/rsos.160960.

Quinn, D. B., Watts, A., Nagle, T., Lentink, D. and Quinn, D. B. (2017) 'A new low-turbulence wind tunnel for animal and small vehicle flight experiments', *Royal Society Open Science*, vol. 4, no. 3 [Online]. DOI: 10.1098/rsos.160960.

Rattenborg, N. C., Voirin, B., Cruz, S. M., Tisdale, R., Dell'Omo, G., Lipp, H. P., Wikelski, M. and Vyssotski, A. L. (2016) 'Evidence that birds sleep in mid-flight', *Nature Communications*, vol. 7, pp. 1–9 [Online]. DOI: 10.1038/ncomms12468.

Renaudin, V., Afzal, M. H. and Lachapelle, G. (2010) 'Complete triaxis magnetometer calibration in the magnetic domain', *Journal of Sensors*, Hindawi, vol. 2010, no. 967245, pp. 1–10 [Online]. DOI: 10.1155/2010/967245.

Rennie S. (2017) 'UK Environmental Change Network (ECN) meteorology data: 1991-2015', NERC Environmental Information Data Centre [Online]. DOI: 10.5285/fc9bcd1c-e3fc-4c5a-b569-2fe62d40f2f5.

Reynolds, A. M., Reynolds, D. R., Smith, A. D. and Chapman, J. W. (2010) 'A single wind-mediated mechanism explains high-altitude "non-goal oriented" headings and layering of nocturnally migrating insects', *Proceedings of the Royal Society B: Biological Sciences*, vol. 277, no. 1682, pp. 765–772 [Online]. DOI: 10.1098/rspb.2009.1221.

Reynolds, K. V. (2016) 'Soaring and Gust Response in the Steppe Eagle', University of Oxford, DPhil Thesis.

Reynolds, K. V., Thomas, A. L. R. and Taylor, G. K. (2014) 'Wing tucks are a response to atmospheric turbulence in the soaring flight of the steppe eagle Aquila nipalensis', *Journal of the Royal Society Interface*, vol. 11, no. 101, pp. 20140645–20140645 [Online]. DOI: 10.1098/rsif.2014.0645.

Richardson, J. (2000) 'Bird Migration and Wind Turbines: Migration Timing, Flight Behavior, and Collision Risk', *Proceedings of National Avian - Wind Power Planning Meeting III*, no. Wind Power Planning, p. 214.

Riley, J. R., Reynolds, D. R., Smith, A. D., Edwards, A. S., Osborne, J. L., Williams, I. H. and McCartney, H. A. (1999) 'Compensation for wind drift by bumble-bees [4]', *Nature*, vol. 400, no. 6740, p. 126 [Online]. DOI: 10.1038/22029.

Ros, I. G. and Biewener, A. A. (2017) 'Pigeons (C. livia) follow their head during turning flight: Head stabilization underlies the visual control of flight', *Frontiers in Neuroscience*, Frontiers, vol. 11, no. DEC, p. 655 [Online]. DOI: 10.3389/fnins.2017.00655.

Safi, K., Kranstauber, B., Weinzierl, R., Griffin, L., Rees, E. C., Cabot, D., Cruz, S. M., Proaño, C., Takekawa, J. Y., Newman, S. H., Waldenström, J., Bengtsson, D., Kays, R., Wikelski, M. and Bohrer, G. (2013) 'Flying with the wind: scale dependency of speed and direction measurements in modelling wind support in avian flight', *Movement Ecology*, BioMed Central, vol. 1, no. 1, p. 4 [Online]. DOI: 10.1186/2051-3933-1-4.

Säfken, B., Rügamer, D., Kneib, T. and Greven, S. (2018) 'Conditional Model Selection in Mixed-Effects Models with cAIC4', pp. 1–31.

Sasaki, T., Mann, R. P., Warren, K. N., Herbert, T., Wilson, T. and Biro, D. (2018) 'Personality and the collective: bold homing pigeons occupy higher leadership ranks in flocks.', *Philosophical transactions of the Royal Society of London. Series B, Biological sciences*, The Royal Society, vol. 373, no. 1746, p. 20170038 [Online]. DOI: 10.1098/rstb.2017.0038.

Schrader, D. K., Min, B. C., Matson, E. T. and Eric Dietz, J. (2016) 'Real-time averaging of position data from multiple GPS receivers', *Measurement: Journal of the International Measurement Confederation*, Elsevier Ltd, vol. 90, pp. 329–337 [Online]. DOI: 10.1016/j.measurement.2016.04.028.

Schwarz, J. S., Sridharan, D. and Knudsen, E. I. (2013) 'Magnetic tracking of eye position in freely behaving chickens', *Frontiers in Systems Neuroscience*, vol. 7, no. November, pp. 1–8 [Online]. DOI: 10.3389/fnsys.2013.00091.

Shepard, Emily L.C., Ross, A. N. and Portugal, S. J. (2016) 'Moving in a moving medium: New perspectives on flight', *Philosophical Transactions of the Royal Society B: Biological Sciences*, vol. 371, no. 1704 [Online]. DOI: 10.1098/rstb.2015.0382.

Shepard, Emily L. C., Ross, A. N. and Portugal, S. J. (2016) 'Moving in a moving medium: new perspectives on flight', *Philosophical Transactions of the Royal Society B: Biological Sciences*, The Royal Society, vol. 371, no. 1704, p. 20150382 [Online]. DOI: 10.1098/rstb.2015.0382.

Shneydor, Neryahu A (1998) *Missile guidance and pursuit: kinematics, dynamics and control*, Elsevier.

Shneydor, N.A. (1998) *Mechanization of Proportional Navigation, Missile Guidance and Pursuit*, Elsevier [Online]. DOI: 10.1533/9781782420590.129.

Sridharan, D., Ramamurthy, D. L., Schwarz, J. S. and Knudsen, E. I. (2014) 'Visuospatial selective attention in chickens', *Proceedings of the National Academy of Sciences*, vol. 111, no. 19, pp. E2056–E2065 [Online]. DOI: 10.1073/pnas.1316824111.

Srygley, R. B. and Oliveira, E. G. (2001) 'Sun compass and wind drift compensation in migrating butterflies', *Journal of Navigation*, vol. 54, no. 3, pp. 405–417 [Online]. DOI: 10.1017/S0373463301001448.

Stamp Dawkins, M. (2002) 'What are birds looking at? Head movements and eye use in chickens', *Animal Behaviour*, vol. 63, no. 5, pp. 991–998 [Online]. DOI: 10.1006/anbe.2002.1999.

Takahashi, H. and Shimoyama, I. (2018) 'Waterproof pitot tube with high sensitive differential pressure sensor and nano-hole array', *Proceedings of the IEEE International Conference on Micro Electro Mechanical Systems (MEMS)*, vol. 2018–Janua, no. January, pp. 214–217 [Online]. DOI: 10.1109/MEMSYS.2018.8346522.

Tarroux, A., Weimerskirch, H., Wang, S. H., Bromwich, D. H., Cherel, Y., Kato, A., Ropert-Coudert, Y., Varpe, Ø., Yoccoz, N. G. and Descamps, S. (2016) 'Flexible flight response to challenging wind conditions in a commuting Antarctic seabird: Do you catch the drift?', *Animal Behaviour*, vol. 113, pp. 99–112 [Online]. DOI: 10.1016/j.anbehav.2015.12.021.

Taylor, Graham K, Reynolds, K. V. and Thomas, A. L. R. (2016) 'Soaring energetics and glide performance in a moving atmosphere', *Philosophical Transactions of the Royal Society B: Biological Sciences*, vol. 371, no. 1704, p. 20150398 [Online]. DOI: 10.1098/rstb.2015.0398.

Taylor, L. A., Portugal, S. J. and Biro, D. (2017) 'Homing pigeons (*Columba livia*) modulate wingbeat characteristics as a function of route familiarity', *The Journal of Experimental Biology*, vol. 220, no. 16, pp. 2908–2915 [Online]. DOI: 10.1242/jeb.154039.

Team, R. D. C. (2008) 'R: A language and environment for statistical computing.', *R Foundation for Statistical Computing, Vienna, Austria. ISBN 3-900051-07-0, URL http://www.R-project.org*, Vienna, Austria, vol. 3 [Online]. DOI: 10.1007/978-3-540-74686-7.

Theunissen, L. M. and Troje, N. F. (2017) 'Head stabilization in the pigeon: Role of vision to correct for translational and rotational disturbances', *Frontiers in Neuroscience*, vol. 11, no. OCT, pp. 1–12 [Online]. DOI: 10.3389/fnins.2017.00551.

Troje, N. F. and Frost, B. J. (2000) 'Head-bobbing in pigeons: how stable is the hold phase?', *The Journal of experimental biology*, vol. 203, no. Pt 5, pp. 935–940 [Online]. DOI: PubMed: 10667977.

Tucker, V. A., Tucker, A., Akers, K. and Enderson, J. (2000) 'Curved flight paths in peregrine falcons', *The Journal of Experimental Biology*, vol. 203, pp. 3755–3763.

Usherwood, J. R., Stavrou, M., Lowe, J. C., Roskilly, K. and Wilson, A. M. (2011) 'Flying in a flock comes at a cost in pigeons', *Nature*, Nature Publishing Group, vol. 474, no. 7352, pp. 494–497 [Online]. DOI: 10.1038/nature10164.

Vyssotski, A. L., Serkov, A. N., Itskov, P. M., Dell'Omo, G., Latanov, A. V., Wolfer, D. P. and Lipp, H.-P. (2006) 'Miniature Neurologgers for Flying Pigeons: Multichannel EEG and Action and Field Potentials in Combination With GPS Recording', *Journal of Neurophysiology*, American Physiological Society, vol. 95, no. 2, pp. 1263–1273 [Online]. DOI: 10.1152/jn.00879.2005.

Wallman, J. and Letelier, J. (1993) *Eye movements, head movements, and gaze stabilization in birds, Vision, brain and behavior in birds*.

Wallraff, H. G. (1994) 'Initial orientation of homing pigeons as affected by the surrounding landscape', *Ethology Ecology and Evolution*, vol. 6, no. 1, pp. 23–36 [Online]. DOI: 10.1080/08927014.1994.9523005.

Wallraff, H. G. (2005) *Avian navigation: Pigeon homing as a paradigm, Avian Navigation: Pigeon Homing as a Paradigm*, Springer Science & Business Media, vol. 208, no. 22 [Online]. DOI: 10.1007/b137573.

Warrick, D. R. (2002) 'Bird maneuvering flight: Blurred Bodies, clear heads', *Integrative and Comparative Biology*, vol. 42, no. 1, pp. 141–148 [Online]. DOI: 10.1093/icb/42.1.141.

Westheimer, G. (1965) 'Visual Acuity', *Annual Review of Psychology*, vol. 16, no. 1, pp. 359–380 [Online]. DOI: 10.1146/annurev.ps.16.020165.002043.

Williams, H. J., Shepard, E. L. C., Duriez, O. and Lambertucci, S. A. (2015) 'Can accelerometry be used to distinguish between flight types in soaring birds?', *Animal Biotelemetry*, BioMed Central, vol. 3, no. 1, pp. 1–11 [Online]. DOI: 10.1186/s40317-015-0077-0.

Wilmers, C. C., Nickel, B., Bryce, C. M., Smith, J. A., Wheat, R. E., Yovovich, V. and Hebblewhite, M. (2015) 'The golden age of bio-logging: How animal-borne sensors are advancing the frontiers of ecology', *Ecology*, Wiley-Blackwell, vol. 96, no. 7, pp. 1741–1753 [Online]. DOI: 10.1890/14-1401.1.

Wiltschko, R. and Wiltschko, W. (2003) 'Avian navigation: From historical to modern concepts', *Animal Behaviour*, vol. 65, no. 2, pp. 257–272 [Online]. DOI: 10.1006/anbe.2003.2054.

Xia, D., Chen, S., Wang, S. and Li, H. (2009) ‘Microgyroscope temperature effects and compensation-control methods’, *Sensors*, vol. 9, no. 10, pp. 8349–8376 [Online]. DOI: 10.3390/s91008349.

Yorzinski, J. L., Patricelli, G. L., Babcock, J. S., Pearson, J. M. and Platt, M. L. (2013) ‘Through their eyes: selective attention in peahens during courtship’, *Journal of Experimental Biology*, vol. 216, no. 16, pp. 3035–3046 [Online]. DOI: 10.1242/jeb.087338.

Yorzinski, J. L. and Platt, M. L. (2014) ‘Selective attention in peacocks during predator detection’, *Animal Cognition*, vol. 17, no. 3, pp. 767–777 [Online]. DOI: 10.1007/s10071-013-0708-x.